

Spring 5-31-2018

Submandibular mechanical stimulation of upper airway muscles to treat obstructive sleep apnea

Ferhat Erdogan
New Jersey Institute of Technology

Follow this and additional works at: <https://digitalcommons.njit.edu/dissertations>



Part of the [Bioimaging and Biomedical Optics Commons](#), and the [Neurosciences Commons](#)

Recommended Citation

Erdogan, Ferhat, "Submandibular mechanical stimulation of upper airway muscles to treat obstructive sleep apnea" (2018). *Dissertations*. 1412.

<https://digitalcommons.njit.edu/dissertations/1412>

This Dissertation is brought to you for free and open access by the Electronic Theses and Dissertations at Digital Commons @ NJIT. It has been accepted for inclusion in Dissertations by an authorized administrator of Digital Commons @ NJIT. For more information, please contact digitalcommons@njit.edu.

Copyright Warning & Restrictions

The copyright law of the United States (Title 17, United States Code) governs the making of photocopies or other reproductions of copyrighted material.

Under certain conditions specified in the law, libraries and archives are authorized to furnish a photocopy or other reproduction. One of these specified conditions is that the photocopy or reproduction is not to be “used for any purpose other than private study, scholarship, or research.” If a user makes a request for, or later uses, a photocopy or reproduction for purposes in excess of “fair use” that user may be liable for copyright infringement,

This institution reserves the right to refuse to accept a copying order if, in its judgment, fulfillment of the order would involve violation of copyright law.

Please Note: The author retains the copyright while the New Jersey Institute of Technology reserves the right to distribute this thesis or dissertation

Printing note: If you do not wish to print this page, then select “Pages from: first page # to: last page #” on the print dialog screen

The Van Houten library has removed some of the personal information and all signatures from the approval page and biographical sketches of theses and dissertations in order to protect the identity of NJIT graduates and faculty.

ABSTRACT

SUBMANDIBULAR MECHANICAL STIMULATION OF UPPER AIRWAY MUSCLES TO TREAT OBSTRUCTIVE SLEEP APNEA

by

Ferhat Erdogan

The extrinsic tongue muscles are activated in coordination with pharyngeal muscles to keep a patent airway during respiration in wakefulness and sleep. The activity of genioglossus, the primary tongue-protruding muscle playing an important role in this coordination, is known to be modulated by several reflex pathways mediated through the mechanoreceptors of the upper airways. The main objective is to investigate the effectiveness of activating these reflex pathways with mechanical stimulations, for the long-term goal of improving the upper airway patency during disordered breathing in sleep. The genioglossus response is examined during mandibular and sub-mandibular mechanical stimulations in healthy subjects during wakefulness. The genioglossus activity is recorded with custom-made sublingual EMG electrode molded out of silicone. Mechanical vibrations are applied to the lower jaw at 8 and 12 Hz with an amplitude of 5 mm in the first experiment, and to the sub-mandibular area at three different intensities (0.2-0.9 mm, 21-33 Hz) in the second experiment. The effects of sub-mandibular mechanical vibrations are also investigated in severe obstructive sleep apnea patients during a whole night sleep study. The major findings of this study are that the genioglossus reflexively responds to the mechanical vibrations applied to the mandible and the sub-mandibular skin surface in healthy subjects during wakefulness and the sub-mandibular stimulations during sleep terminate the apnea earlier and decrease the level of hypoxia with smaller micro arousals.

**SUBMANDIBULAR MECHANICAL STIMULATION OF UPPER AIRWAY
MUSCLES TO TREAT OBSTRUCTIVE SLEEP APNEA**

**by
Ferhat Erdogan**

**A Dissertation
Submitted to the Faculty of
New Jersey Institute of Technology
and Rutgers University Biomedical and Health Sciences – Newark
in Partial Fulfillment of the Requirements for the Degree of
Doctor of Philosophy in Biomedical Engineering**

Department of Biomedical Engineering

May 2018

Copyright © 2018 by Ferhat Erdogan

ALL RIGHTS RESERVED

APPROVAL PAGE

**SUBMANDIBULAR MECHANICAL STIMULATION OF UPPER AIRWAY
MUSCLES TO TREAT OBSTRUCTIVE SLEEP APNEA**

Ferhat Erdogan

Dr. Mesut Sahin, Dissertation Advisor
Professor of Biomedical Engineering, NJIT

Date

Dr. Sergei Adamovich, Committee Member
Professor of Biomedical Engineering, NJIT

Date

Dr. Judith Deutsch, Committee Member
Professor of Rehabilitation and Movement Sciences
Rutgers Biomedical and Health Sciences

Date

Dr. Richard A. Foulds, Committee Member
Professor Emeritus of Biomedical Engineering, NJIT

Date

Dr. Antje Ihlefeld, Committee Member
Assistant Professor of Biomedical Engineering, NJIT

Date

BIOGRAPHICAL SKETCH

Author: Ferhat Erdogan
Degree: Doctor of Philosophy
Date: May 2018

Undergraduate and Graduate Education:

- Doctor of Philosophy in Biomedical Engineering, New Jersey Institute of Technology, Newark, NJ, 2018
- Bachelor of Science in Electrical Engineering, Fatih University, Istanbul, Turkey, 2012

Major: Biomedical Engineering

Presentations and Publications:

Ferhat Erdogan, Mesut Sahin (2017). Human Jaw-Tongue Reflex Evoked by High Frequency Mandibular Vibrations. Biomedical Engineering Society Annual Meeting, Phoenix, AZ.

Ferhat Erdogan, Mesut Sahin (2018). Genioglossal Response to Mechanical Vibrations of the Mandible and the Sub-Mandibular Muscles. Submitted to Journal of NeuroEngineering and Rehabilitation

Dedicated to my parents, Faruk and Ayse Erdogan and my dear wife, Aslinur Erdogan for
all their continuous support.

ACKNOWLEDGMENT

I would like to express my deepest appreciation and thankfulness to Dr. Mesut Sahin, my research advisor, who greatly supported and mentored me throughout my PhD with his deep knowledge and admirable personality. I would also like to thank my PhD dissertation committee members, Dr. Antje Ihlefeld, Dr. Judith Deutsch, Dr. Richard A. Foulds and Dr. Sergei Adamovich for constructive criticism and valuable comments.

I would also like to thank my colleagues and friends, Ozan Cakmak, Sinan Gok, Ahmet Asan, Ali Ersen, Esmâ Cetinkaya, Ahmad Alokaily and Oyindamola Owoeye for creating a motivating and supportive environment as well as for the unlimited discussions I had with them.

Most importantly, I would like to thank my wife, Aslinur Erdogan, for being here with me and for her support, patience and enthusiasm throughout my study. I would also like to thank my parents, Faruk and Ayse Erdogan for their constant support and dedication that brings me to these days.

TABLE OF CONTENTS

Chapter	Page
1 INTRODUCTION	1
1.1 Problem Significance	1
1.2 Objectives	3
1.2.1 Aim 1: Demonstration of Human Jaw-Tongue Reflex During Mandibular Vibrations	4
1.2.2 Aim 2: Human Genioglossus Response to Sub-Mandibular Mechanical Stimulations	4
1.2.3 Aim 3: Effects of Submandibular Mechanical Stimulations in Obstructive Sleep Apnea Patients	4
2 THE JAW-TONGUE REFLEX IN WAKEFULNESS.....	6
2.1 Background Information	7
2.1.1 Jaw-Tongue Reflex (JTR)	7
2.1.2 Genioglossus EMG Recording.....	8
2.2 Experimental Methodology	9
2.2.1 Sublingual Electrode for GG EMG.....	10
2.2.2 Masseter and Mylohyoid Muscle EMG Recordings	12
2.2.3 Mandibular Vibrations	13
2.2.4 Stimulation Protocol.....	14
2.2.5 Signal Processing	16
2.3 Results	17
2.4 Discussion	20

TABLE OF CONTENTS
(Continued)

Chapter	Page
3 GENIOGLOSSUS RESPONSE TO SUB-MANDIBULAR MECHANICAL STIMULATIONS IN WAKEFULNESS	22
3.1 Background Information	23
3.1.1 Pressure Oscillation.....	23
3.1.2 Tonic Vibration Reflex (TVR).....	24
3.2 Experimental Methodology	25
3.2.1 Sublingual Electrode for GG EMG	25
3.2.2 Sub-Mandibular Mechanical Stimulations.....	26
3.2.3 Stimulation Protocol.....	28
3.3 Results	29
3.4 Discussion	32
4 SUBMANDIBULAR MECHANICAL STIMULATIONS IN OSA PATIENTS	35
4.1 Background Information	36
4.1.1 Obstructive Sleep Apnea (OSA)	36
4.1.2 Hypoglossal Nerve Stimulation	37
4.1.3 High Frequency Pressure Oscillation.....	38
4.1.4 Tonic Vibration Reflex (TVR).....	41
4.2 Experimental Methodology	43
4.2.1 OSA Patients	43
4.2.2 Protocol	44

TABLE OF CONTENTS
(Continued)

Chapter	Page
4.2.3 Genioglossus Electrodes	44
4.2.4 Signal Processing	45
4.2.5 Mechanical Vibrations	47
4.2.6 Statistics	47
4.3 Results	48
4.3.1 GG Activity Analysis	48
4.3.2 Individual Patient Characteristics.....	51
4.1.3 EEG Alpha Analysis	57
4.1.4 Snore Classification.....	59
4.4 Discussion	66
5 CONCLUSIONS AND FUTURE WORK.....	69
APPENDIX MATLAB CODE	71
REFERENCES.....	93

LIST OF TABLES

Table		Page
2.1	Statistical Data of the Subjects in Mandibular Vibration Experiment.....	9
3.1	Statistical Data of the Subjects in Sub-Mandibular Vibration Experiment .	26
4.1	Patients Statistics	43
4.2	Statistical Test Results of SpO2, Alpha and GG_EMG	50
4.3	Statistical Results of Snore Features.....	65

LIST OF FIGURES

Figure	Page	
2.1	Computer drawings of the sublingual surface electrode for genioglossus EMG. Stainless steel wires shown as blue-dotted lines are embedded into a silicone (PDMS) mold with the tips exposed underneath (solid blue parts). The top-left figure is the zoomed-in view of the electrode from the bottom. The electrode assembly is placed under the tongue with the two arms on each side of the genioglossus. The thin flat portion protects the wires from and provides an anchor to the teeth when mouth is closed.....	10
2.2	Left: Two-piece mold designed with PTC Creo Parametric. Right: The electrode that was used for GG EMG recordings in the experiments. The two parts of the Sylgard 184 silicone elastomer kit are mixed in a ratio of 10:1. The stainless-steel wires are placed in the mold by leaving the ends out of the mold. The mold is filled with the mix through the hole on the top and cured for 45 minutes at 100°C heat. The cured silicone is removed from mold, the ends of the wires are desheathed and inserted back into the silicone leaving about 5 mm of the wires exposed for EMG recording.....	11
2.3	Subject places the two arms of the silicone piece under the tongue (Right) while slightly biting on the flat part (Left). The exposed ends of the stainless-steel wires were pressing against the GG muscles on each side of tongue	12
2.4	Samples of genioglossus EMG recorded with the sublingual electrode. Bottom: 30 s recording during deep breathing with EMG bursts occurring during inhalation. The red trace is the EMG envelope. Top-Left: Single spikes in GG EMG at a shorter time scale. Top-Right: A single EMG spike from the same data.....	13
2.5	Linear movement was generated by a battery powered reciprocating saw (Milwaukee M12 Reciprocating Saw) and transferred to the mandible via an oil filled Tygon® tubing. A pressure transducer (DPT-100, DELTRAN®) was added to the hydraulic system for measurements of the force applied by the jaw.....	14
2.6	Mandibular vibration setup: Linear movement generated by using a reciprocating mechanism is transferred to the mandible via an oil filled Tygon® tubing	15
2.7	Percent increases in EMG signal power for GG, MS, and MH muscles above the baseline in the mandibular vibration test (mean ± SE)	17

LIST OF FIGURES
(Continued)

Figure	Page
2.8 Stimulus-triggered averages of GG, MS and MH EMG over multiple cycles of displacement from subject M5 at 8 Hz (left) and 12 Hz (right) during twenty trials of 3 s duration. Trials are color coded. Top traces show the displacements averaged across all cycles. Horizontal dash lines: 60 ms	18
2.9 A sample episode from subject M5 during 12 Hz stimulation. Top trace is the displacement of the mandible calculated from the accelerometer. Red lines are the full-wave rectified and low pass filtered (20 Hz) envelopes of the EMG signals	19
2.10 Average coherence between rectified EMGs and the mandibular displacements in all trials for each subject, encoded by the trace color. High coherences occur at the vibrational frequency and its harmonics	20
2.11 Average coherences between rectified EMGs and mandibular displacements at the fundamental frequency (8 Hz or 12 Hz) in all subjects (mean \pm SD).....	21
3.1 Left: A 24 mm DC motor with eccentric rotor (JQ24-35F580C Cylindrical Vibration Motor, Jinlong Machinery & Electronics) for the application of mechanical vibrations, and the acceleration sensor (ADXL335 Triple Axis Accelerometer, Analog Devices) for recording and monitoring the displacement and frequency of the stimulations. Right: 3D printed case for covering the eccentric mass of the motor and attaching the acceleration sensor to the motor	27
3.2 Application of mechanical vibrations generated by an eccentric-load DC motor to the submandibular area using a chin strap	28
3.3 Measured Frequencies and Displacements (Mean \pm SD) in Each Subject at Three Different Voltages (Low, Medium, and High) Used to Drive the DC Motor During the Sub-Mandibular Stimulations	29
3.4 Rectified-filtered GG activity at three different levels of submandibular mechanical stimulation in subject S3 showing the persistence of activity after the stimulation is terminated. Top traces: the mandibular displacement (Disp) and the raw GG activity. Bottom: The EMG envelopes are plotted as the mean (N=17-19 for each trace) and standard error (SE, shaded areas).....	30

LIST OF FIGURES
(Continued)

Figure	Page
3.5 Percent increases in GG signal power during sub-mandibular vibrations (mean \pm SE)	31
3.6 Box-plot for post-stimulus EMG persistence times, calculated as the duration from the stimulus offset point to where the evoked activity fell below one standard deviation around the baseline mean. Maximum measurable delay was limited by 3 s, because the recordings were stopped 3 s after stimulations. Subjects S6 and S7 were excluded (see Methods)	32
4.1 Attachment of the mechanical vibrator over the submandibular skin using a chin strap. A pair of EMG wire electrodes were inserted into the genioglossus unilaterally through the mouth	44
4.2 Sample episode from patient 1. The times of GG_EMG and alpha power baselines measurements are marked with horizontal dash line as an example. The arrows show the intervals where the peak values for the GG_EMG and EEG alpha power were searched. The asterisks indicate the manually marked points of apnea terminations (airflow) and the minimum SpO2 measurements for a pair of unstimulated and stimulated apnea cycles	46
4.3 Top: GG activity during middle of the apnea (baseline) and during apnea terminations for both stimulated and non-stimulated cases. Bottom: Minimum oxygen saturation and alpha peak difference between stimulated and non-stimulated apnea cycle. All GG_EMG and alpha peak powers in both stimulated and non-stimulated cycles are significantly higher than their baseline values ($p < 0.001$, one-sided, unpaired t-test). All values are means \pm SE. The P values can be found in Table 4.2.....	48
4.4 The first two traces are the signal power computed in 4 s running windows for the vibration frequency band (95-105 Hz to capture 99 Hz in this case) and the whole band EMG power (10-500 Hz) respectively. The bottom trace is the raw genioglossal EMG signal. The timings of the stimulations are indicated with the dotted lines	49
4.5 Sample episode from patient 2. The timings of mechanical stimulations are indicated by two vertical dash lines	52

LIST OF FIGURES
(Continued)

Figure	Page
4.6 Sample episode from patient 3. The timings of mechanical stimulations are indicated by two vertical dash lines.....	53
4.7 Sample episode from patient 4. The timings of mechanical stimulations are indicated by two vertical dash lines.....	54
4.8 Sample episode from patient 5. The timings of mechanical stimulations are indicated by two vertical dash lines.....	55
4.9 Sample episode from patient 6. The timings of mechanical stimulations are indicated by two vertical dash lines.....	56
4.10 The peak alpha power measurements in stimulated vs. non-stimulated (spontaneous) apnea terminations in all six patients. The filled circles indicate the instances where the alpha peak is less in a stimulated cycle compared to its neighboring non-stimulated apneic episode. The solid and dash lines show the mean \pm SD of the baseline alpha level in each patient	58
4.11 Classification of the breath cycles and snore events. Post-apneic breath is the first breath after apnea termination. Pre-apneic breath is the last breath before apnea. Mid-breaths are the rest of the breaths between post and pre-apneic breaths. Snore events are also classified by their corresponding breath cycles	61
4.12 Averages of each parameter for each group (mean \pm SE). Statistical test results are summarized in Table 4.3 a) Spectral centroid is the center of mass of the frequency spectrum b) Fundamental frequency is the pitch calculated with autocorrelation method. c) Pitch SD is the standard deviation of the pitches calculated with moving autocorrelation d) Snore duration is the time from beginning and end of snore e) Time interval 1 is the time between beginning of inspiration and end of snore f) Time interval 2 is the time between end of inspiration and end of snore. g) Sound intensity is the spectral power of the snore between 10 and 150 Hz. h) Correlation at pitch is the correlation value calculated from autocorrelation method at fundamental frequency. i) Percent snore occurrences during post, mid and pre-apneic breath cycles	63

CHAPTER 1

INTRODUCTION

1.1 Problem Significance

Obstructive sleep apnea (OSA) is the most common sleep disorder that affects as many as 25 million adults in the US alone (Naresh M Punjabi, 2008). It increases the risk of cardiovascular disease and stroke and leads to a significant decrease in quality of life (Eyal Shahar et al., 2001). It is believed that the problem originates primarily due to the anatomical factors that pre-dispose the upper airways (UAW) for obstructions. The upper airway muscle activity stays high to compensate for the disadvantaged anatomical factors in wakefulness (Robert B Fogel et al., 2001). However, this compensatory mechanism is lost at the alpha-to-theta transition in sleep, and leads to collapsing of the UAWs (Robert B Fogel et al., 2003). The continuous positive airway pressure (CPAP) therapy is the primary treatment method for OSA. However, it requires a mask to be worn by the patient and 46-83% of the OSA patients are non-adherent to the treatment (Terri E Weaver & Ronald R Grunstein, 2008). Hypoglossal (HG) nerve stimulation is a novel technique, which applies small electric currents to the hypoglossal nerve to move the tongue forward during inspiration. Although the HG nerve stimulation is effective, it is an invasive approach that requires surgical implantation of a stimulator lead, a battery and a respiratory sensor.

Many sensory receptors that innervate the oral and pharyngeal regions affect the extrinsic and intrinsic muscles of the tongue and continuously regulate the patency of the airways. For instance, a few groups showed that small amplitude pressure oscillations

similar to those occur during snoring could evoke a strong activity in the UAW muscles by stimulating the mechanoreceptors in the UAW mucosal membrane (Peter R Eastwood et al., 1999; KATHE G Henke & COLIN E Sullivan, 1993). In a different paradigm, opening the mandible increases the activity in the genioglossus (GG), the primary tongue protruding muscle, through the secondary endings of the muscle spindle afferents from the temporalis muscle and it is called the jaw-tongue reflex (JTR) (Y Ishiwata, T Ono, T Kuroda, & Y Nakamura, 2000).

As a third reflex mechanism involving the GG muscle is the tonic vibration reflex (TVR), which is an increase in the muscle activity as a response to mechanical vibrations applied to the muscle belly or its tendon, where Ia fibers generate action potentials locked to each cycle of the mechanical stimulation. The TVR is observed in many skeletal muscles including the masseter and the temporalis (Göran Eklund & K-E Hagbarth, 1966; Karl Erik Hagbarth, Gustaf Hellsing, & L Löfstedt, 1976; Patricia Romaguere, JEAN-PIERRE Vedel, JP Azulay, & S Pagni, 1991). The extrinsic tongue muscles and other pharyngeal muscles that can dilate the UAWs have never been targeted in those studies of the TVR, nor has the effect of sleep on TVR ever been investigated.

It should be emphasized that the UAW patency is maintained not only by the tongue protruding muscles, but also by the retracting and intrinsic tongue muscles, and the muscles of the pharyngeal wall all together (E Fiona Bailey & Ralph F Fregosi, 2004). The main objective in this study is to investigate the effectiveness of reflexively activating the most prominent UAW dilation muscle, the GG, using mechanical vibrations and thereby decreasing the UAW collapsibility.

1.2 Objectives

Our primary hypothesis is that the GG and other muscles that are involved in dilation of the UAWs can be activated synergistically, as it happens naturally during deep breathing, by mechanical stimulation of the UAW muscles. The long-term motivation behind this study is to take advantage of such reflex mechanisms to improve the UAW patency during disordered breathing in sleep. Thus, we set out to demonstrate some of these reflexes in healthy subjects during wakefulness as an initial attempt. The first two aims were designed to examine the response of the GG muscle during sub-mandibular and mandibular mechanical stimulations. The main objective was to demonstrate that mechanical perturbations of the mandibular bone and/or the muscles under the mandible can produce a reflex-like response in the genioglossus (GG), an extrinsic tongue muscle that is responsible for protrusion of the tongue and thereby playing an important role for patency of the UAWs during sleep. It may be argued that the GG activity alone is not sufficient for keeping the airways patent in sleep. The GG activity serves as a representative UAW dilatory muscle here, since it is prohibitively difficult to record from all the muscles involved in pharyngeal dilation. Furthermore, understanding of the reflexes that can affect the GG activity has the potential to provide insights into maintenance of the UAW patency in normals. As a second step towards this goal, the third aim was designed to demonstrate the effects of sub-mandibular stimulation in severe OSA patients ($AHI=51.5\pm 11.8$) during night while recording the GG activity with transorally implanted fine wires.

Our results indeed show that the GG response can be elicited both by vertical movements of the mandible and mechanical vibrations applied to the muscles in the sub-

mandibular region during wakefulness, and the obstructions can be terminated earlier with lower level of hypoxia and smaller micro-arousals with the application of sub-mandibular stimulations during night.

1.2.1 Aim 1: Demonstration of Human Jaw-Tongue Reflex During Mandibular Vibrations

The objective was to investigate the jaw-tongue reflex (JTR) evoked by mandibular vibrations at different frequencies with small amplitude. Eight healthy adult subjects of either gender were recruited for this aim. Three channels of EMG were collected from the genioglossus (GG), mylohyoid (MH) and masseter (MS) muscles. The GG EMG was collected differentially with the sublingual surface electrode molded from silicone.

1.2.2 Aim 2: Human Genioglossus Response to Sub-Mandibular Mechanical Stimulations

This aim was designed to determine if the GG responds to mechanical vibrations as a reflex similar to TVR observed in some other skeletal muscles. Mechanical vibrations were applied to the submandibular area with eccentric vibrational motor attached to a chin strap at three different intensity levels while the subjects lied on a massage bed in a supine position. Ten healthy adult subjects were recruited for this experiment. We recorded EMG signal only from the GG muscle with the sublingual surface electrode.

1.2.3 Aim 3: Effects of Submandibular Mechanical Stimulations in Obstructive Sleep Apnea Patients

The objective was to investigate the effects of mechanical vibrations applied on the submandibular region in six severe OSA patients ($AHI=51.5\pm 11.8$). The genioglossal activity was recorded with transorally implanted fine wire electrodes along with standard

polysomnography data. The mechanical vibrational device was attached using a chin strap over submandibular area. The sleep technician visually detected the UAW obstructions by observing the respiratory pattern and the airflow signals from the nasal sensor. The mechanical vibrational device was turned on manually by the sleep technician and continued until the breathing was resumed.

For statistical analysis, the unstimulated apnea cycles preceding or following the stimulated ones were treated as pairs with the stimulated cycles. The GG EMG activity representing the muscle response to the stimulation, the alpha power as a measure of micro-arousals, and the minimum blood oxygen saturation during the obstructions were marked manually and compared between the paired apnea cycles.

CHAPTER 2

THE JAW-TONGUE REFLEX IN WAKEFULNESS

The tongue position is reflexively controlled by the jaw position during functions such as respiration, swallowing and speech. Studies demonstrated the jaw-tongue reflex (JTR) in both animals and humans by showing increased activity on extrinsic tongue muscles especially the genioglossus (GG) during passive opening of the mandible. However, the response of the GG was not investigated sufficiently in human subjects with small amplitude mechanical vibrations. The purpose of this study was to demonstrate the JTR in human subjects with mechanical vibrations applied to mandible with small amplitudes less than 5 mm.

Eight healthy individuals were recruited to examine the GG response during mandibular mechanical vibrations. We recorded the GG activity using a custom-made sublingual EMG electrode molded out of silicone. Subjects participated in the experiment where 3 s long 5 mm vertical mechanical vibrations were delivered at 8 and 12 Hz to the lower jaw while the masseter (MS) and mylohyoid (MH) EMGs were recorded along with the GG.

The percent increases in EMG signals due to mechanical stimulations were quantified. All three muscle activities were significantly higher during stimulation compared to the baseline ($p < 0.02$) and the increase was higher at 12 Hz vs. 8 Hz ($p < 0.02$). We also demonstrated that all three muscle responses (GG, MS, and MH) had phasic components locked to the vibrational cycle. The major finding of this study is that the GG reflexively responds to the mechanical vibrations applied to the mandible in

healthy subjects during wakefulness. The presence of phasic components with mandibular stimulation suggests a short reflex pathway that may involve lower brain centers.

2.1 Background Information

Upper airway (UAW) muscles are activated in a highly coordinated manner with the extrinsic tongue muscles to keep an open airway passage during respiration. These muscles also act in concert during swallowing, mastication, coughing and other volitional movements to open and close the pharynx as necessary. A great deal of sensory information is taken into account from the pharyngeal area while producing these complex motor patterns. The presence of multiple forms of muscle reflexes that can be evoked in the UAWs suggests that the afferent pathways give rise to motor activity in the same region with short delays, potentially through the brain stem nuclei. These reflexes indicate that the UAWs are highly sensitive to different types of mechanical stimuli, including pressure oscillations, continuous negative pressure, and perturbations of the lower jaw.

2.1.1 Jaw-Tongue Reflex (JTR)

It has been known since 1930s that the tongue position is reflexively controlled by the jaw position. The tongue was retracted during passive jaw opening in cats (R Schoen, 1931) and the involvement of GG and styloglossus in this reflex was confirmed with electromyogram (EMG) recordings (Sigfrid Blom, 1960; R Schoen, 1931). Contrary to this report, a tongue protrusion was observed rather by passive jaw opening both in cats and monkeys (AA Lowe, 1978). This jaw-tongue reflex (JTR) also exists in humans

where opening the mandible increases the GG activity (Y Ishiwata, S Hiyama, K Igarashi, T Ono, & T Kuroda, 1997; AA Lowe, SC Gurza, & BJ Sessle, 1977). It was proposed that receptors responsible for eliciting this reflex are the stretch receptors in the MS muscle and the temporomandibular joint (Sigfrid Blom, 1960; Alan A Lowe & Barry J Sessle, 1973; R Schoen, 1931). However, neither sectioning of the masseteric nerve nor injection of lidocaine into the temporomandibular joint capsule affected the JTR (Toshifumi Morimoto, Hiromitsu TAKEBE, Iwao SAKAN, & Yojiro KAWAMURA, 1978). It was concluded that the secondary endings of the muscle spindle afferents from the temporalis muscle are primarily responsible for evoking the JTR (Y Ishiwata et al., 2000). Morimoto et al. also showed that the application of mechanical vibrations to the mandible evokes strong activity in the styloglossus in the cat. The response was strong with vibration amplitudes larger than 140 μm , but hardly detectable with displacements less than 70 μm . To our knowledge, the GG or any other tongue muscle has never been targeted in humans with mechanical vibrations applied to the mandible, nor the phasic response of the GG has ever been investigated in such a study.

2.1.2 Genioglossus EMG Recording

The genioglossus (GG) activity is usually recorded intramuscularly by inserting needle or wire electrodes into the muscle transorally. However, this method has several drawbacks including the pain and fear with needle insertion and the difficulties of obtaining approval from the institutional review board. Several types of non-invasive surface recording techniques were developed for the GG muscle and the signals were confirmed to originate from the GG by comparing them with their intramuscular counterparts (ELIZABETH A Doble, JAMES C Leiter, SUSAN L Knuth, JA Daubenspeck, & D

Bartlett Jr, 1985; Y Ishiwata et al., 1997; Mary K Milidonis, Charles G Widmer, Richard L Segal, & Steven L Kraus, 1988). Here in this study, we developed a re-usable non-invasive surface EMG electrode for the GG by embedding stainless steel wires in an electrode carrier that was molded from silicone.

Our primary objective is that the GG and other muscles of the UAWs can be activated by mechanical stimulation of the mandible. Thus, we set out to demonstrate the JTR in healthy subjects during wakefulness. As a step toward this goal, the present study was designed to examine the response of the GG, MH and MS muscles during mandibular vibrations.

2.2 Experimental Methodology

Eight healthy subjects were recruited in this study and subject statistics are summarized in Table 2.1. The experimental procedures were approved in advance by the institutional review board of New Jersey Institute of Technology and subjects gave their written informed consent prior to data collection.

Table 2.1 Statistical Data of the Subjects in Mandibular Vibration Experiment

Subject ID	Age	Sex	Weight (kg)	Height (cm)	BMI
M1	30	M	101	184	29.83
M2	27	M	78	175	25.46
M3	26	F	67	163	25.21
M4	28	M	72	183	21.49
M5	53	M	76	171	25.99
M6	33	M	106	180	32.71
M7	32	M	112	181	34.18
M8	28	M	60	167	21.51

2.2.1 Sublingual Electrode for GG EMG

For recording genioglossal activity, a two-part liquid silicone (PDMS, Sylgard® 184, Dow Corning, Shore hardness score of 48A) was molded into a shape shown in Figure 2.1 to securely hold the EMG wire electrodes, a pair of PFA insulated stainless steel wires (50 μm bare diam., #790700, A-M Systems), under the tongue. The ends of the wires were desheathed and inserted back into the silicone leaving about 5 mm of the wires exposed for EMG recording.

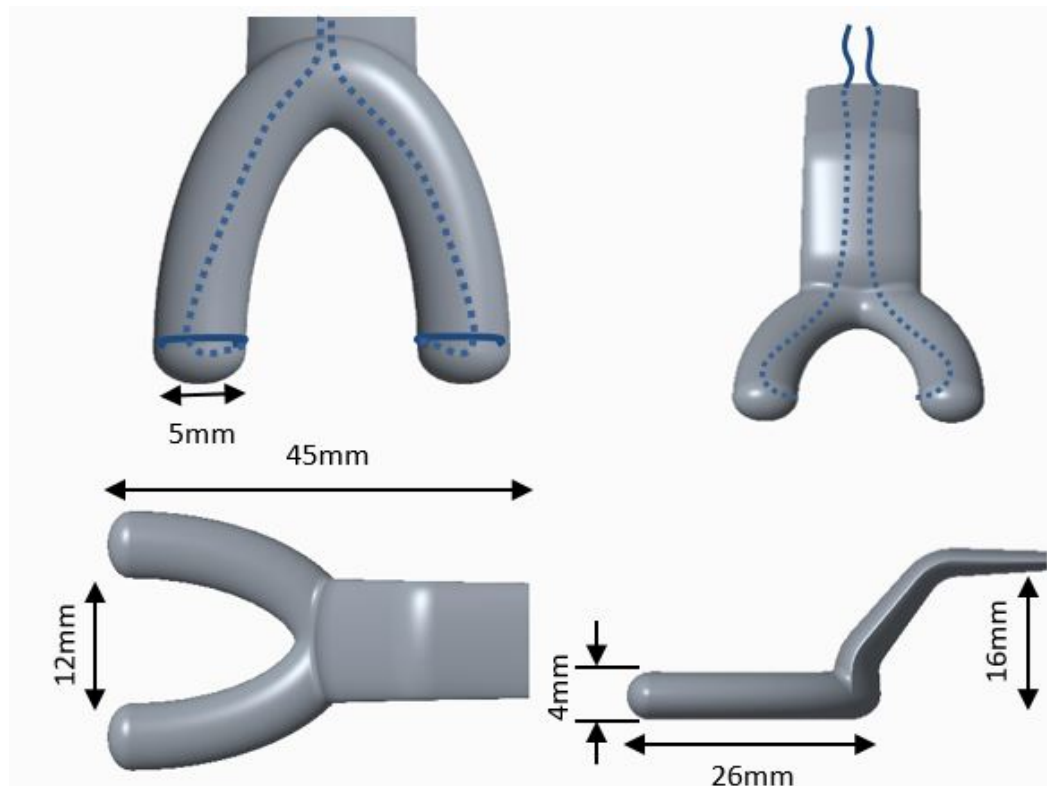


Figure 2.1. Computer drawings of the sublingual surface electrode for genioglossus EMG. Stainless steel wires shown as blue-dotted lines are embedded into a silicone (PDMS) mold with the tips exposed underneath (solid blue parts). The top-left figure is the zoomed-in view of the electrode from the bottom. The electrode assembly is placed under the tongue with the two arms on each side of the genioglossus. The thin flat portion protects the wires from and provides an anchor to the teeth when mouth is closed.

The two pieces 3D printed mold that was designed on PTC Creo Parametric and the molded sublingual electrode which was used in the experiments shown in Figure 2.2. The subjects placed the two arms of the silicone piece under the tongue while slightly biting on the flat part such that the exposed ends of the stainless-steel wires were pressed against the GG muscles on each side of tongue (Figure 2.3).



Figure 2.2 Left: Two-piece mold designed with PTC Creo Parametric. Right: The electrode that was used for GG EMG recordings in the experiments. The two parts of the Sylgard 184 silicone elastomer kit are mixed in a ratio of 10:1. The stainless-steel wires are placed in the mold by leaving the ends out of the mold. The mold is filled with the mix through the hole on the top and cured for 45 minutes at 100°C heat. The cured silicone is removed from mold, the ends of the wires are desheathed and inserted back into the silicone leaving about 5 mm of the wires exposed for EMG recording.

The sublingual electrode assembly was modified and fabricated multiple times to ensure a high signal-to-noise ratio (SNR) in EMG signals. We tested the signal quality by asking the subjects to perform several tasks involving the tongue. The bottom trace in Figure 2.4 represents a 30 s recording during deep breathing from one subject. The

quality of the recordings was sufficiently high such that the electrode could record single units from the GG during regular breathing in most of the subjects (Figure 2.4: Top).

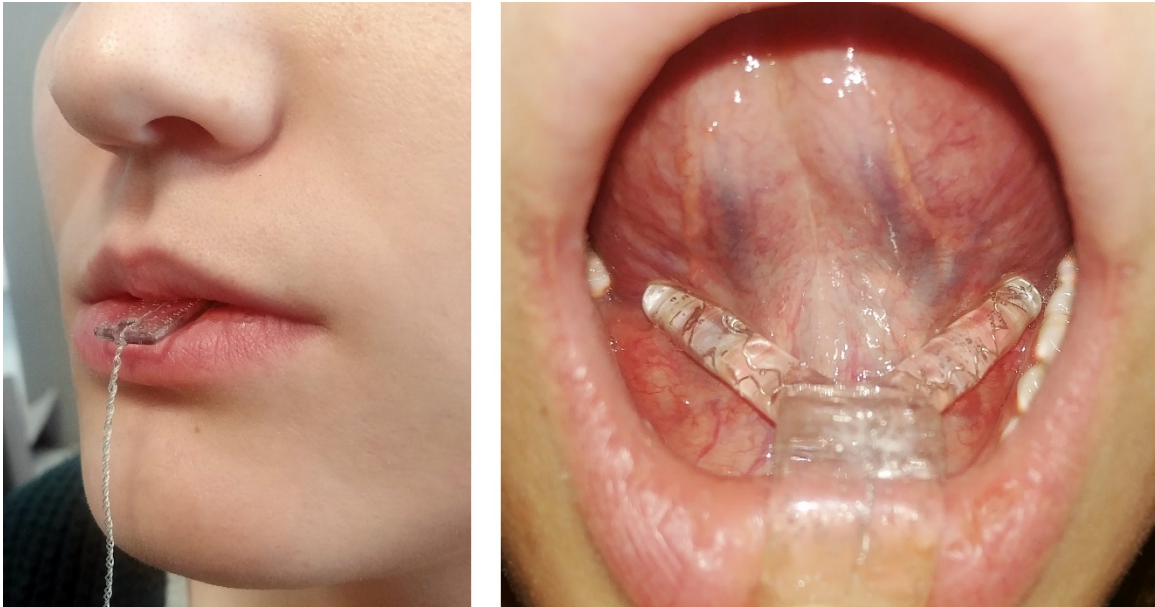


Figure 2.3 Subject places the two arms of the silicone piece under the tongue (Right) while slightly biting on the flat part (Left). The exposed ends of the stainless-steel wires were pressing against the GG muscles on each side of tongue.

The same electrode assembly was used in all participants after cleaning and sterilizing with alcohol, and they did not report any discomfort during data collection. A disposable ECG electrode was attached either on the clavicle or the temporal bone behind the ear as the ground lead for all EMG recording channels.

2.2.2 Masseter and Mylohyoid Muscle EMG Recordings

Two pairs of disposable EMG surface electrodes (Ag/AgCl pad is 10mm in diam.) were placed between the zygomatic and mandibular bones, and on the submandibular area to collect MS and MH muscle activities, respectively. One of the electrodes of the submandibular pair was located about 1 cm from the chin in the middle of the submandibular triangle and the second one about 2 cm away from the first electrode

toward the hyoid bone. This electrode configuration may not completely exclude EMG activity from the anterior digastric muscle, however, maximizes the signal pick-up from the MH muscles being in the middle.

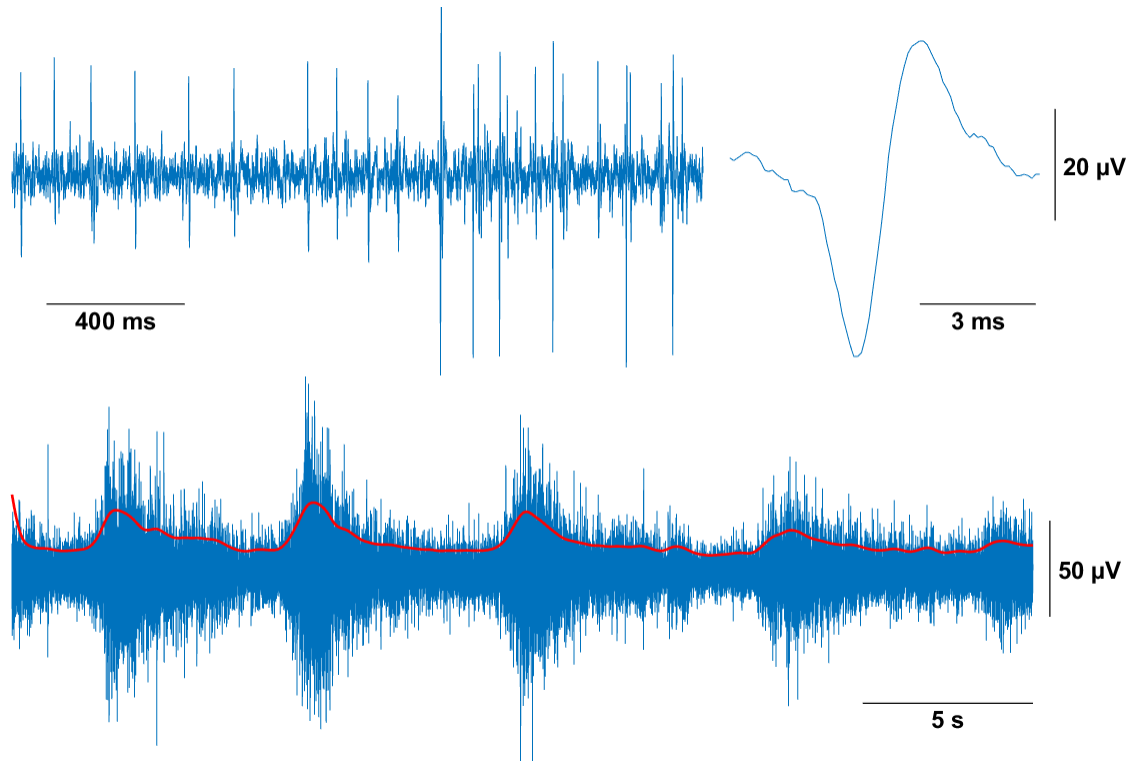


Figure 2.4 Samples of genioglossus EMG recorded with the sublingual electrode. Bottom: 30 s recording during deep breathing with EMG bursts occurring during inhalation. The red trace is the EMG envelope. Top-Left: Single spikes in GG EMG at a shorter time scale. Top-Right: A single EMG spike from the same data.

2.2.3 Mandibular Vibrations

A reciprocating saw (Figure 2.5, Milwaukee M12 Reciprocating Saw) mechanism was utilized to apply vertical movements on the mandible (Figure 2.6). The linear movement of the saw was transferred to the mandible via an oil-filled tubing terminated with a plastic syringe at the end. Subjects were asked to bite passively on the plunger head and the flange extender against the pressure without applying a large force (<5N, Figure 2.6).

Two accelerometers (ADXL335 Triple Axis Accelerometer, Analog Devices) were attached on the syringe for measurements of the plunger and the barrel displacements separately. A pressure transducer (DPT-100, DELTRAN®) was added to the hydraulic system for measurements of the oil pressure and thus the force applied by the jaw during stimulation. Minimum inter-incisal separation was fixed at 20 mm and the linear movements of the saw was adjusted to produce 5 mm vertical displacements of the lower jaw, at 8 or 12 cycles per second (Hz).

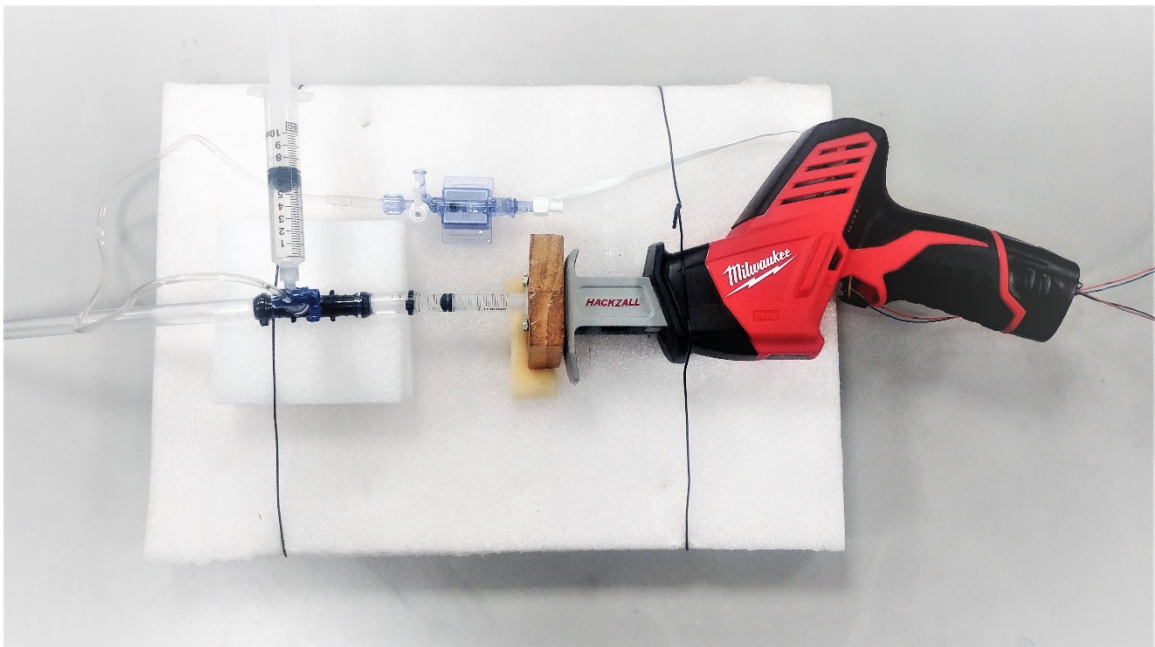


Figure 2.5 Linear movement was generated by a battery powered reciprocating saw (Milwaukee M12 Reciprocating Saw) and transferred to the mandible via an oil filled Tygon® tubing. A pressure transducer (DPT-100, DELTRAN®) was added to the hydraulic system for measurements of the force applied by the jaw.

2.2.4 Stimulation Protocol

Subjects remained seated on a massage chair with their back straight up and the head was on the headrest during the entire experiment. The sublingual EMG electrode was tested first by asking the subject to perform several simple tasks such as taking a deep breath,

tongue protrusion, etc. that would produce a large activity in the GG muscle and allow us to assess the EMG recording quality. Subjects stayed relaxed while several episodes of the baseline GG activity were recorded. These baseline activity levels were monitored by an algorithm running in the background to ensure that the GG is not activated by the subject volitionally before the application of mechanical vibrations. The length of the stimulation trial was set to 3 s and 20 trials were performed at each stimulation frequency (8 and 12 Hz). While the subject remained relaxed, the experimenter initiated the stimulation algorithm that applied mechanical vibrations at two different frequencies in a random order for a total of 40 trials while ensuring a 3 s steady GG baseline before each trial.

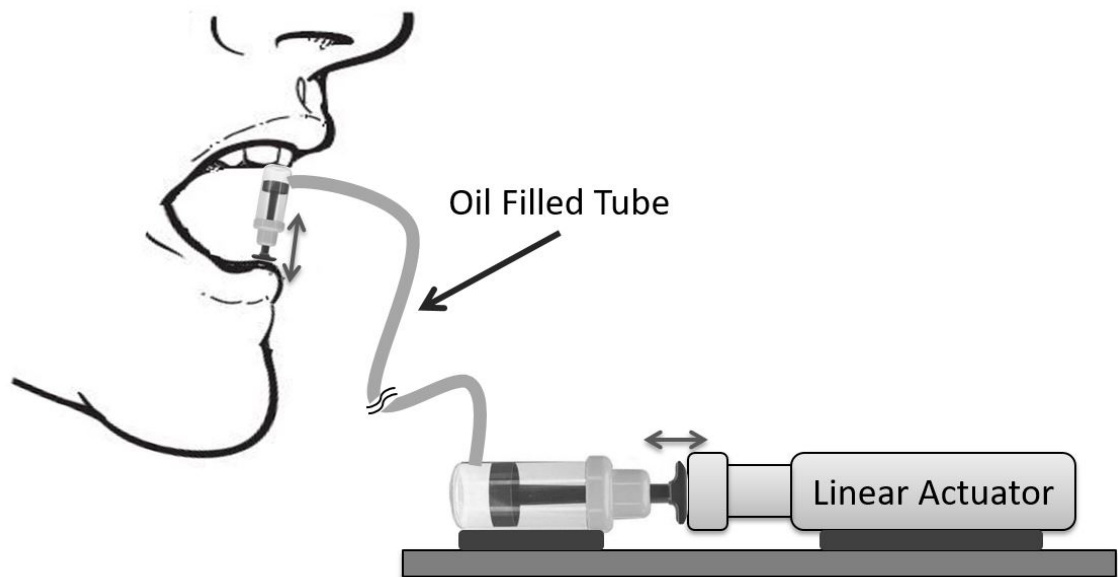


Figure 2.6 Mandibular vibration setup: Linear movement generated by using a reciprocating mechanism is transferred to the mandible via an oil filled Tygon® tubing.

2.2.5 Signal Processing

EMG signals from all three muscles were recorded at 10 kHz sampling rate and passed through an analog band-pass filter (30-1000 Hz, 2nd order Butterworth for each corner) and a 60 Hz notch filter. The EMG signals were then digitally high-pass filtered (60 Hz, 6th order Butterworth) in MATLAB to remove the low frequency motion artifacts caused by the chin movements. The signals were filtered twice, back and forth, using *filtfilt* function in MATLAB in order to avoid introducing phase delays during filtering. The EMG signals were full-wave rectified and low-pass filtered at 2 Hz (4th order Butterworth) to obtain the EMG envelopes. We also computed a second EMG envelope, low-pass filtered at a higher cut-off frequency (20 Hz, 4th order Butterworth) in order to keep the signal components at the mechanical stimulation frequency (8 or 12 Hz).

A coherence between rectified-only EMG signals (without low-pass) and the mandibular displacement signal at the frequency of mechanical stimulation indicated the presence of phasic components. That is, if there were any EMG components increasing and decreasing in synch with the mechanical stimulus, taking the absolute value of the EMG signals (rectifying) brings these high frequency EMG spikes down to the mechanical vibration frequency, and thus allowing detection by coherence. Note that all the low-frequency EMG content due to mechanical or electrical interferences had already been filtered out with 60 Hz high-pass before rectifying and thereby eliminating the possibility of false detections in the coherence plot.

Eight subjects were recruited for this experiment, however, the MS and MH recordings from subject M8 were excluded from analysis due to technical difficulties during data collection.

2.3 Results

To demonstrate the effect of mandibular vibrations on GG, MS and MH, we calculated the spectral power of EMG signals (60-1000 Hz) and compared the total activity before and during each stimulation. The bar plots in Figure 2.7 show the average percent increases in each muscle for each subject.

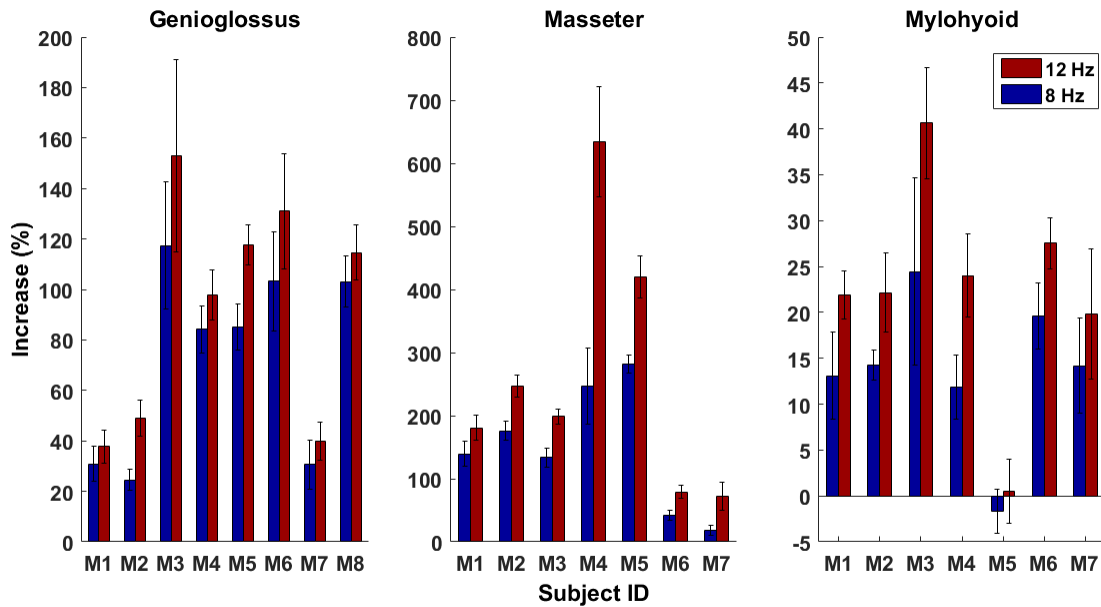


Figure 2.7 Percent increases in EMG signal power for GG, MS, and MH muscles above the baseline in the mandibular vibration test (mean \pm SE).

The GG, MS and MH activities during stimulation were significantly higher compared to the baseline (Wilcoxon signed rank test; GG: $p=0.0078$ for both stimulation frequencies, $N=8$; MS and MH: $p=0.0156$ for both frequencies, $N=7$; adjusted $\alpha=0.0167$). For an equitable comparison between stimulation frequencies, we calculated the EMG power as the root-mean-square (rms) value of signal during the first 60 ms of each vibration cycle, as indicated in Figure 2.8 with horizontal dash lines. According to this analysis, muscle activities increased more during 12 Hz stimulation

compared to that of 8 Hz stimulation (Wilcoxon signed rank test; $p=0.0078$ for GG, $N=8$; $p=0.0156$ for MS and MH, $N=7$; adjusted $\alpha=0.0167$).

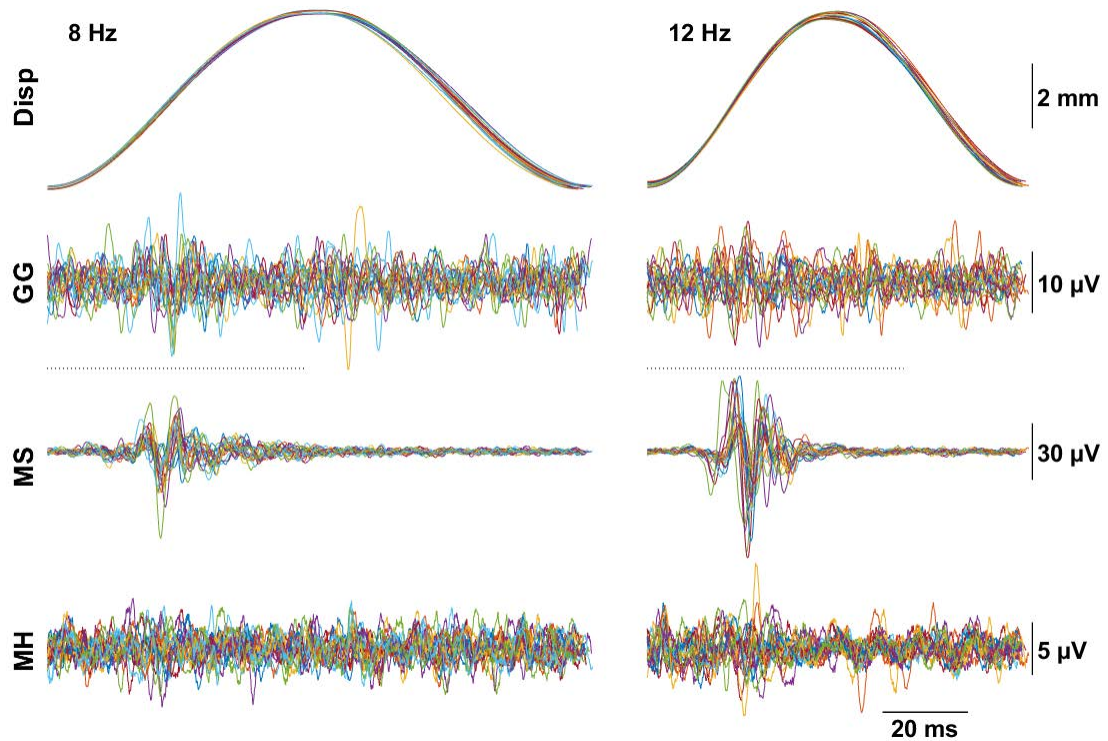


Figure 2.8 Stimulus-triggered averages of GG, MS and MH EMG over multiple cycles of displacement from subject M5 at 8 Hz (left) and 12 Hz (right) during twenty trials of 3 s duration. Trials are color coded. Top traces show the displacements averaged across all cycles. Horizontal dash lines: 60 ms.

Typical muscle responses are plotted along with their envelopes in Figure 2.9 from subject M5 during 12 Hz stimulation. The phasic activity synchronized with the vibration cycles is visible in the figure for all three muscles. Coherence plot between rectified EMG signals and the displacement (Figure 2.10) demonstrates the correlations as a function of frequency up to 40 Hz. The peaks at the stimulation frequency (12 Hz) and its harmonics are seen in all three muscles. The bar plots in Figure 2.11 show that the average coherence at stimulation frequency was significantly higher during 12 Hz stimulation compared to that of 8 Hz stimulation for MH, but the differences were not

significant for GG and MS (Wilcoxon signed rank test; $p=0.31$ for GG, $N=8$; $p=0.30$ for MS and $p=0.016$ MH, $N=7$).

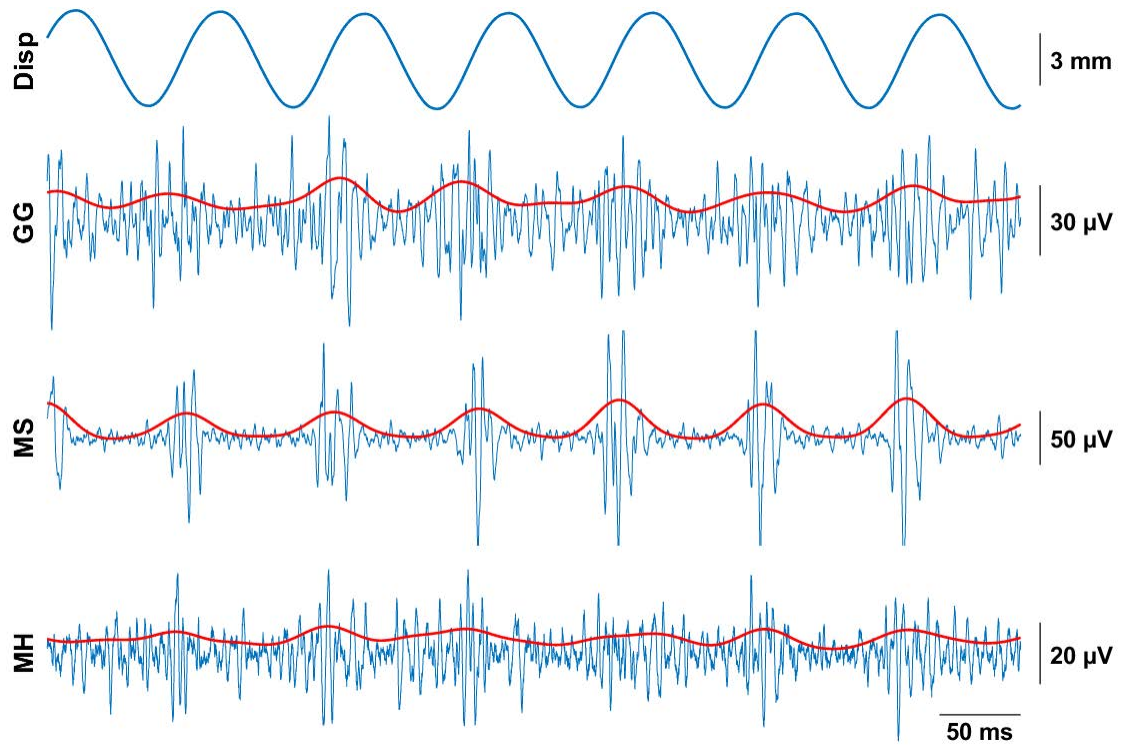


Figure 2.9 A sample episode from subject M5 during 12 Hz stimulation. Top trace is the displacement of the mandible calculated from the accelerometer. Red lines are the full-wave rectified and low pass filtered (20 Hz) envelopes of the EMG signals.

To reveal the shape of phase-locked multi-unit responses, high-pass filtered EMG signals were stimulus-trigger averaged over multiple cycles of the stimulus (36 cycles at 12 Hz) from subject M5 and plotted in Figure 2.8. The plots indicate that the MS response is highly synchronized with the stimulus, whereas the timing of the GG and MH responses greater variability within the stimulus cycle.

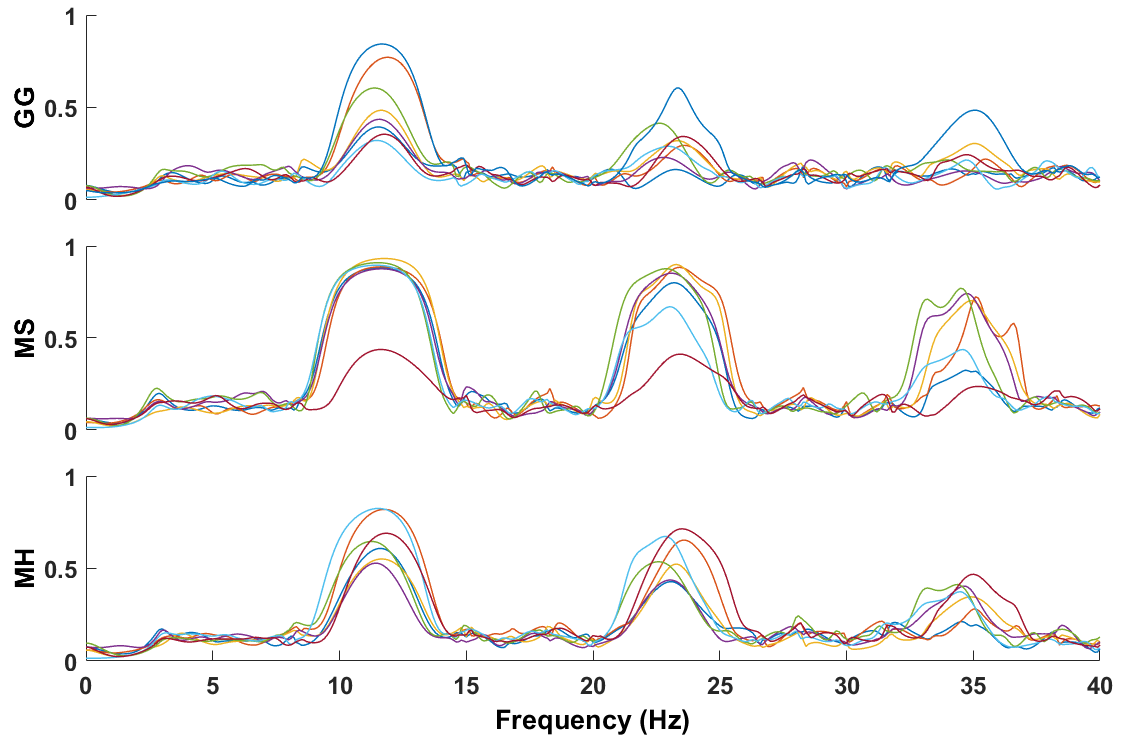


Figure 2.10 Average coherence between rectified EMGs and the mandibular displacements in all trials for each subject, encoded by the trace color. High coherences occur at the vibrational frequency and its harmonics.

2.4 Discussion

Our results demonstrated the presence of phasic activity locked to the vibration cycle not only in the MS in agreement with earlier publications (Jean Edouard Desmedt & Emile Godaux, 1975; Karl Erik Hagbarth et al., 1976), but also in the GG and MH. A significant level of inter-subject variation was observed in the EMG responses to mechanical stimuli. An important factor was the level of volitional components in the recorded muscle signals. Subjects might have volitionally suppressed the muscular activities because they were asked to relax their tongue and the UAW muscles. In these mandibular stimulation experiments, the size of the lower jaw and the maximal inter-incisal opening by volition may have introduced variability among the subjects. The

EMG signals from the MH might have been attenuated by the adipose tissue under the chin, which is supported by the fact that the MH baseline and the increase in subject M5, who happened to be the oldest male in the group with a thick submandibular skin, was almost absent.

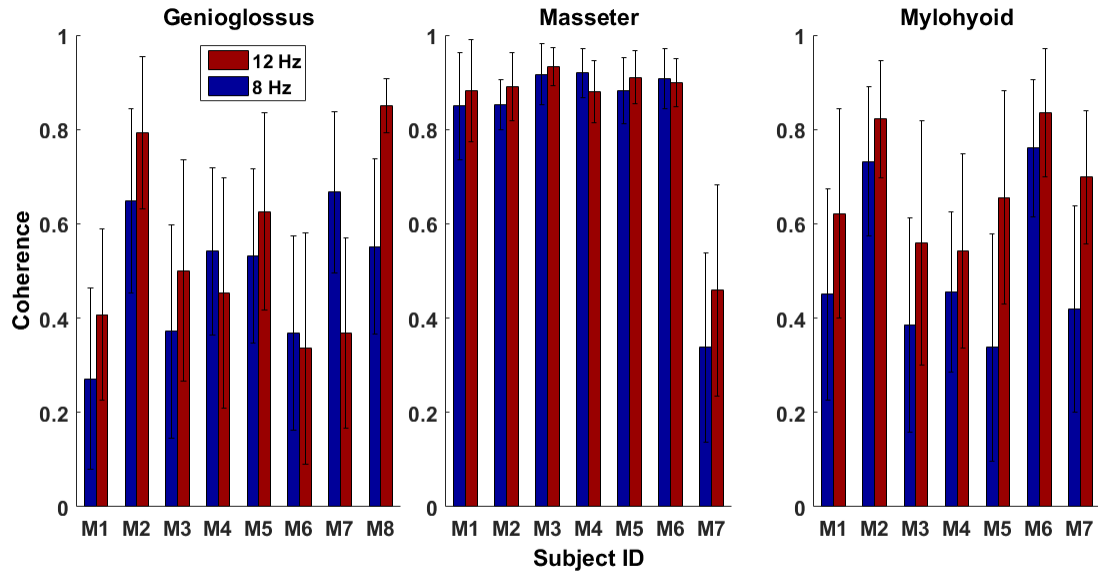


Figure 2.11 Average coherences between rectified EMGs and mandibular displacements at the fundamental frequency (8 Hz or 12 Hz) in all subjects (mean \pm SD).

It was important to confirm that the changes in EMG activity that we recorded were the neurological responses to the mechanical stimulation and not a function of changes in posture or other electrical artifacts. Hence, we mechanically secured and isolated the electrodes and cables against vibrations up to the point they terminate at the amplifier. We also high-pass filtered the EMG signals at 60 Hz to remove possible motion artifact due to the mechanical vibrations, where the stimulation frequency is around 8-12 Hz. We carefully examined the recorded signals in the time and frequency domain from each subject individually to increase the confidence level.

CHAPTER 3

GENIOGLOSSUS RESPONSE TO SUB-MANDIBULAR MECHANICAL STIMULATIONS IN WAKEFULNESS

The extrinsic tongue muscles are activated in coordination with pharyngeal muscles to keep a patent airway during respiration in wakefulness and sleep. The activity of genioglossus (GG), the primary tongue-protruding muscle playing an important role in this coordination, is known to be modulated by several reflex pathways mediated through the mechanoreceptors of the upper airways (UAWs). Our main objective is to investigate the effectiveness of activating these reflex pathways with mechanical stimulations for the long-term goal of improving the UAW patency during disordered breathing in sleep.

Ten healthy individuals were recruited to examine the GG response during sub-mandibular mechanical stimulations. We recorded the GG activity using a custom-made sublingual EMG electrode molded out of silicone. We applied mechanical vibrations at three different stimulation intensities (0.2-0.9 mm, 21-33 Hz) to the sub-mandibular muscles while the subjects laying in a supine position. The percent increases in GG EMG signal due to mechanical stimulations were quantified. In this sub-mandibular mechanical stimulation experiment, the GG activity increased significantly compared to the baseline ($p=0.026$) in nine out of ten subjects. The elevated GG activity persisted after termination of the stimulus for a few seconds. The major finding of this study is that the GG reflexively responds to the mechanical vibrations applied to the sub-mandibular skin surface in healthy subjects during wakefulness. The lack of phasic components with sub-mandibular stimulations indicates a more complex mechanism rather than a simple stretch reflex through GG muscle spindles.

3.1 Background Information

The oral and pharyngeal regions are well integrated functionally and involved in many complex motor responses including respiration, swallowing and speech. Many sensory receptors that innervate these two regions affect the extrinsic and intrinsic muscles of the tongue and continuously regulate the patency of the airway. Furthermore, activation of only the protruding tongue muscles does dilate the airway but has small effect on collapsibility during sleep. However, co-activation of both protruding and retracting tongue muscles does not dilate the airway but decreases the airway collapsibility (DD Fuller, JS Williams, PL Janssen, & RF Fregosi, 1999). Thus, activating the UAW muscles synergistically has higher potential to improve the UAW patency rather than activating only the dilator muscles by electrical stimulation of the hypoglossal nerve.

3.1.1 Pressure Oscillation

As shown in animal and human studies, UAWs contain mechano-receptors that are sensitive to low pressure, high frequency oscillations (Peter R Eastwood et al., 1999; KATHE G Henke & COLIN E Sullivan, 1993). These mechano-receptors must be afferents to a short reflex pathway that innervate the UAW muscles since pressure oscillations (< 1cm H₂O, 30 Hz) induce a strong response in the GG, sternomastoid and diaphragm electromyogram activities in normal and obstructive sleep apnea (OSA) subjects during sleep (KATHE G Henke & COLIN E Sullivan, 1993). Topical anesthesia applied to the UAW eliminates the evoked EMG responses by pressure oscillations, which suggests that the mechanoreceptors involved are located beneath the mucosal surface (Peter R Eastwood et al., 1999). In another study, application of a negative constant pressure (25 cmH₂O) to airways also evoked a strong GG muscle activity in

wakefulness and, although to a lesser degree, in sleep as well (RL Horner, JA Innes, MJ Morrell, SA Shea, & A Guz, 1994).

3.1.2 Tonic Vibration Reflex (TVR)

Research since early 1900s has shown that the muscle stretch receptors are highly sensitive to mechanical vibration (DAVID Burke, KARL-ERIK Hagbarth, L Löfstedt, & B Gunnar Wallin, 1976a, 1976b; Jean Edouard Desmedt & Emile Godaux, 1975; Francis Echlin & Alfred Fessard, 1938; Karl Erik Hagbarth et al., 1976). Primary afferent endings of the muscle spindles have been demonstrated to be the basis of this vibration sensitivity with single fiber recordings (Stephen W Kuffler, Carleton C Hunt, & Juan P Quilliam, 1951). Primary spindle endings can generate action potentials synchronized with each cycle of the vibration at frequencies as high as 220 Hz (DAVID Burke et al., 1976b). This report further showed that the secondary spindle endings and Golgi tendon organs also respond to the mechanical vibrations and they can follow lower frequencies of vibration compared to the primary endings. For instance, the tonic vibration reflex (TVR) can be elicited in the MS, a jaw elevator muscle, where the phase-locking effect to the vibrations becomes stronger with decreasing distances in the conduction path of the proprioceptive reflex arc (Karl Erik Hagbarth et al., 1976). However, the TVR or the stretch reflex was not present in the extrinsic and intrinsic tongue and lip muscles either with application of mechanical vibration or stretching of the tongue (Göran Eklund & K-E Hagbarth, 1966; Peter D Neilson, Gavin Andrews, Barry E Guitar, & Peter T Quinn, 1979).

Our primary hypothesis is that the GG and other muscles that are involved in dilation of the UAWs can be activated synergistically, as it happens naturally during deep

breathing, by mechanical stimulation of the UAW muscles. Thus, we set out to demonstrate one of these reflexes in healthy subjects during wakefulness as an initial attempt. As a step toward this goal, the present study was designed to examine the response of the GG muscle during sub-mandibular mechanical stimulations. The main objective was to demonstrate that mechanical perturbations of the muscles under the mandible can produce a reflex-like response in the GG, an extrinsic tongue muscle that is responsible for protrusion of the tongue and thereby playing an important role for patency of the UAWs during sleep. Furthermore, understanding of the reflexes that can affect the GG activity has the potential to provide insights into maintenance of the UAW patency. Our results indeed show that the GG response can be elicited by mechanical vibrations applied to the muscles in the submandibular region.

3.2 Experimental Methodology

Ten healthy adult subjects were recruited in this study and subject statistics are summarized in Table 3.1. The experimental procedures were approved in advance by the institutional review board of New Jersey Institute of Technology and subjects gave their written informed consent prior to data collection.

3.2.1 Sublingual Electrode for GG EMG

The genioglossus activity was collected differentially with a sublingual surface electrode. The drawings in Figure 2.1 show a silicone (PDMS) mold made to hold the EMG wire electrodes against the genioglossus muscle inside the mouth. A pair of PFA insulated stainless steel wires (50 μm bare diam., #790700, A-M Systems) were inserted into the silicone mold. The ends of the wires were desheathed and inserted back into the silicone

with a 5 mm distance from the origin. See Chapter 2 for detailed information about sublingual GG electrode and recording.

Table 3.1 Statistical Data of the Subjects in Sub-Mandibular Vibration Experiment

Subject ID	Age	Sex	Weight (kg)	Height (cm)	BMI	ST (mm)
S1	30	M	101	184	29.83	9.5
S2	27	M	78	175	25.46	11.5
S3	26	F	67	163	25.21	10
S4	33	M	106	180	32.71	13
S5	28	M	60	167	21.51	5.5
S6	31	F	63	160	24.60	9
S7	27	F	60	156	24.65	10
S8	27	M	86	172	29.06	8
S9	34	M	87	172	29.40	12.5
S10	31	F	56	160	21.87	8

ST: submandibular skin thickness.

3.2.2 Sub-Mandibular Mechanical Stimulations

In ten healthy adult subjects (Table 3.1), mechanical vibrations were applied to the sub-mandibular area in wakefulness while the subjects lied on a massage bed in a supine position. A 24 mm DC motor with eccentric rotor (Figure 3.1: Left, JQ24-35F580C Cylindrical Vibration Motor, Jinlong Machinery & Electronics) was attached to the submandibular area with a chin strap (Figure 3.2). The displacement and frequency of the stimulations were monitored and recorded with an acceleration sensor (ADXL335) attached to the motor (Figure 3.1: Left). The rotation of the eccentric mass on the motor was secured by covering the motor with a 3D printed case, which also has a slot for attaching the acceleration sensor (Figure 3.1: Right).

The tension in the chin strap was measured with a hanging scale and adjusted to 500-600 g to standardize how firmly the motor is pressing against the submandibular

muscles across the subjects. The thickness of the skin and the underlying tissue (ST in Table 3.1) in the submandibular area was measured by pulling the skin away from the mandible manually and placing it between the jaws of a digital caliper that were coated with silicone rubber for softness. Thus, the skin thickness (ST) values in Table 3.1 represent two layers of skin and subdermal tissue.

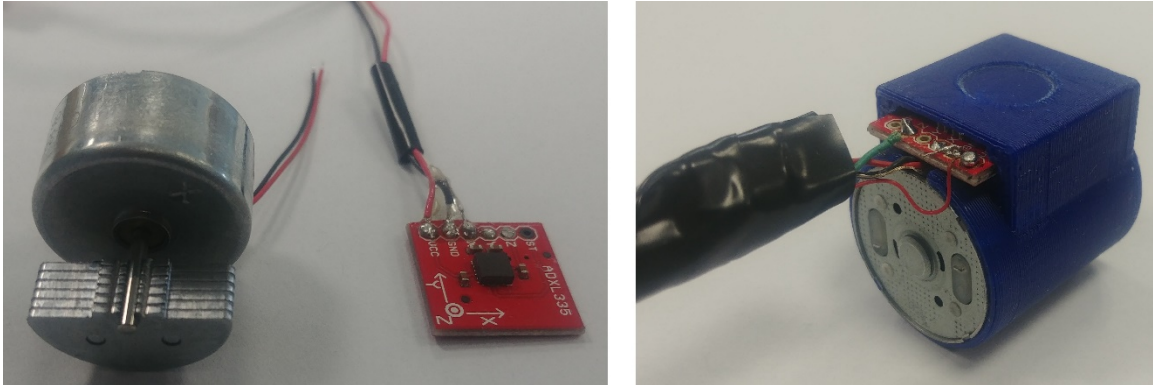


Figure 3.1 Left: A 24 mm DC motor with eccentric rotor (JQ24-35F580C Cylindrical Vibration Motor, Jinlong Machinery & Electronics) for the application of mechanical vibrations, and the acceleration sensor (ADXL335 Triple Axis Accelerometer, Analog Devices) for recording and monitoring the displacement and frequency of the stimulations. Right: 3D printed case for covering the eccentric mass of the motor and attaching the acceleration sensor to the motor.

In this set of experiments, the EMG activity was recorded only from the GG muscle due to contamination of mechanical artifacts into the MS and MH EMGs that we were not able to remove completely. Similar to the mandibular vibration experiment in Chapter 2, the GG EMG was collected differentially using the sublingual surface electrode.

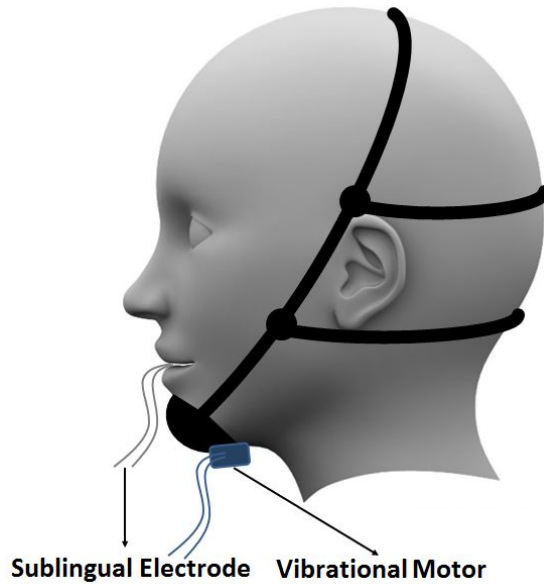


Figure 3.2 Application of mechanical vibrations generated by an eccentric-load DC motor to the submandibular area using a chin strap.

3.2.3 Stimulation Protocol

Subjects were asked to lie on the massage bed in a supine position. Experiments started with testing of the sublingual electrode and the EMG signal quality by asking subjects to perform several volitional tongue movements and deep breathing. A steady baseline activity for the stimulation algorithm was determined in each subject as explained in the first set of experiments. A total of 60 stimulation trials with three different intensities were applied in a random order by supplying 3, 4.5 and 6 V to the DC motor through the computer immediately after detecting a 3 s steady baseline. The high-pass (100 Hz, 6th order Butterworth) filtered GG signal was then full-wave rectified and low-pass filtered at 2 Hz (4th order Butterworth) to obtain the EMG envelope. The spectral power of the GG activity was calculated before and during each stimulation and compared to quantify the stimulus effect. The frequency range of the mechanical stimulations (20-35 Hz) was excluded from the spectral power by summing the FFT coefficients from 100 to 1000 Hz.

To suppress the electrical noise of the motor, the FFT components at the harmonics of the vibrational frequency were also excluded from power calculations.

3.3 Results

For the same motor voltage, the vibration frequencies were similar among the subjects, however the displacement varied (Figure 3.3), most likely due to differences in the volume and thickness of the submandibular tissue where the mechanical stimulations were applied (see skin thicknesses-ST in Table 3.1).

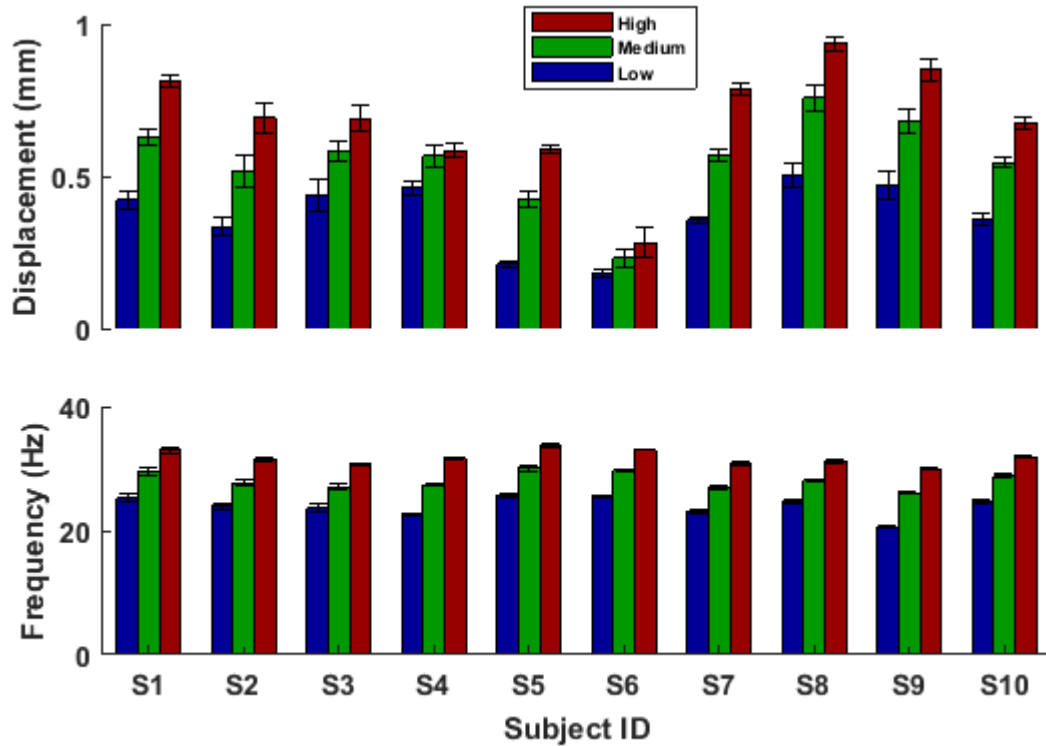


Figure 3.3 Measured Frequencies and Displacements (Mean \pm SD) in Each Subject at Three Different Voltages (Low, Medium, and High) Used to Drive the DC Motor During the Sub-Mandibular Stimulations.

In most of the trials in nine of the ten subjects, GG activity increased with the mechanical stimulation strength applied to submandibular area, as illustrated in Figure 3.4 with a typical response from subject S3. The percent increases were calculated with respect to the baseline in each trial and shown as a bar plot for each subject (Figure 3.5).

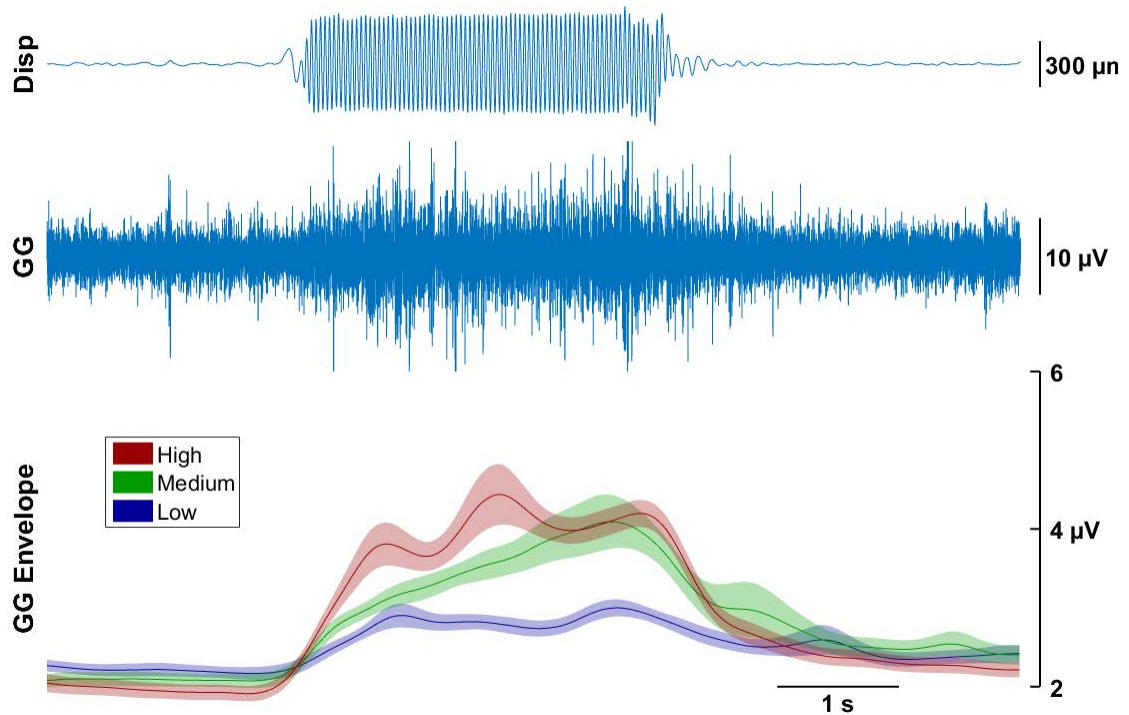


Figure 3.4 Rectified-filtered GG activity at three different levels of submandibular mechanical stimulation in subject S3 showing the persistence of activity after the stimulation is terminated. Top traces: the mandibular displacement (Disp) and the raw GG activity. Bottom: The EMG envelopes are plotted as the mean (N=17-19 for each trace) and standard error (SE, shaded areas).

According to the results from 10 subjects, there was a statistically significant difference between the stimulation levels and the baseline (repeated ANOVA, Greenhouse-Geiser corrected p value = 0.026). The increases in GG activity were statistically significant for each stimulation intensity compared to the baseline (Wilcoxon signed rank test, $p < 0.002$ for all three stimulation levels, adjusted $\alpha = 0.008$).

Furthermore, the responses at Level 2 and 3 were significantly higher compared to the response at Level 1 (Wilcoxon signed rank test, $p=0.002$, $p=0.004$, respectively, adjusted $\alpha=0.0083$), but the difference was not significant between Level 2 and 3 ($p=0.065$).

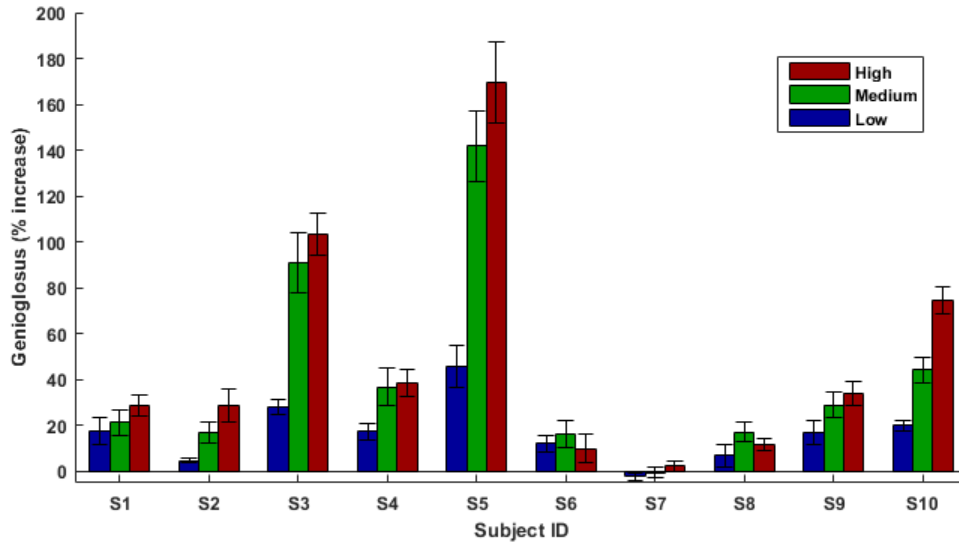


Figure 3.5 Percent increases in GG signal power during sub-mandibular vibrations (mean \pm SE).

Pearson correlations were calculated between average GG EMG increases and both BMI and ST values across the subjects. Correlations were not significant ($r = -0.46$, $p=0.17$ for BMI and $r = -0.53$, $p=0.11$ for ST). The ST, on the other hand, was correlated positively with the BMI ($r = 0.68$, $p=0.029$). We also observed a post-stimulus persistence of the GG activity in most trials as demonstrated with stimulus-triggered averages of the GG envelopes (Figure 3.4: Bottom). The mean duration was 1.94 ± 1.08 s ($N=8$). The post-stimulus persistence was not analyzed for subject S6, who showed no response to the stimulations, and subject S7, who had a high and variable baseline activity. We defined the post-stimulus activity duration from the stimulus offset to where the evoked activity fell below one standard deviation around the baseline mean (Figure

3.6). In contrast to mandibular stimulation, a phasic EMG response to the vibration cycle was not observed in any one of the subjects.

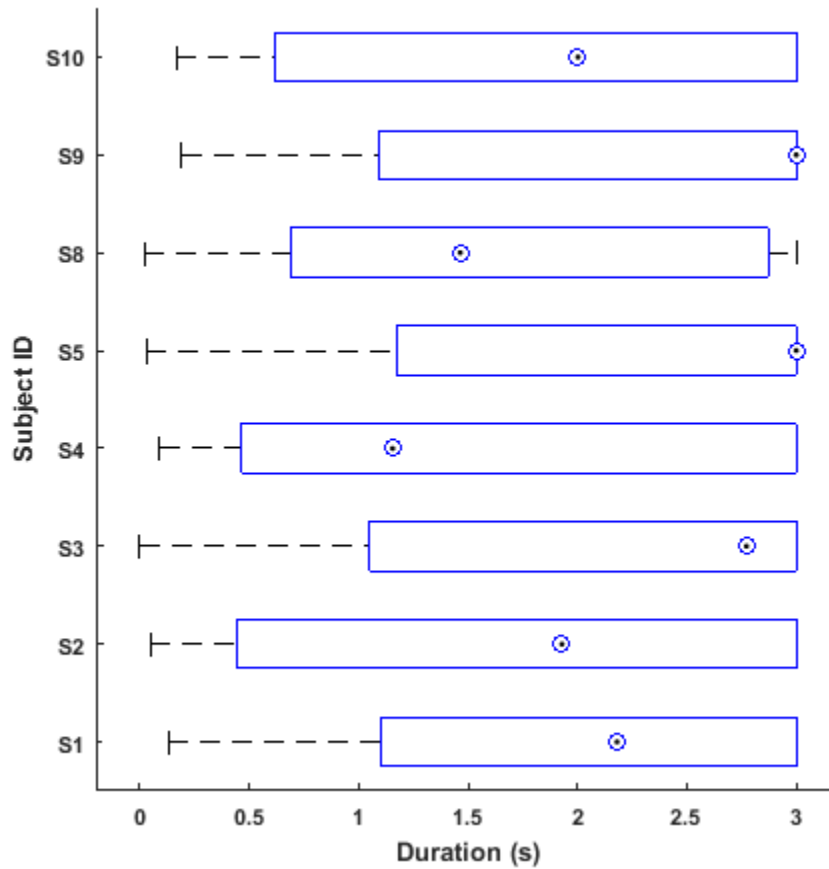


Figure 3.6 Box-plot for post-stimulus EMG persistence times, calculated as the duration from the stimulus offset point to where the evoked activity fell below one standard deviation around the baseline mean. Maximum measurable delay was limited by 3 s, because the recordings were stopped 3 s after stimulations. Subjects S6 and S7 were excluded (see Methods).

3.4 Discussion

In this experiment, the EMG signals did not have a detectable phasic component similar to a tonic vibratory reflex as demonstrated in several skeletal muscles in humans. The absence of phasic activity is consistent with the published work where the reports agreed upon that the GG does not have a stretch reflex (Göran Eklund & K-E Hagbarth, 1966;

Peter D Neilson et al., 1979). Therefore, we conclude that the GG response to the mechanical vibrations must be mediated not through the GG's own muscle spindles but most likely via an indirect reflex pathway involving other UAW afferents, potentially the spindles of other pharyngeal muscles or the mechanoreceptors of the UAW mucosal membrane. The elongation of the elevated GG activity after termination of the stimulus is also an indication that the GG response is given rise by an increased population activity in a group of neurons, rather than a simple reflex pathway.

We observed a significant level of between subject variation in the GG EMG responses to sub-mandibular stimulations. The most important factor is the level of volitional components in the recorded GG activity. The response to mechanical vibrations might have volitionally suppressed by subjects because they were asked to relax their tongue during experiment. Some of the variability can also be explained by the skin and subcutaneous tissue thickness, although a strong correlation with percent EMG increases was not found. The subcutaneous adipose tissue may dampen the strength of mechanical stimulations before reaching the underlying UAW and extrinsic tongue muscles.

In subject S5, who had the smallest submandibular skin thickness, the GG response to sub-mandibular mechanical stimulation was several times higher than some others. Both experimental setups were tested on this particular subject many times during system development. Thus, we conjecture that this subject might have developed a sensitivity to sub-mandibular mechanical stimulations over the course of multiple applications. If the GG muscle can be trained to respond more strongly by repeated applications of mechanical stimuli, this may in fact be useful treatment option for

improving the UAW patency. Whether the elevated levels of GG response can be maintained during sleep is a question that warrants further research.

The experimental setup was carefully designed to ensure that the recorded signals were of neuromuscular origin and not due to changes in subjects' posture or an electrical contamination from the DC motor. The EMG electrodes and input cables were mechanically secured against vibrations and electrically isolated from electromagnetic sources up to the point they terminate at the amplifier. The EMG signals were also high-pass filtered with sharp filters to remove possible motion artifacts. The sixth harmonic of the DC motor's vibrational frequency and its multiples were observed in the EMG signals with small amplitudes, most probably generated by the switching currents at the motor brushes. These electromagnetic interferences were eliminated from EMG power calculations, even though the noise power was much smaller than the muscle signals. The recorded signals were carefully examined in the time and frequency domain from each subject individually to increase the confidence level in the source of signals and eliminate any source of electrical or mechanical artifacts.

Here in this study, we developed a surface EMG electrode for the GG by embedding stainless steel wires in an electrode carrier that was molded from silicone as an alternative to recording with intramuscularly by inserting needle electrodes into the muscle. With the help of this non-invasive recording technique, we performed the experiments without needing a medical doctor during experiments or without any pain or fear reported from the subjects which is common during intramuscular recording with needle insertions.

CHAPTER 4

SUBMANDIBULAR MECHANICAL STIMULATIONS IN OSA PATIENTS

The effects of mechanical vibrations applied on the submandibular region were investigated in six severe obstructive sleep apnea (OSA) patients ($AHI=51.5\pm 11.8$). Genioglossal (GG) activity was recorded with transorally implanted fine wires along with standard polysomnography data. The mechanical vibrations were turned on manually upon observation of obstructions and remained on until breathing was resumed.

The GG activity increased following the stimulus onset, the apnea was terminated, and the minimum levels of the blood SpO₂ was raised during the stimulated cycles of obstructions compared to spontaneously terminated apneas. The response time to mechanical vibrations varied from 2.25 ± 0.72 s in one subject to more than 10 s in some others. The EEG alpha power increased at the time of apnea terminations both in stimulated and non-stimulated cycles. In two patients, the micro arousals (i.e. alpha power increase) were statistically smaller in stimulated apnea cycles compared to the spontaneously terminated apneas. When individual apnea cycles were inspected, however, there were many stimulated episodes in each patient where the micro arousals were smaller than the spontaneous ones.

These results argue favorably that a submandibular mechanical vibration device may improve blood deoxygenation by terminating the obstructive episodes earlier than they are due, but with smaller micro arousals. The increase in the activity of the upper airway muscles, such as the GG, is proposed as the mechanism for apnea terminations. A

longitudinal study is warranted to investigate if a lesser degree of sleep fragmentation may be achieved through habituation to mechanical vibrations.

4.1 Background Information

4.1.1 Obstructive Sleep Apnea (OSA)

Obstructive sleep apnea (OSA) is characterized by repetitive complete or partial occlusion of upper airways (UAWs) resulting in frequent arousals during sleep. In general, it is believed that the problem emerges primarily due to anatomical factors that pre-dispose the UAWs for obstruction. Several sleep studies have shown that the UAW of the patients with OSA is anatomically small compared to the control subjects, and it makes the airways more collapsible (Richard J. Schwab, Warren B. Gefter, Eric A. Hoffman, Krishanu B. Gupta, & Allan I. Pack, 1993).

Excess weight and obesity is the major risk factor for OSA and the majority of the patients with OSA are overweight or obese (Helen Bearpark et al., 1995; Eyal Shahar et al., 2001). Obesity and excess weight leads to storing soft adipose tissue around the UAWs which makes it more vulnerable to collapse (Dorit Koren, Magdalena Dumin, & David Gozal, 2016). Another cause of OSA is anatomical factors such as enlarged tonsil or tongue that makes UAWs narrower and leads to increased airway collapsibility (Surendra K Sharma et al., 2015).

The elevated neural outflow to the UAW muscles dilates the airways and compensate for the disadvantaged anatomical factors in wakefulness (Robert B Fogel et al., 2001). However, these neural compensatory mechanisms are lost at the alpha-to-theta transition in NREM sleep, thereby leading to occlusions of the anatomically

compromised UAWs (Robert B Fogel et al., 2003). Consequently, the treatment attempts for OSA have focused on both restoring the lost UAW dilating muscle activity via electrical stimulation, and also mechanical devices that can help the UAWs become less collapsible under negative pressure.

Obstructive sleep apnea is the most common sleep disorder and the prevalence of clinically significant OSA is estimated to be 3-7% for adult in general population (Naresh M Punjabi, 2008). The prevalence is greater in men than in woman and the estimates show that the male/female ratio varying between 2:1 and 4:1 (Carl J Stepnowsky Jr, William C Orr, & Terence M Davidson, 2004). The prevalence of mild to severe OSA ($AHI \geq 5$) increased from %26.4 to 33.9 for men and from %13.2 to 17.4 for women during 1994 to 2010 (Paul E Peppard et al., 2013).

Patients with OSA suffer from poor sleep quality associated with increased daytime sleepiness, depression, reduced quality of life and increased risk of motor vehicle accident. Furthermore, there are adverse cardiovascular consequences associated with three key pathological features of OSA: hypoxemia (low blood oxygen saturation), excessive negative intrathoracic pressure against the occluded airway and arousals from sleep which contributes to abrupt surges in heart rate and blood pressure (Richard ST Leung & T Douglas Bradley, 2001; Micha T Maeder, Otto D Schoch, & Hans Rickli, 2016).

4.1.2 Hypoglossal Nerve Stimulation

Hypoglossal nerve (HG) stimulation and that of its medial branch was proposed almost two decades ago as a method to remove UAW obstructions (David W Eisele, Philip L Smith, Daniel S Alam, & Alan R Schwartz, 1997; Alan R Schwartz et al., 1993). Closed-

loop stimulation of the HG nerve using its own activity as a feedback signal was demonstrated in a dog model of OSA (Mesut Sahin, DH Durand, & Musa A Haxhiu, 2000). Selective activation of the HG nerve with a multi-contact cuff electrode was proposed for generation of multiple modes of UAW dilation and thereby increasing the success rate by accounting for anatomical differences between subjects (Jingtao Huang, Mesut Sahin, & Dominique M Durand, 2005; Paul B Yoo, Mesut Sahin, & Dominique M Durand, 2004). Many years of collective data by several groups have lead the way to successful clinical trials in recent years. In multicenter clinical trials, HG stimulation using implantable electrodes have been shown to reduce the number of apnea-hypopnea episodes at the end of a 12-month study period (Eric J Kezirian et al., 2014; Patrick J Strollo Jr et al., 2014), with sustained improvements at 18 months in one of these trials, where the withdrawal group returned to the baseline (B Tucker Woodson et al., 2014).

HG nerve stimulation technique is an exciting development in the field as a treatment method of OSA, despite the fact that it is an invasive approach. However, non-invasive methods will continue to be searched as potential alternatives even if the benefits are marginal.

4.1.3 High Frequency Pressure Oscillation

An interesting finding in the field was that the mechano-receptors in the UAW mucosal membrane were shown to be very sensitive to pressure oscillations similar to those occur during snoring. The effect of high frequency pressure oscillations at 30Hz were studied in humans (KATHE G Henke & COLIN E Sullivan, 1993), and in experimental animals (Peter R Eastwood et al., 1999; LOUISE Plowman, DESMOND C Lauff, MICHAEL Berthon-Jones, & COLIN E Sullivan, 1990; SHAOPING Zhang & OOMMEN P

Mathew, 1992). In both cases it was confirmed that small amplitude pressure oscillations, even smaller than those observed during snoring ($\pm 1\text{cmH}_2\text{O}$, (KATHE G Henke & COLIN E Sullivan, 1993)), could evoke a strong activity in the upper airway muscles including the genioglossus (GG).

Henke and Sullivan reported that in almost half the trials the increase in GG activity accompanied a partial or complete reversal of obstructions in human subjects during both NREM and REM sleep. If the pressure amplitudes were higher (± 2 to $\pm 4\text{cmH}_2\text{O}$), the inspiratory cycle was terminated early or the expiratory cycle was extended depending on the timing of the pressure onset (Peter R Eastwood et al., 1999).

Eastwood et al. asserted that the mechanoreceptors stimulated by the pressure oscillations are close to the mucosal surface in the UAWs since the responses were eliminated by topical anesthesia. Single fiber recordings from the superior laryngeal nerve in anesthetized dogs confirmed that vast majority of the laryngeal mechanoreceptors were activated by high frequency oscillations ($\pm 2.5\text{ cmH}_2\text{O}$ at 10, 20, and 30Hz) applied to the UAWs (SHAOPING Zhang & OOMMEN P Mathew, 1992). Plowman et al. argued that oscillatory pressure waves, as they occur in snoring, produce reflex responses that help maintain upper airway patency during sleep. In most of the reports cited here, the GG response was primarily in the form of a tonic response, except that of Henke and Sullivan in OSA subjects where the phasic component was prominent, as seen in their figures.

There are also reports contradicting these findings regarding the effect of oscillatory pressures. Forced oscillation technique is a clinical tool that was developed for measurements of respiratory impedance in assessment of UAW mechanical properties

during sleep. Needless to say, the technique should not be altering the UAW muscle activity in order not to interfere with the measurements. A study conducted in moderate-to-severe OSA patients reported that the forced oscillations (1.0 cmH₂O peak-to-peak at 5 and 30Hz) did not elicit significant changes in the surface recorded GG activity during obstructive or flow limited episodes of stable sleep (JR Badia et al., 2001). They argued that the GG responses observed by Henke and Sullivan were accompanied by sleep arousals caused by the larger oscillation amplitudes they employed (± 1.0 cmH₂O, i.e. 2 cmH₂O peak-to-peak). They also commented that the patient group selected in their study might have had higher response thresholds due to obesity and not having had CPAP therapy prior to the study. Whether the high-frequency oscillations can cause sufficient elevation in the UAW muscle activity, tonic and/or phasic, to prevent UAW obstructions without arousals demands further investigation. The common experience of the public suggests that non-obstructive snoring usually does not awaken the subject from sleep, though there may be micro arousals.

Oronasal application of pressure oscillations require a mask to be worn by the subject. A less intrusive approach may be the application of mechanical vibrations through the skin to the UAW muscles, in which case the muscle spindles and skin mechanoreceptors would be stimulated as much as the pharyngeal mucosal mechanoreceptors. All of these sensory mechanisms are presumably activated during a snoring event as well. We anticipated that the mechanical vibrations applied to the UAWs during sleep should be well tolerated, as it happens during snoring. Activation of the muscle spindles alone may also increase the UAW muscle tone as a reflex, as discussed below. If snoring can be induced in place of obstructions, this would certainly be

improvement in the sleep pattern. The critical pressures for UAW closing in snorers is slightly less negative than that of normals and much lower than the OSA patients (Jason P Kirkness, Vidya Krishnan, Susheel P Patil, & Hartmut Schneider, 2006). To our knowledge, this paradigm has not been tested in the past and thus we do not have direct supporting evidence that externally applied mechanical vibrations might have such an effect. A more important question is that if this effect can be generated without causing sleep arousals.

4.1.4 Tonic Vibration Reflex

It was established decades ago that tonic muscle contractions can be evoked as a reflex to mechanical vibrations (Karl Erik Hagbarth et al., 1976; PBC Matthews, 1966) either applied to the muscle belly or transcutaneously to its tendon. This so called tonic vibration reflex (TVR) has been demonstrated in various limb muscles and shown to be mediated mainly through activation of Ia muscle spindle endings at higher frequencies, and secondary muscle spindle endings and Golgi tendon organs at lower frequencies of the mechanical vibration (DAVID Burke et al., 1976b; PB Matthews, 1984). With an acute application to a relaxed muscle, the Ia fibers can generate action potentials locked to each cycle of the mechanical stimulation at frequencies as high as ~200 Hz (DAVID Burke et al., 1976b; JP Roll, JP Vedel, & E Ribot, 1989). The phase-locking to the vibrations is even stronger in the masseter, a jaw elevator muscle, than the leg muscles (Karl Erik Hagbarth et al., 1976). The shortness of the reflex arc that the neural impulses needed to propagate from and to the masseter was offered as a potential explanation for lesser jitter and thereby stronger phase-locking. Interestingly, discharges of voluntarily

driven motor units in the masseter also became phase-locked to the mechanical oscillations as soon as the vibrator was applied in this study.

Single muscle unit recordings using microelectrodes revealed that TVR discharge is composed of impulses some of which are locked and others unlocked to the vibration cycle (Keidai Hirayama, Saburo Homma, Muneaki Mizote, Yasuo Nakajima, & Shiro Watanabe, 1974). This suggested involvement of both monosynaptic and polysynaptic pathways respectively. The role of the monosynaptic pathway was thought to merely consist of organizing the temporal pattern of the motor outflow of the TVR, which mainly involved polysynaptic mechanisms (Karl Erik Hagbarth et al., 1976). The gradually increasing pattern seen in TVR contractions and the strong effect of barbiturate anesthesia indicated the involvement of polysynaptic pathways. However, a study on wrist extensor muscles provided evidence that the monosynaptic pathway plays a major role in the initial phase of the TVR response after the vibration is turned on and plays a significant role in maintaining the reflex contractions (Patricia Romaguere et al., 1991).

To our knowledge, the GG or any other tongue muscle has never been targeted in those studies on the mechanical vibration reflex, nor has the effect of sleep on TVR ever been investigated. In a somewhat related study, mechanical vibrations applied to the anterior temporalis (TA) in order to induce jaw-tongue reflex evoked TVR in the GG along with the TA (K Igarashi, 1996).

Therefore, we set out to investigate the effects of mechanical vibrations applied externally under the chin (submandibular area) primarily targeting the genioglossus in OSA patients during NREM sleep. Standard polysomnography measurements were made including the GG electromyography. The mechanical vibrations were turned on and off

by the experimenter whenever cessation in breathing was observed. In this study, the main objective was to study the effect of the vibrations on the GG activity and other measures of apnea termination during individual obstructive episodes, rather than evaluating the overall impact of vibrations on sleep quality.

4.2 Experimental Methodology

4.2.1 OSA Patients

Nine OSA patients (8 male, 1 female) were recruited, however, three of the male subjects were excluded from the study due to the difficulties in collecting the genioglossal signals. All the remaining 6 subjects (5 males, 1 female; age 51 ± 6.5) were severe OSA patients (AHI = 51.5 ± 11.8) with body-mass index of larger than 29. The experimental procedures were approved in advance by the ethical committee of Bezmialem Vakıf University, Istanbul. Patient statistics are summarized in Table 4.1.

Table 4.1 Patient Statistics

Subject	Sex	Age	Weight(kg)	BMI	AHI
1	F	47	71	31	58.3
2	M	54	85	39	55.9
3	M	45	90	31	44.7
4	M	62	125	41	66.7
5	M	52	92	29	32.9
6	M	46	106	36	50.5

AHI: Apnea/Hypopnea Index.

4.2.2 Protocol

Complete polysomnographic recordings including the body position and the tracheal sounds were obtained. Each sleep session took approximately six hours over night under the supervision of a sleep technician who visually detected the UAW obstructions by observing the respiratory pattern and the airflow signals from the nasal sensor. Upon detection of an obstruction, a mechanical vibrational device, attached to a chin strap over the submandibular area (Figure 4.1), was turned on manually and continued until the breathing was resumed. In each subject sub-mandibular mechanical vibrations were applied approximately 60-120 times, distributed across the night.

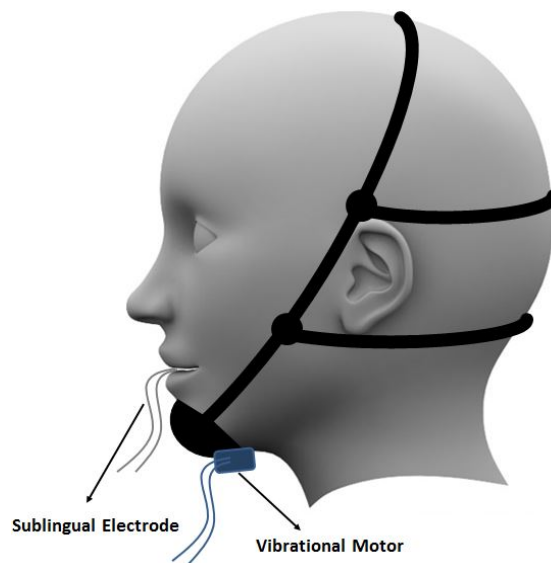


Figure 4.1 Attachment of the mechanical vibrator over the submandibular skin using a chin strap. A pair of EMG wire electrodes were inserted into the genioglossus unilaterally through the mouth.

4.2.3 Genioglossus Electrodes

Genioglossus activity was collected with fine wire electrodes (GG_EMG). A pair of PFA insulated stainless steel wires (50 μm bare diam., #790700, A-M Systems) were inserted

into a 25 g needle; the ends of the wires were desheathed for ~2 mm; the tips were staggered by a few mm and implanted through the mouth about 2 cm into the belly of the GG muscle either to the right or left off the midline. Mechanical vibrations were tested during wakefulness in each subject first to determine if the vibration strength was at a comfortable level.

4.2.4 Signal Processing

The GG_EMG activity was sampled at 10 kHz and filtered with an analog notch filter to remove 50 Hz contamination from the main power. The GG_EMG signal envelope was calculated on the computer by rectifying and low-pass filtering the raw signal with a 6th order Butterworth filter at 5 Hz. To quantify the effect of mechanical stimuli on GG muscle activity, we calculated the area under the rectified-filtered GG_EMG activity during a 5 s interval after termination of an apnea as determined by the nasal airflow (cannula). Results were expressed in arbitrary units (a.u.) due to the dependency of signal amplitudes on the tip separation of the bipolar EMG electrodes. Baseline GG activities were measured toward the middle of apneic episodes where the amplitudes were minimum (see Figure 4.2 for markings).

To remove artifacts and large amplitude low frequency components, EEG signals (C3-A2 and C4-A1) were passed through a 4 Hz high-pass filter first. The alpha band EEG signal power (8-12 Hz) was computed using FFT coefficients within a 4 s sliding window that was advanced in 0.25 s steps. The *baseline alpha* measurement was taken at the lowest level during the apnea cycle (horizontal dash line in Figure 4.2). In spontaneously terminated apneas, *the alpha peak* was searched within the time window that started 2 s before the apnea termination and lasted 10 s after (first horizontal arrow in

Figure 4.2). In stimulated cycles, *the alpha peak* was looked for within the time window starting at the onset of the mechanical vibrations and extended 10 s after the apnea was terminated (second horizontal arrow in Figure 4.2). Both in stimulated and spontaneously terminated apnea cycles, the corresponding lowest point in SpO₂ was easily identified and manually marked after taking a delay of about 15-20 s into account (asterisks in Figure 4.2).

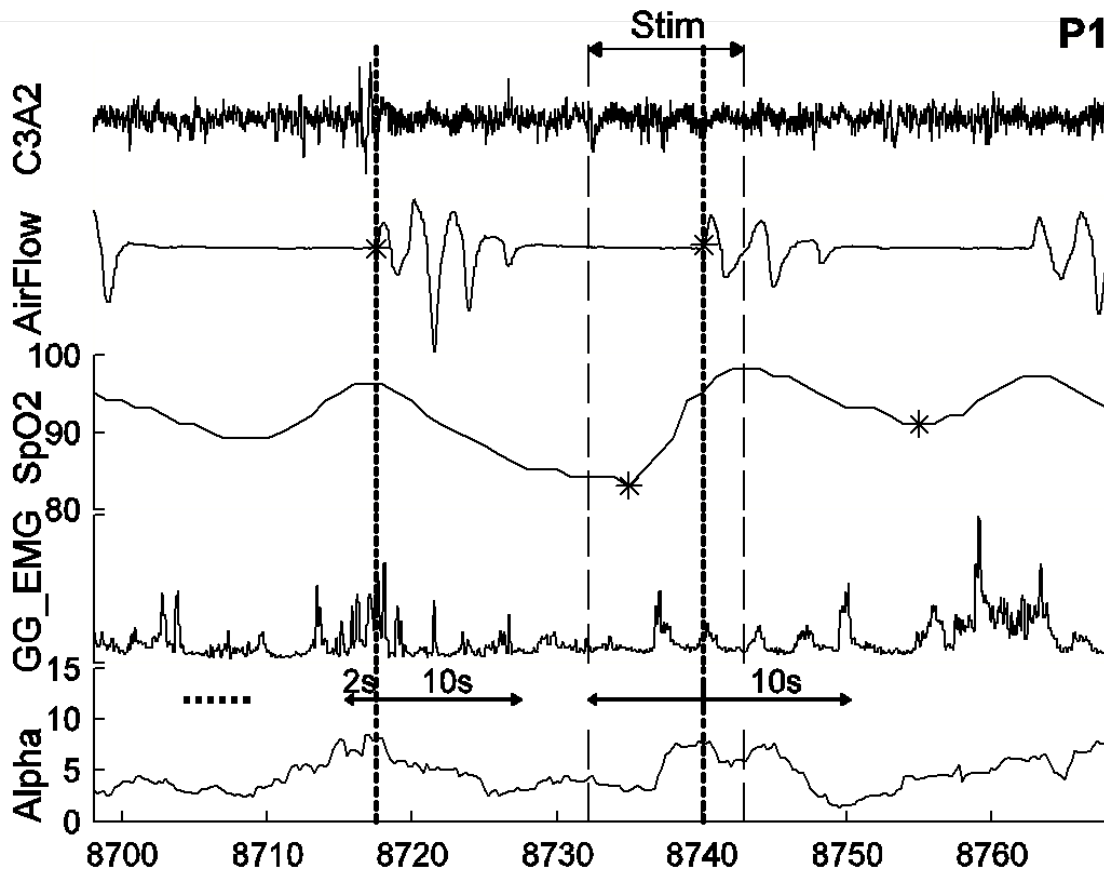


Figure 4.2 Sample episode from patient 1. The times of GG_EMG and alpha power baselines measurements are marked with horizontal dash line as an example. The arrows show the intervals where the peak values for the GG_EMG and EEG alpha power were searched. The asterisks indicate the manually marked points of apnea terminations (airflow) and the minimum SpO₂ measurements for a pair of unstimulated and stimulated apnea cycles.

4.2.5 Mechanical Vibrations

The submandibular mechanical vibrations (SMVs) generated by the mechanical device (Pico Vibe 307-100, Precision Microdrives, UK) was tested while it was attached to the chin strap on a subject, at various voltage levels for their frequency (Hz) and acceleration (g). According to the test results and patient feedbacks, we decided to use two different levels of the stimulus, comfortable to the subjects. For the low level of stimulus, we applied 1.3 V to the motor, which produced 89 Hz vibrations at 1.72 g (g: gravitational acceleration). For the high level of stimulus, we applied 1.5 V to the motor, which produced 99 Hz vibrations with 2.25 g acceleration. The technician applied low and high levels of stimulus randomly in each study. When the data were grouped according to the vibration strength, there was not a significant difference. Thus, the results were pooled together.

4.2.6 Statistics

The unstimulated apnea cycles preceding or following the stimulated ones are considered as a pair. Occasionally the same unstimulated episode was used as a pair for two stimulated cycles because there was not a gap between stimulations. The measurement points for the GG_EMG, the *alpha power*, and the minimum SpO2 were marked manually (see Figure 4.2 for markings) and the paired values were compared using one-tailed, paired t-test for SpO2 and both sided, paired t-test for *alpha power* and GG_EMG, after confirming that the data had normal distribution (Figure 4.3). Only the baseline values were performed in an unpaired fashion because there were a larger number of

baseline GG_EMG measurements available (N1 in Table 4.2) than the stimulated/unstimulated cycle pairs (N2).

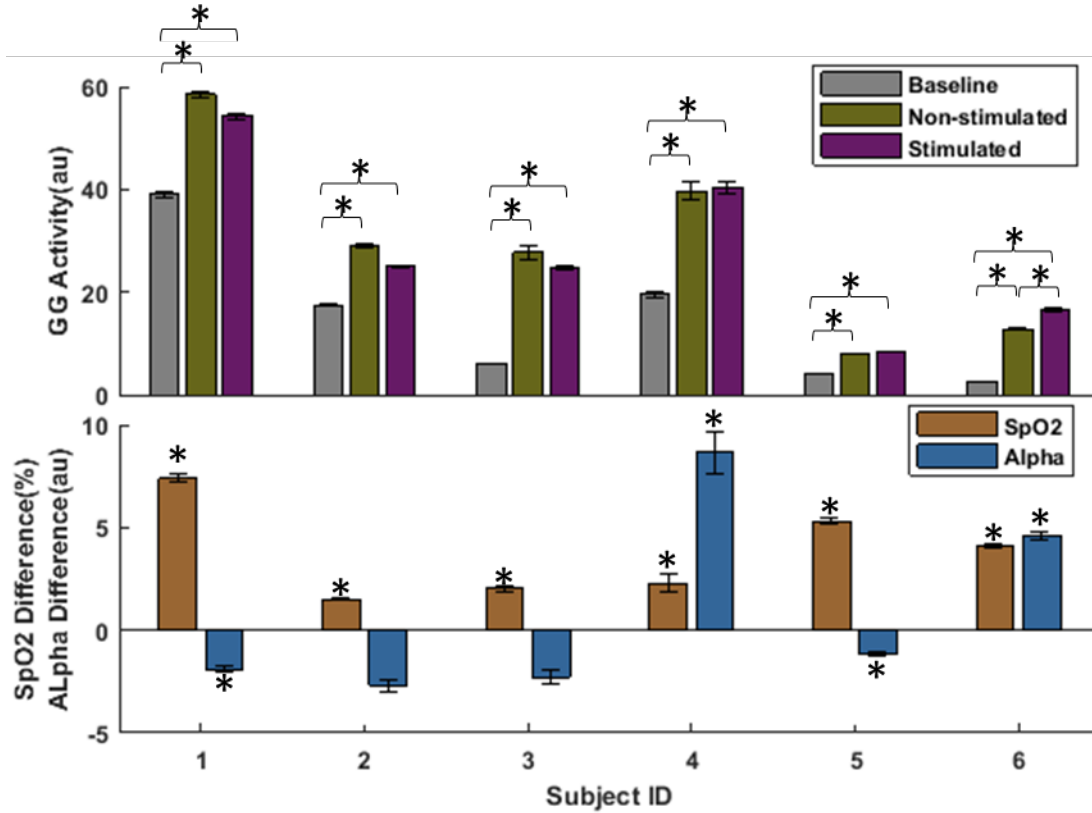


Figure 4.3 Top: GG activity during middle of the apnea (baseline) and during apnea terminations for both stimulated and non-stimulated cases. Bottom: Minimum oxygen saturation and alpha peak difference between stimulated and non-stimulated apnea cycle. All GG_EMG and alpha peak powers in both stimulated and non-stimulated cycles are significantly higher than their baseline values ($p < 0.001$, one-sided, unpaired t-test). All values are means \pm SE. The P values can be found in Table 4.2.

4.3 Results

4.3.1 GG Activity Analysis

As an evidence towards showing that the observed GG response was evoked by the mechanical stimulations, we searched for the GG_EMG components at the frequency of mechanical stimulus in a few patients under the premise that the EMG activity will be

higher during stimulated episodes. Assuming that the EMG signal power at the vibration frequency should contain the mechanical artifacts due to mechanical coupling between the vibrator and the EMG wires, we compared the EMG envelopes after band-pass filtering the signals to contain the vibrational frequencies only and the broader band.

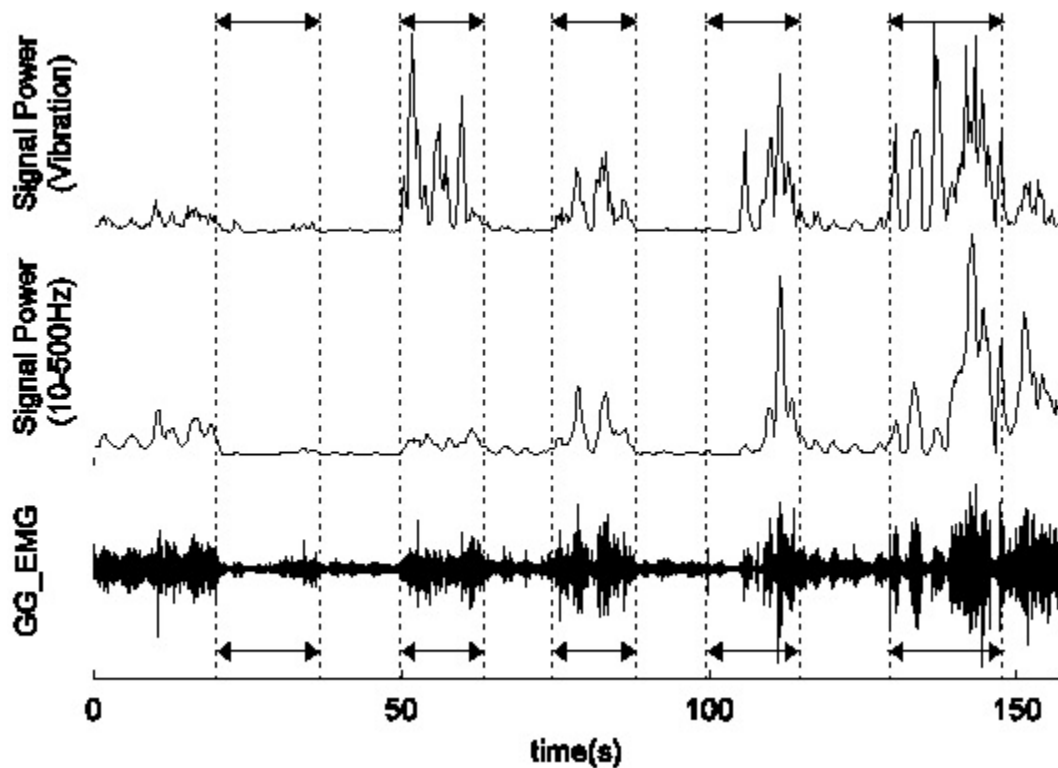


Figure 4.4 The first two traces are the signal power computed in 4 s running windows for the vibration frequency band (95-105 Hz to capture 99 Hz in this case) and the whole band EMG power (10-500 Hz) respectively. The bottom trace is the raw genioglossal EMG signal. The timings of the stimulations are indicated with the dotted lines.

The signal power at the vibration frequency (89 or 99 Hz) did not follow the GG_EMG pattern in general (compare top two traces in Figure 4.4), which suggested that the signal was not a simple mechanical artifact due to proximity of the vibrator to the recording electrodes, in which case the signal power would follow the exact pattern of the GG_EMG envelope with broader filtering (10-500 Hz). The fact that the two EMG

envelopes were different during the stimulated episodes suggested the presence of evoked EMG activity that was not a mechanical artifact. The results in one of the subjects clearly showed that the GG activity had frequency components that were phased-locked to the mechanical stimulations. This specific observation however did not extrapolate to the other subjects, most probably because the EMG wires are inherently too large to record from single muscle units.

Table 4.2 Statistical Test Results of SpO2, Alpha and GG_EMG

Patient	N1	Min SpO2	Alpha (a.u.)	Baseline Alpha (a.u.)	Response Time	Baseline GG_EMG	GG_EMG (a.u.)	N2
1	44	86.1+/-7.21	9.43+/-2.98	3.73+/-0.93	12.8+/-7.76	39.0+/-18.9	51.2+/-20.5	39
		78.7+/-5.74	11.3+/-4.9				58.6+/-25.9	
		P < 0.001	P = 0.034				P = 0.057	
2	51	88.4+/-2.58	34.1+/-11.3	14.4+/-5.51	10.7+/-5.72	17.5+/-5.08	25.3+/-10.4	37
		86.9+/-2.47	36.7+/-20.1				28.9+/-12.8	
		P < 0.001	P = 0.19				P = 0.08	
3	37	90.7+/-2.66	25.8+/-8.88	6.17+/-1.54	8.47+/-7.56	6.10+/-4.12	22.1+/-12.2	20
		88.7+/-3.47	28.1+/-11.2				27.3+/-23.5	
		P = 0.0066	P = 0.3				P = 0.43	
4	11	84.5+/-5.81	29.8+/-14.8	8.48+/-0.91	5.96+/-6.18	19.5+/-5.53	33.3+/-8.7	4
		82.2+/-2.35	21.1+/-12.4				39.6+/-7.0	
		P = 0.07	P = 0.033				P = 0.08	
5	31	95.9+/-1.52	6.29+/-2.05	2.97+/-0.70	2.25+/-0.72	4.02+/-1.25	7.99+/-3.40	28
		90.6+/-3.34	7.43+/-2.56				7.91+/-2.98	
		P < 0.001	P = 0.04				P = 0.91	
6	53	89.1+/-5.30	15.0+/-8.21	3.71+/-0.88	16.6+/-11.1	2.67+/-2.78	16.8+/-13.5	52
		85.0+/-3.11	10.4+/-5.19				12.8+/-8.11	
		P < 0.001	P < 0.001				P = 0.01	

Highlighted rows indicate stimulated apnea cycles in each patient. N1 is the number of stimulated/unstimulated cycle pairs that applies to all the columns except the GG_EMG, for which the number of pairs is shown as N2. All values are means \pm std. The P values of statistical significance test (one-sided, paired t-test) between stimulated and un-stimulated cycles are given for each patient below each measurement type. All GG_EMG and alpha peak powers in both stimulated and non-stimulated cycles are significantly higher than their baseline values ($p < 0.001$, one-sided, unpaired t-test).

The GG activity presented highly variable patterns, with and without phasic components, and sometimes completely out of phase with respiration. The EMG measurements in general indicated that the GG activity is highly correlated with the start

and termination of UAW obstructions. In all patients, the GG activity increased significantly compared to the baseline ($p < 0.001$, unpaired t-test) at the time of apnea terminations (measured as the average of activity within the following 5 s window) both during spontaneously ended and stimulated episodes. In most patients, the increase in the mean GG as a response to mechanical vibrations was comparable to or little less than those measured during spontaneous apnea terminations, as suggested by the p values in Table 4.2 (Figure 4.3). Only in patient 6 the GG activity during stimulations increased more than the spontaneous cases (Figure 4.3, $p = 0.01$). Data do not show conclusively if the GG responds to the SMVs directly, or indirectly as a result of micro arousals. The EEG analysis below suggests that there is a direct GG response to SMVs at least in a certain number of episodes in each patient.

4.3.2 Individual Patient Characteristics

Patient 1: Both phasic and tonic components of GG_EMG were present in patient 1 throughout the night, however, the GG_EMG did not present immediate increases as a response to mechanical vibrations in general (Figure 4.2). The apneas were terminated within 12.8 ± 7.8 s (mean \pm SD) after the onset of the mechanical vibrations. The EEG alpha power peaks were a little less in the stimulated periods compared to the immediately preceding or following non-stimulated breaths, where the apneas were terminated spontaneously (9.43 ± 2.98 vs. 11.34 ± 4.86 , $p = 0.034$, $N = 44$, Table 4.2, Figure 4.3), suggesting smaller micro arousals. Despite the fact that GG_EMG amplitudes were slightly lower during the stimulated breaths compared to the spontaneously terminated apneas (51.24 vs. 58.55 , $p = 0.057$), the minimum SpO₂ values observed during the apneas were substantially higher in the stimulated episodes ($86.1 \pm 7.2\%$ vs. $78.7 \pm 5.7\%$,

$p < 0.001$), which was due to the fact that the mechanical vibrations terminated the apneas earlier than their due times for spontaneous termination. The long response time to the stimuli may be due to the low amplitude of the mechanical vibrations.

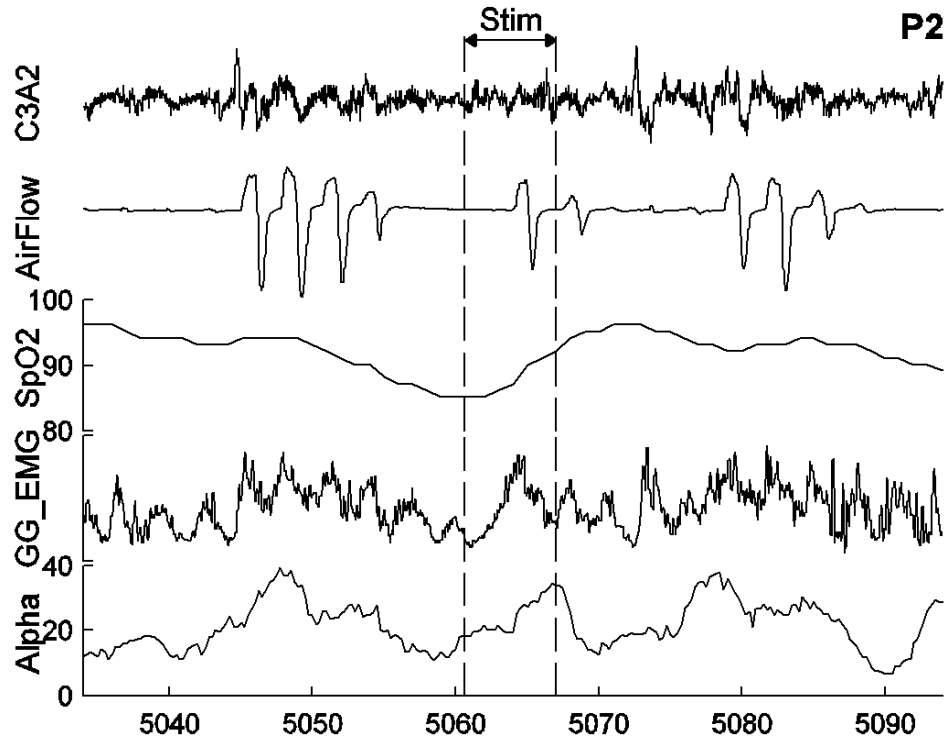


Figure 4.5 Sample episode from patient 2. The timings of mechanical stimulations are indicated by two vertical dash lines.

Patient 2: Both tonic and phasic GG_EMG was present also in this patient, however there was also a noticeable increase particularly in the tonic component as a response to SMVs (Figure 4.5). The spontaneous apnea terminations were coinciding quite well with GG_EMG increases (e.g. $t=5,040-50$ s). The apneas were not always terminated immediately upon stimulus application and the response time was 10.7 ± 5.72 s ($N=51$). The alpha power in EEG and the GG_EMG immediately after the stimulus onset were slightly less than those of the spontaneously terminated apneas on average but not with very strong statistics ($p=0.19$ and $p=0.08$, respectively, Table 4.2, Figure 4.3). The

minimum SpO₂ values during stimulated periods were significantly higher as in other patients ($88.4 \pm 2.6\%$ vs. $86.9 \pm 2.5\%$, $p < 0.001$). This subject presented a similar picture to patient 1 overall, except that the GG_EMG had a clear response to the mechanical stimuli. Substantial improvements in SpO₂ desaturation were achieved along with similar GG_EMG increases to that of the spontaneously terminated apneas, although accompanied by slightly less but similar alpha arousals.

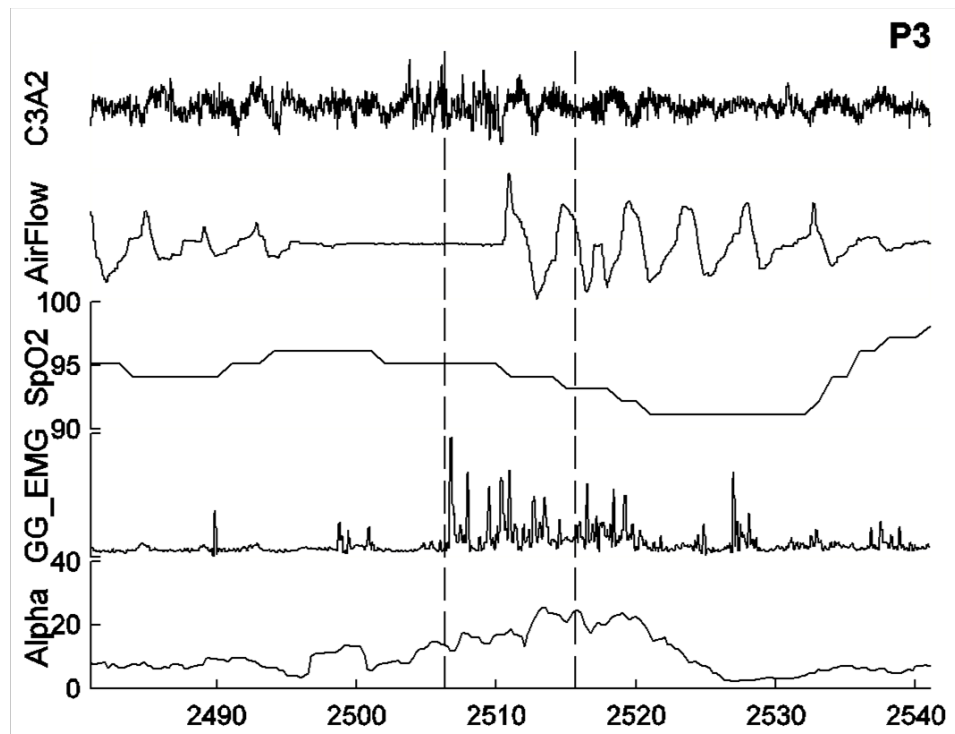


Figure 4.6 Sample episode from patient 3. The timings of mechanical stimulations are indicated by two vertical dash lines.

Patient 3: This subject had much stronger GG_EMG responses, usually not phasic with the breathing cycle (Figure 4.6). The apneas were terminated sooner following the mechanical stimuli (8.47 ± 7.56 s, Table 4.2, Figure 4.3) compared to the previous patients. The EEG alpha power and GG_EMG during stimulations were not significantly different than that of the spontaneously terminated apneas ($p=0.3$ and

p=0.43). However, the min SpO₂ values were again significantly higher during the stimulated apnea cycles ($90.7\pm 2.7\%$ vs. $88.7\pm 3.5\%$, $p<0.01$).

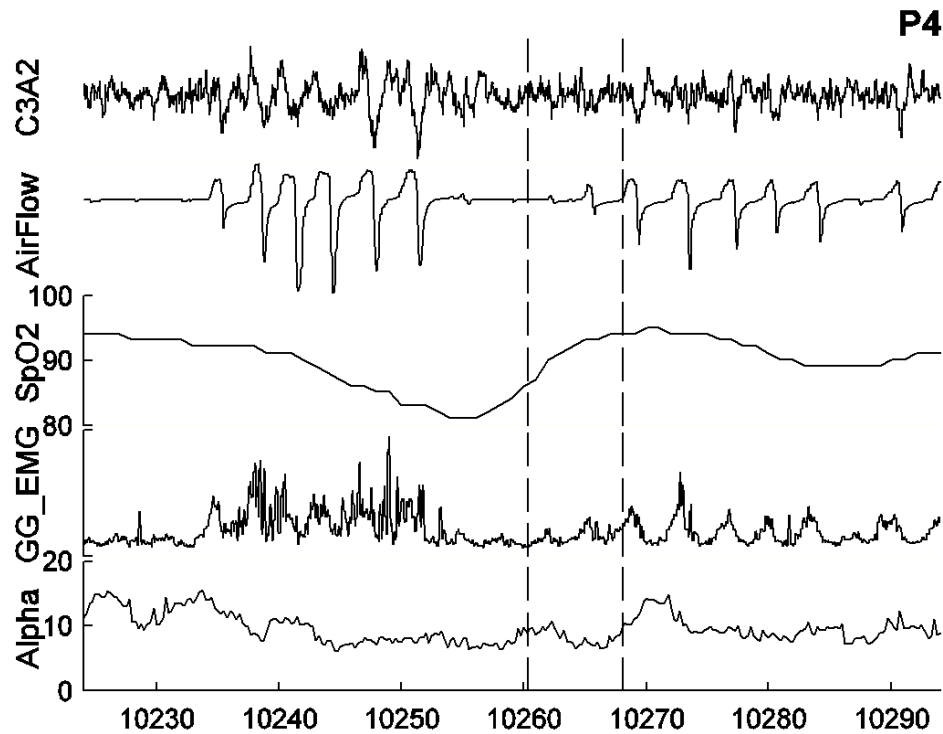


Figure 4.7 Sample episode from patient 4. The timings of mechanical stimulations are indicated by two vertical dash lines.

Patient 4: The phasic GG_EMG increased at times of apnea terminations, spontaneously and by mechanical vibrations, and ceased almost completely during the obstructed breaths (Figure 4.7). The mechanical vibrations caused similar levels of increase both in alpha power and the GG_EMG compared to the spontaneously terminated apneas, which were significantly higher than the baseline levels. This patient had only four stimulated episodes with GG_EMG recording available for comparison. However, the response times from stimulus to apnea terminations were shorter than the previous patients (5.96 ± 6.18 s, $N=11$, Table 4.2, Figure 4.3).

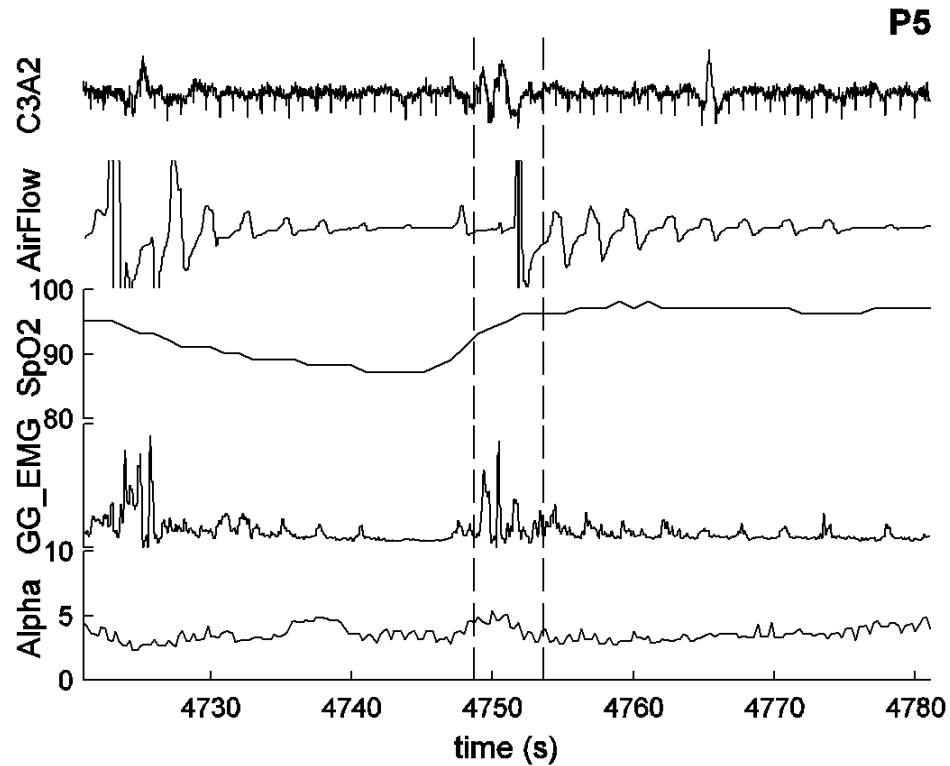


Figure 4.8 Sample episode from patient 5. The timings of mechanical stimulations are indicated by two vertical dash lines.

Patient 5: This patient was the most responsive among all to the mechanical vibrations, as suggested by the short response times (2.25 ± 0.72 s). The GG_EMG was increasing clearly in stimulated apnea terminations as well as in STAs (Figure 4.8). The stimulations were terminating the apneas earlier than their due time for spontaneous UAW opening. In this patient as in patient 1, the alpha power in EEG increased significantly less compared to the non-stimulated episodes (6.29 ± 2.05 vs. 7.43 ± 2.56 , $p=0.04$, $N=31$, Table 4.2, Figure 4.3), despite the fact that the minimum SpO2 values were substantially higher with mechanical vibrations ($95.9 \pm 1.5\%$ vs. $90.6 \pm 3.3\%$, $p<0.001$). The GG response in stimulated breaths were very similar to that of spontaneous apnea terminations (7.99 ± 3.40 vs. 7.91 ± 2.98 $p=0.91$). Overall, this patient produced the most promising results regarding the effects of mechanical vibrations by

terminating the apneas with the shortest delays, comparable increases in the GG activity upon stimulation, and weaker micro arousals.

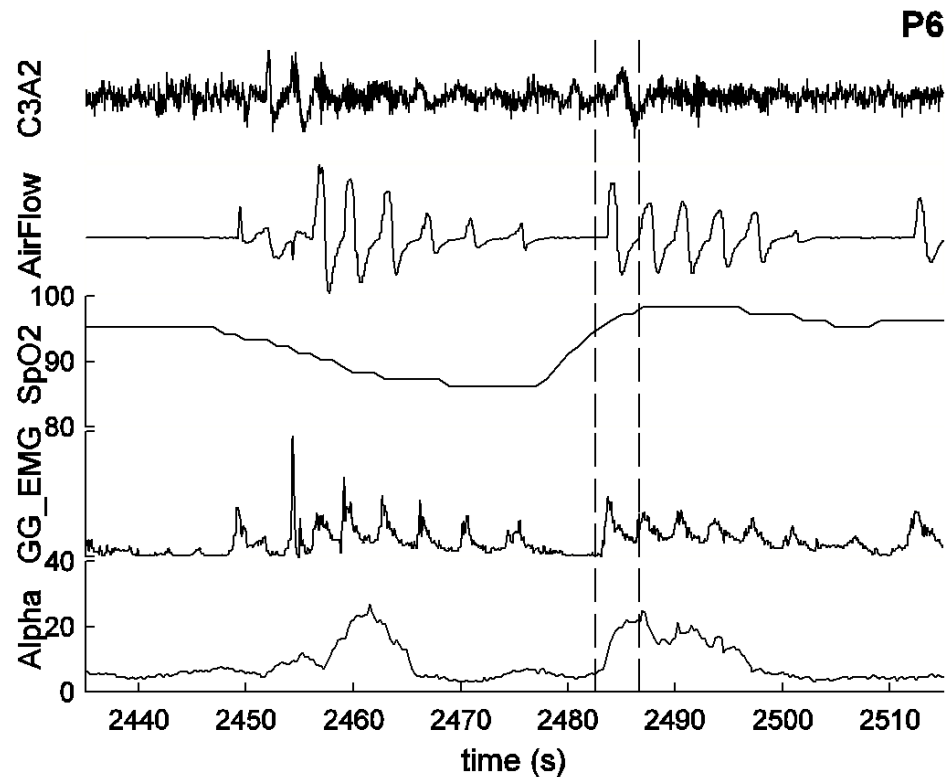


Figure 4.9 Sample episode from patient 6. The timings of mechanical stimulations are indicated by two vertical dash lines.

Patient 6: This subject also had a clear association of the GG_EMG with spontaneous termination of obstructions as well as with stimulations (Figure 4.9). Alpha power in EEG increased significantly compared to the non-stimulated episodes (15.0 ± 8.21 vs. 10.4 ± 5.19 , $p < 0.001$, Table 4.2, Figure 4.3). The response times were very long (16.6 ± 11.1 s), which cast a doubt whether the mechanical vibrations played any role in termination of UAW obstructions, even though the GG_EMG amplitudes were significantly higher at the time of stimulated apnea terminations (16.8 ± 13.5 vs. 12.8 ± 8.11 , $p = 0.01$, $N = 52$).

4.3.3 EEG Alpha Analysis

In all patients, the alpha power values both during stimulated and spontaneously terminated apneas were higher than the baseline values ($p < 0.0001$, see Table 4.2 for N1 values). The peaks of alpha were detected in stimulated and nearby episodes of spontaneously terminated apneas as described above and compared in pairs. Considering that the effects of the mechanical vibrations as well as the blood deoxygenation on micro arousals may vary according to the sleep stage, the peak alpha values taken in pairs from the stimulated and spontaneously terminated apnea episodes are plotted against each other in Figure 4.10. Those points above the line with a slope of unity are the cases where the alpha peak is less in the stimulated episode than the nearby spontaneously terminated apnea episode, and *vice versa*. The solid and dash lines show the mean \pm SD of the baseline alpha.

In all patients, in a large percentage of episodes the stimulated alpha peak was less than its non-stimulated pair and, in some cases, fell into the baseline mean \pm SD range. We can assume that those points near the baseline alpha should be considered as smaller arousals and should have less of an effect on sleep fragmentation. Therefore, in many cases the mechanical stimulations caused lesser arousals than the blood deoxygenation would evoke during spontaneously terminated apneas. These cases comprised 64%, 49%, 57%, 27%, 71%, and 30% of the total number of pairs in each patient respectively, thereby resulting smaller micro arousals in more than 50% of the episodes in 3 patients (patients 1, 3, and 5). This suggests an improvement in SpO₂ values with lesser degrees of sleep fragmentation in half the patients involved in this study.

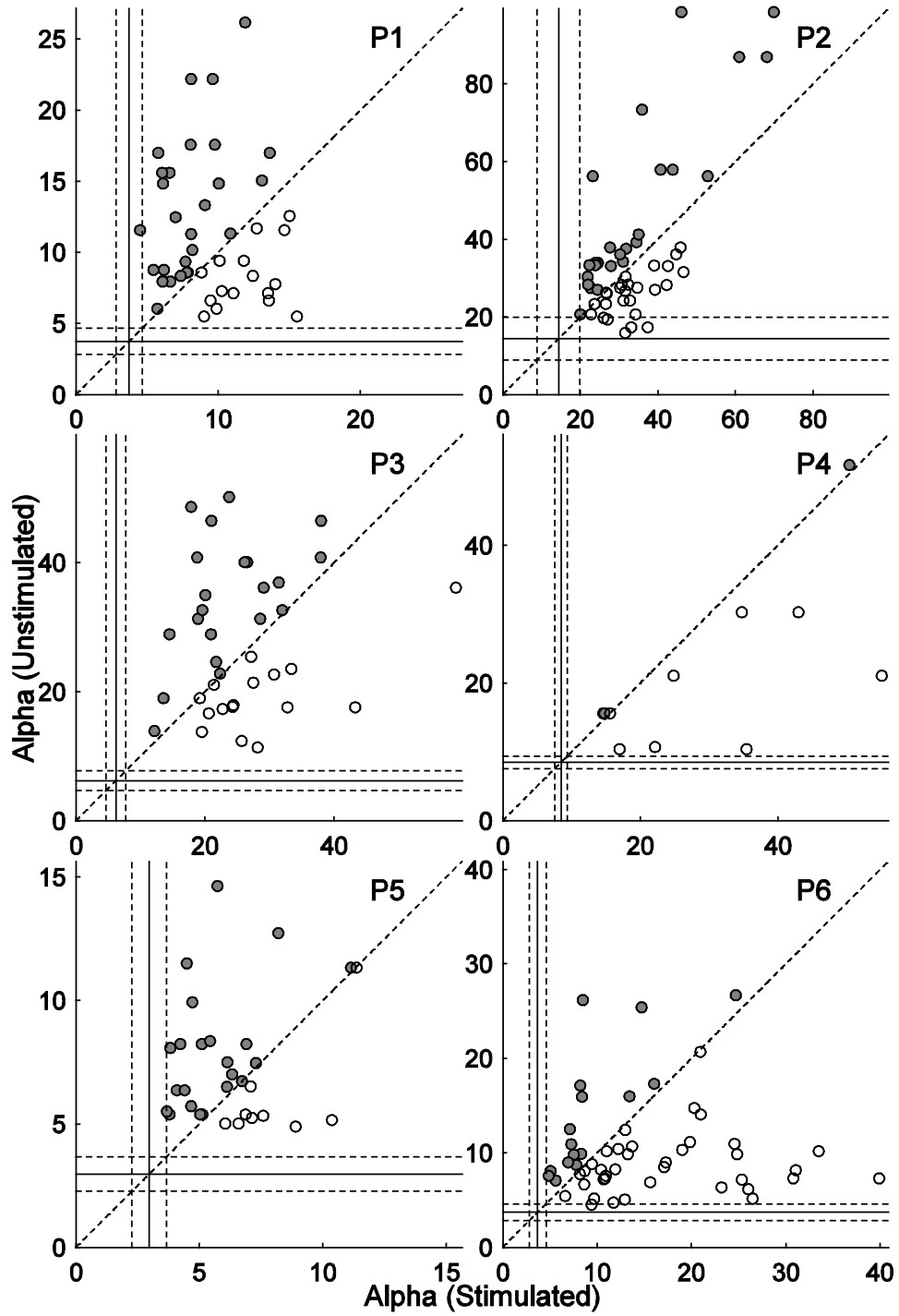


Figure 4.10 The peak alpha power measurements in stimulated vs. non-stimulated (spontaneous) apnea terminations in all six patients. The filled circles indicate the instances where the alpha peak is less in a stimulated cycle compared to its neighboring non-stimulated apneic episode. The solid and dash lines show the mean \pm SD of the baseline alpha level in each patient.

4.3.4 Snore Classification

Our results from six severe OSA patients showed that the application of mechanical vibration to the UAWs can increase the muscle activity and terminate the apneas earlier. The long-term objective is to develop a mechanical device that tracks the patient's respiration during sleep and apply mechanical stimulations immediately after a reduction in airflow is observed. The applied mechanical vibration is expected to increase the upper airway activity and prevent the airway from occlusion. This non-invasive stimulation method may increase the sleep quality of OSA patients by reducing the number of obstructive episodes and arousals.

According to our results, recovering completely blocked airway requires much more muscle activity compared to the activity during regular breathing through non-occluded airway because of the excessive negative intrathoracic pressure against the occluded pharynx. The timing of the mechanical stimulations here plays an important role for preventing the obstructions instead of recovering the completely blocked airway. Therefore, it is essential to sense any signs of obstruction earlier for preventing the occlusions by starting the stimulation early.

The relationship between snoring and OSA was shown in the literature. It was reported that OSA patients generated significantly higher snoring sound intensity levels than simple snorer patients (Kent Wilson et al., 1999). Other groups also showed that there are different spectral shapes of snores between OSA and simple snorers that can be used to separate OSA patients from others (JA Fiz et al., 1996; W Whitelaw, 1993). Fundamental frequency of snore was used for classification of these groups (J Sola-Soler,

R Jane, JA Fiz, & J Morera, 2002; Jordi Sola-Soler, Raimon Jane, Jose Antonio Fiz, & Jose Morera, 2000).

There are many automatic pitch detection methods for speech in the literature. The oldest and most reliable one, autocorrelation method was used in pitch analysis in snoring sounds (J Sola-Soler et al., 2002; Jordi Sola-Soler et al., 2000). The pitch estimations from autocorrelation method was verified with the manual estimations and it was shown that the automatic pitch estimations are smoother version of the manual estimations, and the autocorrelation method is able to detect pitch absence in snore (Jordi Sola-Soler et al., 2000).

Snoring sounds were recorded from all subjects with a pressure transducer placed in front of the mouth during the full night sleep study along with the other 26 channel polysomnography data. The snore analysis explained below was performed on patient 6. The snore signal was passed through an analog band-pass filter between 10 and 150 Hz and sampled at 512 Hz. The recorded signal did not include background noise from the sleep room due to the proximity of the sensor pipe to the mouth. Therefore, further noise reduction was not necessary.

Detection of snore events was done by computing the envelope of the snore signal by using Hilbert transformation and passing through a low-pass filter at 2 Hz. Threshold is defined as the 30 percent of the smallest amplitude snore event that was found by visual inspection. Any time interval where the envelope is higher than the threshold is marked as “event” in the signal. Then, the events that are shorter than 0.2 s and longer than 2 s (stimulation artifact) are excluded as noise. The remaining events are marked as snore and stored for further processing.

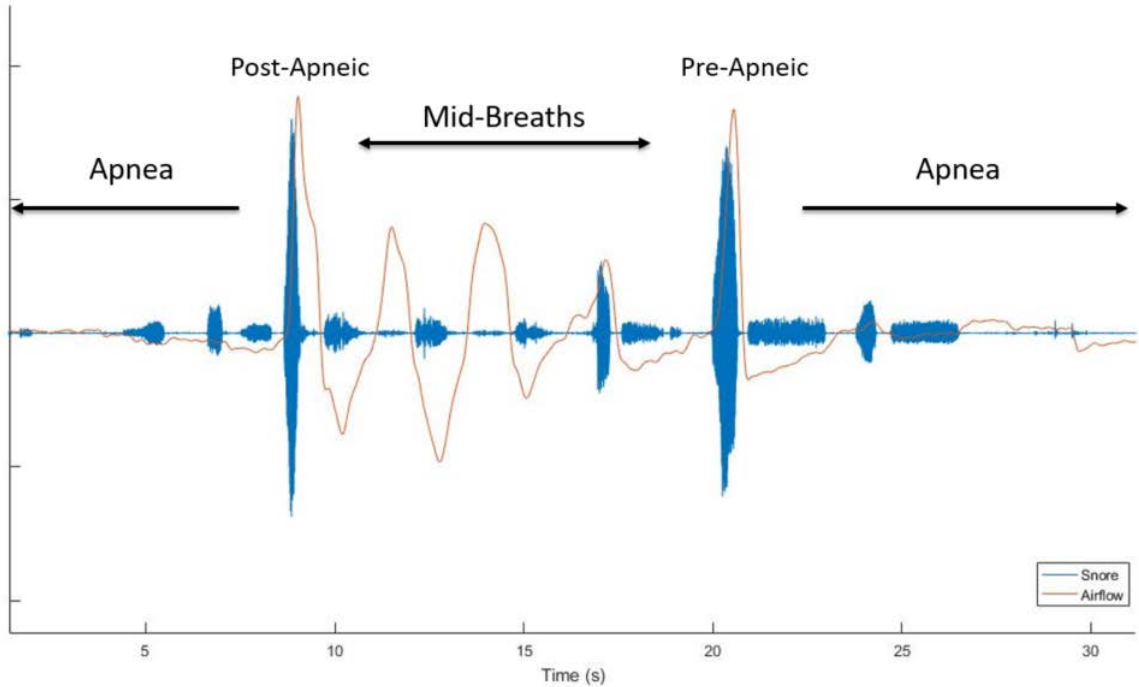


Figure 4.11 Classification of the breath cycles and snore events. Post-apneic breath is the first breath after apnea termination. Pre-apneic breath is the last breath before apnea. Mid-breaths are the rest of the breaths between post and pre-apneic breaths. Snore events are also classified by their corresponding breath cycles.

Respiratory cycles and occlusions are detected with simple peak detection algorithm from the airflow signal which is band-pass filtered between 0.1 and 4 Hz. Breath cycles are separated into three categories as post-apneic, pre-apneic and mid-breath (Figure 4.11). Total of 192 post-apneic, 192 pre-apneic, 634 mid-breath cycles was found. Snore events that occur during inspiratory phase of the breath cycles are extracted and separated into the same three categories as breath cycles. Finally, total of 153 post-apneic, 114 pre-apneic and 118 mid snore events were selected for further analysis.

Autocorrelation method is selected out of many pitch detectors that was developed in literature. The window length is fixed at 125 ms with an overlap of 25 ms, which is sufficiently enough to cover pitch range for snores and moved along the snore for pitch tracking. Autocorrelation is computed with “xcorr” function in MATLAB for

each window. The algorithm detects the maximum of the peaks on the positive site of the autocorrelation signal in the range of 8-25 ms (corresponding to 40-125 Hz). Pitch is determined as the corresponding frequency of the location of the detected peak for each window.

We then extracted eight parameters from the snore events for statistical analysis. Snore duration is calculated as the time between beginning and the end of the snore. Time interval 1 is the time between the beginning of the inspiration and the end of snore. Time interval 2 is the time between the end of inspiration and the end of snore. The snore intensity is calculated as the spectral power of the snore between 10 and 150 Hz. Spectral centroid represents the center of mass of the frequency spectrum and is calculated by multiplying FFT coefficients with corresponding frequencies and dividing by the sum of FFT coefficients. The fundamental frequency is the pitch calculated with autocorrelation method. The pitch SD is the standard deviation of the calculated pitches during each snore event. Correlation at pitch is the calculated correlation value from the autocorrelation method at the fundamental frequency.

The snore detection method explained above found 153 post-apneic, 118 mid and 114 pre-apneic snores out of 192, 634 and 192 breath cycles, respectively. Percent snore occurrence during mid-breath cycles is %18.6 which is significantly low compared to the snore occurrence of post-apneic and pre-apneic breath cycles, 79.7 and 59.4 respectively (Figure 4.12i).

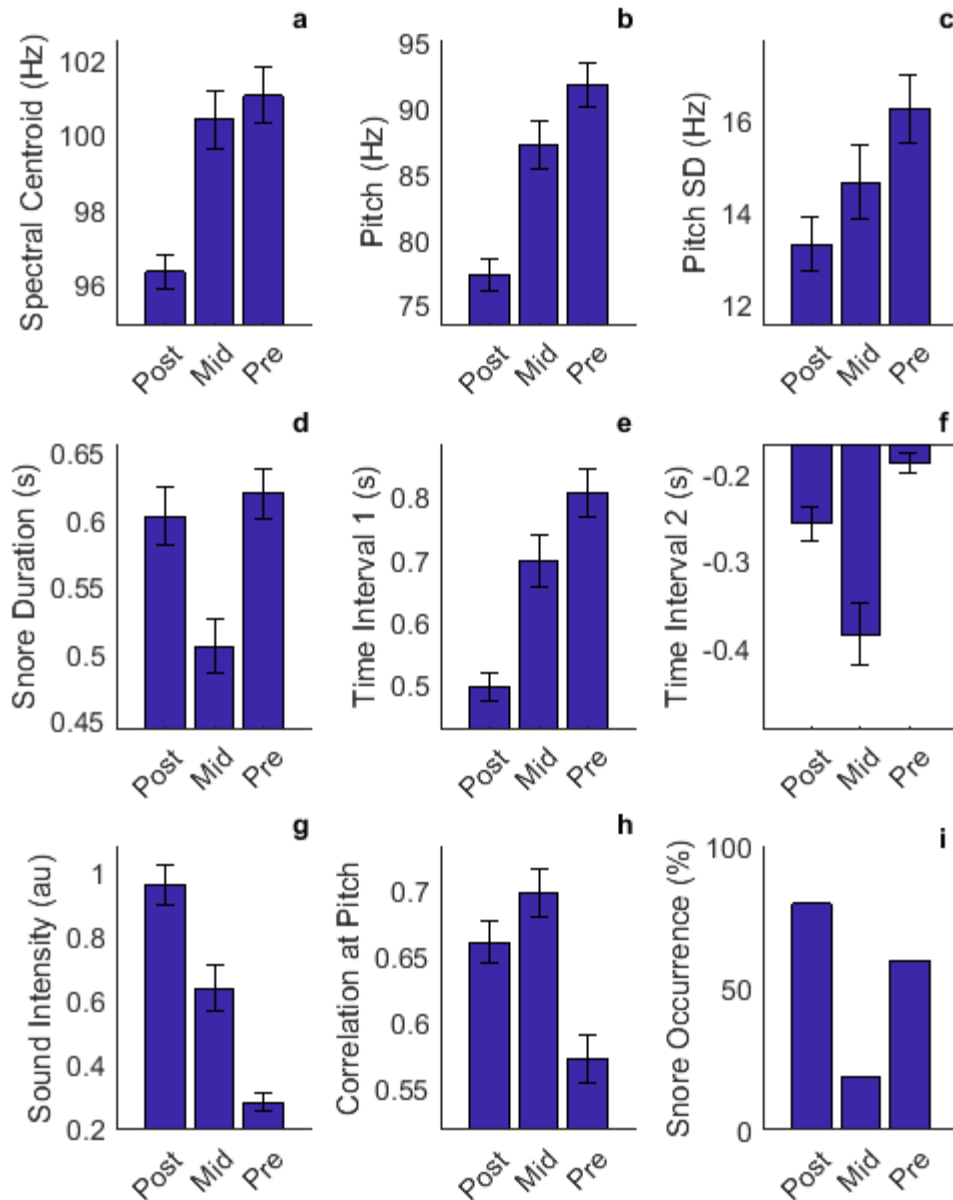


Figure 4.12 Averages of each parameter for each group (mean \pm SE). Statistical test results are summarized in Table 4.3 a) Spectral centroid is the center of mass of the frequency spectrum b) Fundamental frequency is the pitch calculated with autocorrelation method. c) Pitch SD is the standard deviation of the pitches calculated with moving autocorrelation d) Snore duration is the time from beginning and end of snore e) Time interval 1 is the time between beginning of inspiration and end of snore f) Time interval 2 is the time between end of inspiration and end of snore. g) Sound intensity is the spectral power of the snore between 10 and 150 Hz. h) Correlation at pitch is the correlation value calculated from autocorrelation method at fundamental frequency. i) Percent snore occurrences during post, mid and pre-apneic breath cycles.

One-way Multivariate Analysis of Variance (MANOVA) was performed over eight features extracted from snore to test the hypothesis that the means of each group are the same n-dimensional multivariate vector. According to the results from MANOVA, we reject the null hypothesis that the multivariate means lie on the same line ($p < 0.0001$). We then performed one-way ANOVA on each dependent variable to test which of the parameters are significantly different between groups at the significance level of 0.0063 (adjusted alpha). Then Tukey's honest significance test was performed for pairwise comparison between groups for each parameter.

We found that the mean snore duration during mid-cycles is significantly shorter than the duration of snore events during pre-apneic and post-apneic breaths (Table 4.3, Figure 4.12d). Besides that, snore sound intensity showed decreasing pattern from post-apneic to pre-apneic breaths (Table 4.3, Figure 4.12g). Time interval between the beginning of inspiratory phase and the end of snore (Time Interval 1) is significantly lower on post-apneic breaths than the mid and pre-apneic snores (Table 4.3, Figure 4.12e). The mean time interval between the end of inspiratory phase and the end of snore (Time Interval 2) is also significantly higher during mid breaths compared to the post and pre-apneic breaths (Table 4.3, Figure 4.12f).

According to the results of the pitch analysis, we found that the estimated pitch is significantly lower during post-apneic snores compared to the other groups (Table 4.3, Figure 4.12b). Estimated pitch was also slightly lower during mid snores compared to during pre-apneic snores, however the difference was not significant. We also saw that the correlation value at the pitch was significantly lower for pre-apneic snores compared to the other groups, which shows that the irregularity of pitch increases with the

upcoming occlusion (Table 4.3, Figure 4.12h). The standard deviation of pitches, which also represents irregularity, presented similar increasing trends through the pre-apneic breaths, however the differences were not significant at the significance level of 0.0063 ($p=0.01$, Table 4.3, Figure 4.12c). Similar to the fundamental frequency, the mean spectral centroid of the snore was significantly lower during post-apneic breaths compared to the other N groups (Table 4.3, Figure 4.12a).

Table 4.3 Statistical Results of Snore Features

	Group 1 Post-Apneic N = 153	Group 2 Mid N=118	Group 3 Pre-Apneic N=114	One-Way ANOVA	Significance Between Groups
Spectral Centroid (Hz)	96.31±0.60	100.40±0.69	101.05±0.70	$p<0.001^*$	1-2 $p<0.001^*$ 1-3 $p<0.001^*$ 2-3 $p=0.788$
Fundamental Frequency (Hz)	77.25±1.42	87.16±1.62	91.72±1.65	$p<0.001^*$	1-2 $p<0.001^*$ 1-3 $p<0.001^*$ 2-3 $p=0.118$
Pitch SD (Hz)	12.60±0.66	13.64±0.75	15.65±0.76	$p=0.010$	1-2 $p=0.549$ 1-3 $p=0.007^*$ 2-3 $p=0.140$
Snore Duration (s)	0.60±0.02	0.51±0.02	0.62±0.02	$p<0.001^*$	1-2 $p=0.002^*$ 1-3 $p=0.834$ 2-3 $p=0.001^*$
Time Interval 1 (s)	0.50±0.03	0.70±0.03	0.81±0.04	$p<0.001^*$	1-2 $p<0.001^*$ 1-3 $p<0.001^*$ 2-3 $p=0.073$
Time Interval 2 (s)	-0.26±0.02	-0.39±0.03	-0.19±0.03	$p<0.001^*$	1-2 $p<0.001^*$ 1-3 $p=0.105$ 2-3 $p<0.001^*$
Sound Intensity (au)	0.96±0.05	0.64±0.06	0.28±0.06	$p<0.001^*$	1-2 $p<0.001^*$ 1-3 $p<0.001^*$ 2-3 $p<0.001^*$
Correlation at Pitch	0.66±0.02	0.70±0.02	0.57±0.02	$p<0.001^*$	1-2 $p=0.275$ 1-3 $p=0.001^*$ 2-3 $p<0.001^*$

Group averages states as mean ± SE. Tukey's honest significance test was used for pairwise comparison between groups.

According to these results, most of the parameters differ significantly between breath groups and could be a potential metric to be used in prediction of the occlusions before they occur. These promising results are from only one patient and the recorded snore signal is analyzed only in one frequency range. More spectral information can be extracted from the snore signal that is recorded at higher sampling rates.

4.4 Discussion

In our small group of OSA patients, we observed significant effects of submandibular mechanical vibrations on apnea terminations, the minimum SpO₂, and the GG activity. The stimulations might have had varying degrees of strength due to different amounts of muscle/fat under the chin and the coupling efficiency of the vibrator to the submandibular tissue. In a subset of stimulation trials, the mechanical stimuli increased the GG activity and terminated the apneas with smaller arousals than the spontaneously terminated apneas. Stimulation strength was standardized in this study by applying one of the two pre-selected voltages to the vibrational device. In future trials, the patient may be titrated during the initial segment of the night to decide on an optimum strength that produces a sizeable GG response in the absence of micro arousals in the EEG pattern.

The vibration frequency varied as a function of the voltage applied to the device and thus it was not possible to set the frequency independent of the vibration strength. The frequency can be investigated as a separate variable in terms of its effect on the UAW muscles and the sleep arousal threshold. Previous research on UAW mechanoreceptor sensitivity to pressure oscillations was mostly conducted at lower frequencies, typically at 30 Hz, whereas the tonic vibration reflex (TVR) studies were usually done at frequencies above 100 Hz.

In this study, we did not score the apnea/hypopnea index (AHI) as an outcome measure because the initiation and duration of the mechanical stimuli were decided by the experimenter and not automated based on a set of predetermined criteria. Moreover, it is not clear if the AHI would be the right measure to use for assessing the sleep quality in this study. The number of apneas per hour will artificially be increased because each apnea is terminated by the stimulus earlier than the time it would spontaneously be terminated by asphyxia. The size of the micro arousals may have to be factored in as a parameter to evaluate the sleep quality, along with the number of arousals.

The ultimate objective is to maintain normal levels of blood oxygenation while avoiding micro arousals as much as possible. Current evidence suggests a strong relation between the number of intermittent hypoxemia and re-oxygenation episodes during sleep, as typically seen in obstructive apneas, with cardiovascular diseases such as hypertension, coronary artery disease, atrial fibrillation, and heart failure (for a review see (C Gonzaga, A Bertolami, M Bertolami, C Amodeo, & D Calhoun, 2015)). Therefore, maintaining normal levels of blood oxygenation during sleep is the key for cardiovascular health, as well as avoiding sleep fragmentation.

We speculate that the primary mechanism underlying the observed physiological changes is either through the stimulation of the UAW muscle spindles or the mucosal mechano-receptors. Other UAW muscles may have been activated by the same stimulus along with the GG, although we did not record their activities. Indeed, a concerted effort involving most of the UAW muscles would be much more effective to remove the obstructions. Electrical activation of the GG muscle through HG nerve stimulation is a technique that recently received much attention. Although the GG is the primary muscle

that is responsible for forward traction of the tongue, it should be recognized that the UAW patency is maintained not only by the extrinsic tongue muscles but by the pharyngeal wall muscles as well. The coordinated recruitment of UAW muscles that spontaneously occurs during inhalation and dilates the airways in all directions is a very difficult activation pattern to achieve via electrical stimulation of extrinsic tongue muscles (Jingtao Huang et al., 2005; Paul B Yoo et al., 2004).

The long-term effects of the submandibular mechanical stimulation need to be investigated in longitudinal studies. The observed GG response may diminish over time due to habituation. On the other hand, patients may adapt to vibrations and sleep through even stronger amplitudes in repeated trials. A future goal is to extend this study to a larger patient population where the stimuli will be turned on and off automatically upon detection of apneas using a set of predetermined criteria.

CHAPTER 5

CONCLUSIONS AND FUTURE WORK

This study demonstrated for the first time the presence of phasic activity in the GG, an UAW dilating muscle, with sinusoidal displacements of the lower jaw in healthy subjects during wakefulness. Another major finding of this study was that the GG activity is elevated as a response to the mechanical vibrations applied to the submandibular muscles. The elevated GG activity persisted after termination of the submandibular stimulation for a few seconds. These results support the previous studies that the GG response to mechanical stimulations of the submandibular muscles may not be simple reflex through a short pathway. The results show the presence of a more complex response that resembles an output from a neuronal network activated by UAW afferents. The results from sleep studies on six OSA patients also showed that the sub-mandibular mechanical stimulations terminated the obstructive events earlier than their spontaneously due times, but with a smaller decrease in the blood oxygen levels and resulted smaller micro-arousals compared to spontaneously terminated ones.

It may be difficult to compare the effects of submandibular mechanical stimulations in sleep and wakefulness because the vibrational motor that was used in the sleep experiments was much smaller compared to the one used in awake subjects. The vibration amplitude generated during sleep was approximately 0.1 mm at 95 Hz, which is significantly smaller compared to 0.5 mm displacements at 30 Hz that the large motor produced during wakefulness. Moreover, there was a large difference between the average BMIs of the subjects in the two set of experiments. The BMI was positively

correlated with the submandibular skin thickness, which may have limited the transmission of vibrations to the UAW muscles (average BMI=34.5 and 26.5 for sleep and wakefulness experiments, respectively).

In a subset of stimulation trials in sleep experiments, the GG muscle activity was elevated during obstructions to the activity levels observed during unobstructed breathing. However, it was not sufficient to remove the obstructions because of the excessive negative intrathoracic pressure against the occluded pharynx. Therefore, we concluded that the stimulation paradigm for future sleep studies should be modified in a way such that the stimulations should be started immediately upon sensing any signs of upcoming obstructions. For instance, changes in the spectral or time domain parameters of snore sounds can be used as a metric to this end.

As the next step for future studies, the GG reflex needs to be investigated in healthy subjects during sleep, rather than in wakefulness. Healthy subjects would be preferred for examining the effects of sleep on the GG response to sub-mandibular stimulations since the UAW patency is very chaotic in OSA patients. After determining the stimulation amplitude that is adequate for evoking a GG reflex in NREM sleep without causing arousal, the second step would be studying the effects of the sub-mandibular stimulations progressively on mild, moderate and severe OSA patients by performing double night sleep studies. Investigation of the outcome measures such as apnea-hypopnea index (AHI), the average blood oxygen saturation, the heart rate, and the sleep arousals between stimulation and control nights can provide conclusive results in these patient groups.

APPENDIX

MATLAB CODE

All the analyses of sub-mandibular mechanical vibration were performed using the code below.

```
load('subjectnames')
for klm=1:length(subjects)
    clearvars -except subjects klm
    subjectname = subjects{klm};
    cd Google Drive\VIB'
    asd = dir(subjectname);
    path = strcat(Google Drive\VIB\',subjectname,'\',asd(3).name);
    asdd = dir(path);
    data1 = [];
    k=1;

    f = [100 1000];
    fr = 1/3;
    load(strcat(path,'\','baseline'))
    for i=1:10-1-h.nstim
        y = abs(fft(data(i*h.fs+1:(i+h.nstim)*h.fs,1))); y(1) = []; y(15000:end) = [];
        baseline_pow(i) = sum(y((f(1)/fr):(f(2)/fr)))/(3*h.fs);
    end
    basepow1 = mean(baseline_pow);
    fr = 1/8;
    y = abs(fft(data(1*h.fs+1:9*h.fs,1))); y(1) = []; y(40000:end) = [];
    basepow2 = sum(y((f(1)/fr):(f(2)/fr)))/(8*h.fs);

    load(strcat(path,'\','max_activity'))
```

```

fr = 1/3;
for i=1:10-1-h.nstim
    y = abs(fft(data(i*h.fs+1:(i+h.nstim)*h.fs,1))); y(1) = []; y(15000:end) = [];
    max_pow(i) = sum(y((f(1)/fr):(f(2)/fr)))/(3*h.fs);
end
maxpow1 = mean(max_pow);
fr = 1/8;
y = abs(fft(data(1*h.fs+1:9*h.fs,1))); y(1) = []; y(40000:end) = [];
maxpow2 = sum(y((f(1)/fr):(f(2)/fr)))/(8*h.fs);

for i=5:length(asdd)
    load(strcat(path,'\',asdd(i).name))
    %   lvl = strcat('level',num2str(h.freq));
    lvls = h.randorder(k:k+length(trl)-1);
    k = k+length(trl);
    for j=1:length(trl)
        lvl = strcat('level',num2str(lvls(j)));
        if isfield(data1,lvl)
            data1.(lvl)(end+1) = trl(j);
        else
            data1.(lvl) = trl(j);
        end
    end
end
clearvars -except h data1 subjectname f maxpow1 basepow1 subjects klm
data = data1;
clearvars -except h data subjectname f maxpow1 basepow1 subjects klm
fc = 100;
[B, A] = butter(3,2*fc/h.fs,'high');
fc = 40;
[B1, A1] = butter(4,2*fc/h.fs,'low');
fc = 5;
[B2, A2] = butter(2,2*fc/h.fs,'high');

```

```

fc = 2;
[B3, A3] = butter(2,2*fc/h.fs,'low');
fc = 1;
[B4, A4] = butter(2,2*fc/h.fs,'low');
frange_mscohere = 0:.2:60;
levels = sort(fieldnames(data));
for jj=1:length(levels)
    lvl = char(levels(jj));
    for i=1:length(data.(lvl))
        % displacement
        acc = 9807*1000*(data.(lvl)(i).data(:,2))/(h.vs*100);
        %     acc = filtfilt(B2,A2,acc);
        vel = cumsum(acc)/h.fs;
        %     vel = filtfilt(B2,A2,vel);
        disp = cumsum(vel)/h.fs;
        data.(lvl)(i).disp = filtfilt(B2,A2,disp);
        data.(lvl)(i).acc = filtfilt(B2,A2,acc/9807);
        %     Force = ((data.(lvl)(i).data(:,5)-0.5)*13.6)/(0.32*h.vs);
        [YUPPER1, YLOWER1] = envelope(data.(lvl)(i).disp,round(h.fs/40),'peak');
        ENV = YUPPER1 - YLOWER1;
        data.results.(lvl)(1).meddisp(i) = mean(ENV((h.nstim+1)*h.fs+1:(h.nstim+h.stim-1)*h.fs));
        [YUPPER1, YLOWER1] = envelope(data.(lvl)(i).acc,round(h.fs/40),'peak');
        ENV = YUPPER1 - YLOWER1;
        data.results.(lvl)(1).amplitude(i) =
mean(ENV((h.nstim+1)*h.fs+1:(h.nstim+h.stim-1)*h.fs));

        pkss = data.(lvl)(i).disp((h.nstim+0.3)*h.fs:(h.nstim+h.stim)*h.fs);
        [pks, locs] = findpeaks(pkss,'MinPeakHeight',0);
        data.results.(lvl)(1).meanfreq(i) = 1/(median(diff(locs))/h.fs);
        fun_frq = data.results.(lvl)(1).meanfreq(i);

```

```

d = min(diff(locs));
for j=1:1
    data.(lv1)(i).fdata(:,j) = filtfilt(B,A,data.(lv1)(i).data(:,j)); % high pass filter
    data.(lv1)(i).henvdata(:,j) = filtfilt(B1,A1,abs(data.(lv1)(i).fdata(:,j))); % low
pass filter for envelope (high freq env)
    %
    data.(lv1)(i).lenvdata(:,j) =
flipud(filter(B3,A3,flipud(abs(data.(lv1)(i).fdata(:,j))))); % low pass filter for envelope
(low freq env)
    data.(lv1)(i).lenvdata(:,j) = filtfilt(B3,A3,abs(data.(lv1)(i).fdata(:,j))); % low
pass filter for envelope (low freq env)
    data.(lv1)(i).lenvdata2(:,j) = filtfilt(B4,A4,abs(data.(lv1)(i).fdata(:,j))); % low
pass filter for envelope (low freq env)

% spectral power calculation
fr = 1/h.nstim;
ff = 0:fr:f(2);
y = abs(fft(data.(lv1)(i).data(0*h.fs+1:h.nstim*h.fs,j))); y(1) = []; y(15000:end)
= [];
y2 = y;

data.results.(lv1)(j).npow(i) = sum(y((f(1)/fr):(f(2)/fr)))/(h.nstim*h.fs);
data.results.(lv1)(j).npow2(i) = std(data.(lv1)(i).fdata(.1*h.fs+1:h.nstim*h.fs,j));
data.results.(lv1)(j).basestd(i) = std(data.(lv1)(i).lenvdata(:,j));
fr = 1/h.stim;
y=abs(fft(data.(lv1)(i).data((h.nstim+0.1)*h.fs+1:(h.nstim+h.stim+0.1)*h.fs,j)));
y(1) = []; y(15000:end) = [];
[Y, I] = max(y);
I1 = ((I-1)*y(I-1)+I*y(I)+(I+1)*y(I+1))/(y(I-1)+y(I)+y(I+1));
y1 = y;
for kk=1:6
    rg = [round(I1*6*kk-15), round(I1*6*kk+15)];
    y1(rg(1):rg(2)) = 0;
    y2(rg(1):rg(2)) = 0;
end
data.results.(lv1)(j).npow3(i) = sum(y2((f(1)/fr):(f(2)/fr)))/(h.stim*h.fs);

```

```

data.results.(lv1)(j).pow(i) = sum(y((f(1)/fr)+1:(f(2)/fr)+1))/(h.stim*h.fs);
data.results.(lv1)(j).pow2(i) =
std(data.(lv1)(i).fdata((h.nstim+.1)*h.fs+1:(h.nstim+h.stim)*h.fs,j));
data.results.(lv1)(j).pow3(i) = sum(y1((f(1)/fr):(f(2)/fr)))/(h.stim*h.fs);
data.results.(lv1)(j).inc(i) = 100*(data.results.(lv1)(j).pow(i)-
data.results.(lv1)(j).npow(i))/data.results.(lv1)(j).npow(i);
data.results.(lv1)(j).inc2(i) = 100*(data.results.(lv1)(j).pow2(i)-
data.results.(lv1)(j).npow2(i))/data.results.(lv1)(j).npow2(i);
data.results.(lv1)(j).inc3(i) = 100*(data.results.(lv1)(j).pow3(i)-
data.results.(lv1)(j).npow3(i))/data.results.(lv1)(j).npow3(i);
data.results.(lv1)(j).inc4(i) = 100*(data.results.(lv1)(j).pow(i)-
data.results.(lv1)(j).npow(i))/(maxpow1-basepow1);
% correlation peaks
data.results.(lv1)(j).corrpeak(i) =
(max(xcorr(data.(lv1)(i).disp((h.nstim+1)*h.fs+1:(h.nstim+h.stim-
1)*h.fs),data.(lv1)(i).henvdata((h.nstim+1)*h.fs+1:(h.nstim+h.stim-1)*h.fs,j)-
mean(data.(lv1)(i).henvdata((h.nstim+1)*h.fs+1:(h.nstim+h.stim-1)*h.fs,j),'coeff')))^2;
[Cxy,F] = mscohere(data.(lv1)(i).disp((h.nstim+0.3)*h.fs+1:
(h.nstim+h.stim)*h.fs),abs(data.(lv1)(i).fdata((h.nstim+0.3)*h.fs+1:(h.nstim+h.stim)*h.fs,
j)),[],[],frange_mscohere,h.fs);
data.results.(lv1)(j).mscohere(i,:) = Cxy;
data.results.(lv1)(j).mscohere1(i,:) = max(Cxy(round(fun_frq*5)+1-
10:round(fun_frq*5)+1+10));
% sum of each cycles
sm = zeros(d+1,1);
sm2 = zeros(d+1,1);
sm3 = zeros(d+1,1);
for k=1:length(locs)-1
sm = sm + data.(lv1)(i).fdata(locs(k):locs(k)+d,j); % sum of filtered data
sm2 = sm2 + data.(lv1)(i).henvdata(locs(k):locs(k)+d,j); % sum of envelope
sm3 = sm3 + acc(locs(k):locs(k)+d); % sum of acceleration
% dll = [dll;locs1((locs1-locs(k))>0&(locs1-locs(k))<d)-locs(k)];
end
% data.results.(lv1)(j).hst = [data.results.(lv1)(j).hst; dll];
data.(lv1)(i).avg(:,j) = sm/(length(locs)-1);
data.(lv1)(i).sm2(:,j) = sm2;

```

```

        data.(lvl)(i).sm3(:,j) = sm3;
    end
end
end

if not(strcmp(subjectname,'subject1'))
    rsst = load(strcat('Google Drive\VIB\results1\',subjectname,'.mat'));
    data.results.level1.delay = rsst.result.level1.delay;
    data.results.level2.delay = rsst.result.level2.delay;
    data.results.level3.delay = rsst.result.level3.delay;
end
result = data.results;
end
%%
path = \Google Drive\VIB\results';
cd (path)
asdd = dir(path);
data1 = [];
k = 1;
for i=3:length(asdd)
    load(strcat(path,'\',asdd(i).name))
    label = ['subject',num2str(k)];
    rslt.(label) = result;
    k = k+1;
    clear result h
end

levels = sort(fieldnames(rslt.subject1));
sbj = fieldnames(rslt);
chn=1;
asddisp = [];
asdfreq = [];
for i=1:length(levels)

```

```

for j=1:length(sbj)
    mr(j,i) = mean(rslt.(char(sbj(j))).(char(levels(i)))(chn).inc3);
    sr(j,i) =
std(rslt.(char(sbj(j))).(char(levels(i)))(chn).inc3)/sqrt(length(rslt.(char(sbj(j))).(char(levels
(i)))(chn).inc3));

    mrnp(j,i) = mean(rslt.(char(sbj(j))).(char(levels(i))).npow3);
    srnp(j,i) =
std(rslt.(char(sbj(j))).(char(levels(i))).npow3);%/length(rslt.(char(sbj(j))).(char(levels(i)))(c
hn).npow3);
    mrp(j,i) = mean(rslt.(char(sbj(j))).(char(levels(i))).pow3);
    srp(j,i) =
std(rslt.(char(sbj(j))).(char(levels(i))).pow3);%/length(rslt.(char(sbj(j))).(char(levels(i)))(c
hn).pow3);
    [H P] = ttest(rslt.(char(sbj(j))).(char(levels(i)))(chn).npow3,rslt.(char(sbj(j))).(char(
levels(i)))(chn).pow3,'alpha',0.05);
    hh(j,i) = H;

    cpm(j,i) = mean(rslt.(char(sbj(j))).(char(levels(i))).corrpeak);
    cps(j,i) = std(rslt.(char(sbj(j))).(char(levels(i))).corrpeak);

    mcoh1(j,i) = mean(rslt.(char(sbj(j))).(char(levels(i)))(chn).mscohere1);
    scoh1(j,i) = std(rslt.(char(sbj(j))).(char(levels(i)))(chn).mscohere1);

    md(j,i) = mean(rslt.(char(sbj(j))).(char(levels(i)))(chn).meddisp);
    sd(j,i) = std(rslt.(char(sbj(j))).(char(levels(i)))(chn).meddisp);
    mf(j,i) = mean(rslt.(char(sbj(j))).(char(levels(i)))(chn).meanfreq);
    sf(j,i) = std(rslt.(char(sbj(j))).(char(levels(i)))(chn).meanfreq);
    ma(j,i) = mean(rslt.(char(sbj(j))).(char(levels(i)))(chn).amplitude);
    sa(j,i) = std(rslt.(char(sbj(j))).(char(levels(i)))(chn).amplitude);
    asddisp = [asddisp rslt.(char(sbj(j))).(char(levels(i)))(chn).meddisp];
    asdfreq = [asdfreq rslt.(char(sbj(j))).(char(levels(i)))(chn).meanfreq];
end
end
%%

```

```

%Repeated measures analysis of variance (ranova)
t=table(mr(:,1),mr(:,2),mr(:,3),'VariableNames',{'Low','Medium','High'});
rm = fitrm(t,'Low-High~1','WithinDesign',[1 2 3]);
ranovatbl = ranova(rm)
tbl = mauchly(rm) % Mauchly's test for sphericity

% normality test - one-sample Kolmogorov-Smirnov test
[h,p] = kstest(mr(:,1)-mr(:,2))
[h,p] = kstest(mr(:,1)-mr(:,3))
[h,p] = kstest(mr(:,2)-mr(:,3))

% post-hoc paired ttest if normal, Wilcoxon signed rank test if not
alpha = 0.05/6;
[p,h] = signrank(mr(:,1),0,'alpha',alpha)
[p,h] = signrank(mr(:,2),0,'alpha',alpha)
[p,h] = signrank(mr(:,3),0,'alpha',alpha)
[p,h] = signrank(mr(:,1),mr(:,2),'alpha',alpha)
[p,h] = signrank(mr(:,1),mr(:,3),'alpha',alpha)
[p,h] = signrank(mr(:,2),mr(:,3),'alpha',alpha)

```

All the analyses performed for mandibular vibration using the code below.

```

Load('subjectnames')
for klm=1:length(subjects)
    clearvars -except subjects klm
    subjectname = subjects{klm};
    cd '\Google Drive\JTR'
    asd = dir(subjectname);
    path = strcat('\JTR\',subjectname,'\',asd(3).name);
    asdd = dir(path);
    data1 = [];
    k=1;

```

```

for i=4:length(asdd)
    load(strcat(path,'\',asdd(i).name))
    %   lvl = strcat('level',num2str(h.freq));
    lvls = h.randorder(k:k+length(trl)-1);
    k = k+length(trl);
    for j=1:length(trl)
        lvl = strcat('level',num2str(lvls(j)));
        if isfield(data1,lvl)
            data1.(lvl)(end+1) = trl(j);
        else
            data1.(lvl) = trl(j);
        end
    end
end
clearvars -except h data1 subjectname subjects klm
data = data1;
clearvars -except h data subjectname subjects klm
fc = 60;
[B, A] = butter(3,2*fc/h.fs,'high');
fc = 20;
[B1, A1] = butter(4,2*fc/h.fs,'low');
fc = 2;
[B2, A2] = butter(2,2*fc/h.fs,'high');
fc = 2;
[B3, A3] = butter(2,2*fc/h.fs,'low');
f = [60 1000];
frange_mscohere = 0:.1:40;

levels = fieldnames(data);
for jj=1:length(levels)
    lvl = char(levels(jj));
    for i=1:length(data.(lvl))
        if not(strcmp(subjectname,'yusuf')) || i~=20 || not(strcmp(lvl,'level2'))

```

```

% displacement
acc = 9807*1000*(data.(lvl)(i).data(:,h.acc(2))-
data.(lvl)(i).data(:,h.acc(1)))/(h.vs*100);
vel = cumsum(acc)/h.fs;
disp = filtfilt(B2,A2,cumsum(vel)/h.fs);
data.(lvl)(i).disp = disp;

[pks, locs] = findpeaks(-data.(lvl)(i).disp,'MinPeakHeight',.8);
locs(locs<(h.nstim+0.3)*h.fs) = [];
locs(locs>(h.nstim+h.stim)*h.fs) = [];

data.results.(lvl)(1).meanfreq(i) = 1/(median(diff(locs))/h.fs);
fun_frq = data.results.(lvl)(1).meanfreq(i);
[YUPPER1,YLOWER1] = envelope(disp,round(h.fs/16),'peak');
ENV = YUPPER1 - YLOWER1;
data.results.(lvl)(1).meddisp(i) =
mean(ENV((h.nstim+1)*h.fs+1:(h.nstim+h.stim-1)*h.fs));
d = min(diff(locs));
force = h.adj*data.(lvl)(i).data(:,6);
fforce = filtfilt(B3,A3,force);
data.results.(lvl)(1).force(i,:) = force;
data.results.(lvl)(1).fforce(i,:) = fforce;
for j=1:3
    data.(lvl)(i).fdata(:,j) = filtfilt(B,A,data.(lvl)(i).data(:,j)); % high pass filter
    data.(lvl)(i).henvdata(:,j) = filtfilt(B1,A1,abs(data.(lvl)(i).fdata(:,j))); % low
pass filter for envelope (high freq env)
    data.(lvl)(i).lenvdata(:,j) =
flipud(filter(B3,A3,flipud(abs(data.(lvl)(i).fdata(:,j))))); % low pass filter for envelope
(low freq env)
    data.(lvl)(i).hilbertenv(:,j) = envelope(abs(data.(lvl)(i).fdata(:,j)),600,'peak');

% spectral power calculation
fr = 1/h.nstim;
ff = 0:fr:f(2);

```

```

y = abs(fft(data.(lvl)(i).data(0.3*h.fs+1:h.nstim*h.fs,j)));
data.results.(lvl)(j).npow(i) = sum(y((f(1)/fr)+1:(f(2)/fr)+1))/(h.nstim*h.fs);
data.results.(lvl)(j).npow2(i) =
std(data.(lvl)(i).fdata(.3*h.fs+1:h.nstim*h.fs,j));
fr = 1/h.stim;
y = abs(fft(data.(lvl)(i).data((h.nstim+.3)*h.fs+1:(h.nstim+h.stim)*h.fs,j)));

plot(data.(lvl)(i).data((h.nstim+.1)*h.fs+1:(h.nstim+h.stim)*h.fs,j)); pause
data.results.(lvl)(j).pow(i) = sum(y((f(1)/fr)+1:(f(2)/fr)+1))/(h.stim*h.fs);
data.results.(lvl)(j).pow2(i) =
std(data.(lvl)(i).fdata((h.nstim+.3)*h.fs+1:(h.nstim+h.stim)*h.fs,j));
data.results.(lvl)(j).inc(i) = 100*(data.results.(lvl)(j).pow(i)-
data.results.(lvl)(j).npow(i))/data.results.(lvl)(j).npow(i);
data.results.(lvl)(j).inc2(i) = 100*(data.results.(lvl)(j).pow2(i)-
data.results.(lvl)(j).npow2(i))/data.results.(lvl)(j).npow2(i);
% correlation peaks, r^2
data.results.(lvl)(j).corrpeak(i) =
(max(xcorr(data.(lvl)(i).disp((h.nstim+1)*h.fs+1:(h.nstim+h.stim-
1)*h.fs),data.(lvl)(i).henvdata((h.nstim+1)*h.fs+1:(h.nstim+h.stim-1)*h.fs,j)-
mean(data.(lvl)(i).henvdata((h.nstim+1)*h.fs+1:(h.nstim+h.stim-1)*h.fs,j),'coeff')))^2;

[Cxy,F] =
mscohere(data.(lvl)(i).disp((h.nstim+0.3)*h.fs+1:(h.nstim+h.stim)*h.fs),abs(data.(lvl)(i).f
data((h.nstim+0.3)*h.fs+1:(h.nstim+h.stim)*h.fs,j)),[],[],frange_mscohere,h.fs);
data.results.(lvl)(j).mscohere(i,:) = Cxy;
data.results.(lvl)(j).mscohere1(i,:) = max(Cxy(round(fun_frq*10)+1-
9:round(fun_frq*10)+1+11));

data.results.(lvl)(j).norminc(i) = data.results.(lvl)(j).inc(i)/(length(locs)-1);
data.results.(lvl)(j).norminc2(i) = data.results.(lvl)(j).inc2(i)/(length(locs)-1);

data.results.(lvl)(j).hilbpow(i) =
mean(data.(lvl)(i).hilbertenv((h.nstim+0.3)*h.fs:(h.nstim+h.stim)*h.fs,j));
data.results.(lvl)(j).hilbnpow(i) =
mean(data.(lvl)(i).hilbertenv(0.3*h.fs+1:h.nstim*h.fs,j));

```

```

data.results.(lv1)(j).hilbinc(i) = 100*(data.results.(lv1)(j).hilbpow(i)-
data.results.(lv1)(j).hilbnpow(i))/data.results.(lv1)(j).hilbnpow(i);

% sum of each cycles
sm = zeros(d+1,1);
sm2 = zeros(d+1,1);
sm3 = zeros(d+1,1);

% [pks1, locs1] =
findpeaks(data.(lv1)(i).fdata(:,j),'MinPeakDistance',50,'MinPeakHeight',0.08);
% dll = [];
sss = [];
sss1 = [];
sss2 = [];
for k=1:length(locs)-1
    sm = sm + data.(lv1)(i).fdata(locs(k):locs(k)+d,j); % sum of filtered data
    sm2 = sm2 + data.(lv1)(i).henvdata(locs(k):locs(k)+d,j); % sum of
envelope
    sm3 = sm3 + disp(locs(k):locs(k)+d); % sum of acceleration
    %dll = [dll;locs1((locs1-locs(k))>0&(locs1-locs(k))<d)-locs(k)];

    sss1 = [sss1; std(abs(data.(lv1)(i).fdata(locs(k):locs(k)+d,j)))];
    sss2 = [sss2; std(data.(lv1)(i).henvdata(locs(k):locs(k)+d,j))];
    % 60ms power over each cycle
    sss = [sss; std(data.(lv1)(i).fdata(locs(k):locs(k)+60*10-1,j))];
end
data.results.(lv1)(j).cyclepow(i) = mean(sss);
% data.results.(lv1)(j).hst = [data.results.(lv1)(j).hst; dll];
data.(lv1)(i).avg(:,j) = sm/(length(locs)-1);
data.(lv1)(i).sm2(:,j) = sm2/(length(locs)-1);

data.results.(lv1)(j).phasicstd(i) = std(data.(lv1)(i).avg(:,j));
data.results.(lv1)(j).tonicstd(i) = mean(sss1);

```



```

dspp{2} = [];
frqq{2} = [];

for i=1:length(levels)
    for j=1:length(sbj)
        for chn=1:3

            mr1(j,i,chn) = mean(rslt.(char(sbj(j))).(char(levels(i)))(chn).inc2);
            sr1(j,i,chn) =
std(rslt.(char(sbj(j))).(char(levels(i)))(chn).inc2)/sqrt(length(rslt.(char(sbj(j))).(char(levels
(i)))(chn).inc2));
            mcoh1(j,i,chn) = mean(rslt.(char(sbj(j))).(char(levels(i)))(chn).mscohere1);
            scoh1(j,i,chn) = std(rslt.(char(sbj(j))).(char(levels(i)))(chn).mscohere1);
            [H, P] =
ttest(rslt.(char(sbj(j))).(char(levels(i)))(chn).npow,rslt.(char(sbj(j))).(char(levels(i)))(chn).
pow);
            hh(j,i,chn) = H;
        end
        md(j,i) = mean(rslt.(char(sbj(j))).(char(levels(i)))(1).meddisp);
        sd(j,i) = std(rslt.(char(sbj(j))).(char(levels(i)))(1).meddisp);
        mf(j,i) = mean(rslt.(char(sbj(j))).(char(levels(i)))(1).meanfreq);
        sf(j,i) = std(rslt.(char(sbj(j))).(char(levels(i)))(1).meanfreq);

        dspp{i} = [dspp{i} ;rslt.(char(sbj(j))).(char(levels(i)))(1).meddisp'];
        frqq{i} = [frqq{i} ;rslt.(char(sbj(j))).(char(levels(i)))(1).meanfreq'];
    end
end

```

Snore analysis was performed using the code below.

```

P = 9;
[header,Pdata] = edfread([' ' num2str(P) '.edf']); % load sleep data
N = header.ns;
for i = 1:N

```

```

    assignin('base',header.label{1,i},Pdata(i,1:header.records*header.samples(1,i)))
end
clear Pdata

% create time vectors for different sampling rates
t512 = 1/512:1/512:header.records;
t256 = 1/256:1/256:header.records;
t64 = 1/64:1/64:header.records;

% filter the airflow signal
fc = 4;
fnc=2*fc/(64);
[B,A] = butter(4,fnc,'low');
fAirflow2 = filtfilt(B,A,Airflow2);
fc = 0.1;
fnc=2*fc/(64);
[B,A] = butter(4,fnc,'high');
fAirflow2 = filtfilt(B,A,fAirflow2);

% Respiration cycle detection
[pks lcs width] = findpeaks(fAirflow2,'MinPeakDistance',96,'MinPeakHeight',10);
dlcs = diff(lcs);
[pks2 lcs2 width2] = findpeaks(dlcs,'MinPeakDistance',0,'MinPeakHeight',15*64); %%
64 is fs of airflow. 15*64 is total length.
dlcs2 = diff(lcs2);%% Number of airflow between two apnea.

% separate the breath cycles into groups
resp{16,7} = [];
for i=1:length(dlcs2)
    if dlcs2(i)>=4 && dlcs2(i)<=7
        resp{1,dlcs2(i)} = [resp{1,dlcs2(i)}; lcs(lcs2(i)+1:lcs2(i+1))];
        resp{2,dlcs2(i)} = [resp{2,dlcs2(i)}; pks(lcs2(i)+1:lcs2(i+1))];
    end
end

```

```

    resp{16,dlcs2(i)} = [resp{16,dlcs2(i)}; width(lcs2(i)+1:lcs2(i+1))]; % width (half
prominence)
%    resp{19,dlcs2(i)} = [resp{19,dlcs2(i)}; pksss(lcs2(i)+1:lcs2(i+1))]; % width (half
prominence)
    end
end

```

```

% exclude the cycles with more than 4 second delay between breaths

```

```

for i=4:7

```

```

    resp{3,i} = diff(resp{1,i},1,2)/64;
    [I, ~] = (find(resp{3,i}>4));
    resp{1,i}(I,:) = [];
    resp{2,i}(I,:) = [];
    resp{3,i} = [];
    resp{16,i}(I,:) = [];
end

```

```

%%

```

```

% fc = 150;
% fnc=2*fc/(512);
% [B,A] = butter(4,fnc,'low');
% fMic = filtfilt(B,A,Mic);

```

```

% snore hilbirt envelope

```

```

[yupper,ylower] = envelope(Mic,2*512,'analytic');

```

```

fc = 2;

```

```

fnc=2*fc/(64);

```

```

[B,A] = butter(4,fnc,'low');

```

```

fyupper = filtfilt(B,A,yupper);

```

```

fylower = filtfilt(B,A,ylower);

```

```

fenv = fyupper - fylower;

```

```

th = 0.02;
fenvt = fenv - th;
fenvt(find(fenvt<0))=0;
fenvt(find(fenvt>0))=1;
dfenvt = diff(fenvt);

locs(1,:) = find(dfenvt==1);
locs(2,:) = find(dfenvt==-1);
locs(3,:) = locs(2,)-locs(1,);

for i=1:length(locs)
    locs(4,i) = mean(fenv(locs(1,i):locs(2,i)));
    if locs(3,i)<100 || locs(3,i)>1024 || locs(4,i)<0.05
        fenvt(locs(1,i):locs(2,i)) = 0;
    end
end

locs(:,find(locs(3,)<100))=[];
locs(:,find(locs(3,)>1024))=[];
locs(:,find(locs(4,)<0.05))=[];
sn(:,1) = find(diff(fenvt)==1);
sn(:,2) = find(diff(fenvt)==-1);

for ii=4:7
    for i=1:length(resp{1,ii})
        for j=1:size(resp{1,ii},2)
            resp{3,ii}(i,j) = resp{1,ii}(i,j)-find(flip(fAirflow2(1:resp{1,ii}(i,j)))<2,1); %
beginning of inspiration
            resp{4,ii}(i,j) = resp{1,ii}(i,j)+find(fAirflow2(resp{1,ii}(i,j):end)<2,1); % end of
inspiration
            resp{17,ii}(i,j) = resp{4,ii}(i,j)- resp{3,ii}(i,j); % airflow width
            resp{18,ii}(i,j) = trapz(abs(fAirflow2(resp{3,ii}(i,j):resp{4,ii}(i,j)))); % area
under the curve (airflow)

```

```

resp{19,ii}(i,j) = j; % airflow number
resp{23,ii}(i,j) = trapz(abs(Mic(8*resp{3,ii}(i,j):8*resp{4,ii}(i,j)))); % area under
the curve (snore) during airflow
if mean(fenvt(8*resp{3,ii}(i,j):8*resp{4,ii}(i,j)))>0 % check if any snore during
respiration
    [I, ~] = find(sn(:,2)>8*resp{3,ii}(i,j),1);
    resp{5,ii}(i,j) = sn(I,1); % beginning of snore
    resp{6,ii}(i,j) = sn(I,2); % end of snore
    resp{6,ii}(i,j) = resp{6,ii}(i,j) + mod(resp{6,ii}(i,j)-resp{5,ii}(i,j)+1,2); %
make length of snore even number
    L = resp{6,ii}(i,j) - resp{5,ii}(i,j) + 1;

    xd = Mic(resp{5,ii}(i,j):resp{6,ii}(i,j));

    resp{22,ii}(i,j) = trapz(abs(xd)); % area under the curve (snore)

    resp{7,ii}(i,j) = L/512; % length of snore (seconds)
    resp{8,ii}(i,j) = ((resp{5,ii}(i,j)+resp{6,ii}(i,j))/2-8*resp{3,ii}(i,j))/512; % time
between beginning of inspiration and middle of snore
    resp{24,ii}(i,j) = ((resp{6,ii}(i,j))-8*resp{3,ii}(i,j))/512; % time between
beginning of inspiration and end of snore
    resp{25,ii}(i,j) = ((resp{5,ii}(i,j))-8*resp{3,ii}(i,j))/512; % time between
beginning of inspiration and end of snore
    resp{26,ii}(i,j) = ((resp{6,ii}(i,j))-8*resp{4,ii}(i,j))/512; % time between end of
inspiration and end of snore
    resp{27,ii}(i,j) = ((resp{5,ii}(i,j))-8*resp{4,ii}(i,j))/512; % time between end of
inspiration and end of snore

    td=(0:L-1)/512;
    ft = abs(fft(xd)/L);
    ft = ft(1:L/2+1);
    ft(2:end-1) = 2*ft(2:end-1);
    f = 512*(0:(L/2))/L;
    resp{9,ii}(i,j) = sum(f.*ft)/sum(ft); % spectral centroid
    [~, I] = max(ft);

```

```

resp{10,ii}(i,j) = 10000*sum(ft.^2)/L; % sound intensity
resp{11,ii}(i,j) = f(1); % max frequency snore

% pitch detection
maxlag = 32; pi1=4; pi2=12;
r = xcorr(xd, maxlag, 'coeff');
d=1000*(-maxlag:maxlag)/512;
r1 = r(maxlag+2:end);
[maxi,idx]=max(r1(pi1:pi2));
resp{12,ii}(i,j) = 512/(pi1+idx-1); % pitch calculated with whole snore
resp{13,ii}(i,j) = maxi; % correlation

[R, d] = movingpitch(xd,512,64,16,32,[4 12]);
resp{14,ii}(i,j) = mean(R(1,:)); % mean pitch calculated from moving pitch
resp{15,ii}(i,j) = std(R(1,:)); % std pitch

else
    for kk=[5:15,24:27]
        resp{kk,ii}(i,j) = 0;
    end
    resp{22,ii}(i,j) = 0;
end
end
end
end
resp{20,ii} = [zeros(length(resp{1,ii}),1) diff(resp{2,ii},[],2)];
resp{21,ii} = [zeros(length(resp{1,ii}),1) diff(resp{1,ii},[],2)];
end

resp{30,30} = [];
for i = 1:27
    for ii=4:7
        resp{i,10} = [resp{i,10}; resp{i,ii}(:,1)];
        resp{i,12} = [resp{i,12}; resp{i,ii}(:,end)];
    end
end

```

```

    for j=2:ii-1
        resp{i,11} = [resp{i,11}; resp{i,ii}(:,j)];
    end
end
end
end

```

```

labels{7} = 'Snore Duration (s)'; labels{8} = 'Interval (s)'; labels{9} = 'Spectral Centroid (Hz)'; labels{10} = 'Sound Intensity (au)'; labels{11} = 'Maximum frequency '; labels{12} = 'Pitch (Hz)'; labels{13} = 'Correlation at Pitch'; labels{14} = 'Mean Fundamental Frequency (Hz)'; labels{15} = 'Pitch SD (Hz)'; labels{16} = 'Airflow width (half prominence)'; labels{17} = 'airflow width'; labels{18} = 'area under the curve(airflow)'; labels{19} = 'airflow number'; labels{20} = 'peak amplitude diff'; labels{21} = 'airflow peak to peak interval'; labels{22} = 'area under the curve(snore)'; labels{23} = 'area under the curve(MIC) during airflow'; labels{24} = 'Time Interval 1 (s)'; % bi and es labels{25} = 'bi and bs'; labels{26} = 'Time Interval 2 (s)'; % ei and es labels{27} = 'ei and bs';

```

```

postsnorerate = 100*sum(resp{5,10} ~= 0)/length(resp{5,10});
midsnorerate = 100*sum(resp{5,11} ~= 0)/length(resp{5,11});
presnorerate = 100*sum(resp{5,12} ~= 0)/length(resp{5,12});

```

```

sublabels = {'a','b','c','d','e','f','g','h','i'};

```

```

m = [];

```

```

e = [];

```

```

fts = [9,12,15,7,24,26,10,13];

```

```

fpr = 3;

```

```

for j=1:length(fts)

```

```

    i = fts(j);

```

```

    subplot(fpr,ceil(length(fts)/fpr),j)

```

```

    m = [mean(resp{i,10}(resp{i,10}~=0)), mean(resp{i,11}(resp{i,11}~=0)), mean(resp{i,12}(resp{i,12}~=0))];

```

```

    e = [std(resp{i,10}(resp{i,10}~=0))/sqrt(sum(resp{i,10}~=0)), std(resp{i,11}(resp{i,11}~=0))/sqrt(sum(resp{i,11}~=0)), std(resp{i,12}(resp{i,12}~=0))/sqrt(sum(resp{i,12}~=0))];

```

```

    barwitherr(e,m)

```

```

% errorbar(m,e,'o')

```

```

% xlim([0 3])
ylabel(labels(i))
ylim([min(m-3*e) max(m+2*e)])
xticklabels({'Post','Mid','Pre'})
box off
xtickangle(45)
text(0.90,1.15,sublabels{j},'Units',          'Normalized',          'VerticalAlignment',
'Top','FontWeight','bold')
% pause;
end
j=j+1;
subplot(fpr,ceil(length(fts)/fpr),j)
bar([postsnorerate,midsnorerate,presnorerate])
ylabel('Snore Occurrence (%)')
ylim([0 100])
xticklabels({'Post','Mid','Pre'})
box off
xtickangle(45)
text(0.90,1.1,sublabels{9},'Units',          'Normalized',          'VerticalAlignment',
'Top','FontWeight','bold')

%% statistics and table
for i = 1:27
    features(:,i) = [resp{i,10};resp{i,11};resp{i,12}];
end
groups          =          [ones(length(resp{5,10}),1);          2*ones(length(resp{5,11}),1);
3*ones(length(resp{5,12}),1)];

features = [features groups];
features(features(:,5)==0,:)=[];
x = features(:,fts);
xn = (x-mean(x))./std(x);
grp = features(:,end);

```

```

inputsnore = [xn grp];
inputsnore = inputsnore(randperm(size(inputsnore,1)),:);

[d, p, stats] = manova1(x,grp)

for j=1:length(fts)
    i = fts(j);
    [p,tbl,stats] = anova1(features(:,i),grp);
    [c,mm,h,gnames] = multcompare(stats);
    t1{j,1} = labels{i}; %string(labels{i});
    t1{j,2} = [num2str(mm(1,1),'%.2f') '±' num2str(mm(1,2),'%.2f')];
    t1{j,3} = [num2str(mm(2,1),'%.2f') '±' num2str(mm(2,2),'%.2f')];
    t1{j,4} = [num2str(mm(3,1),'%.2f') '±' num2str(mm(3,2),'%.2f')];
    t1{j,5} = ['p=' num2str(p,'%.3f')];
    t1{j,6} = ['1-2 p=' num2str(c(1,6),'%.3f') newline '1-3 p=' num2str(c(2,6),'%.3f')
newline '2-3 p=' num2str(c(3,6),'%.3f')];
end
t11 = string(t1);

% for i=1:size(mf,1)
%   for j=1:size(mf,2)
%       frq{i,j} = [num2str(mf(i,j),'%.2f') '±' num2str(sf(i,j),'%.2f')];
%       dsp{i,j} = [num2str(md(i,j),'%.2f') '±' num2str(sd(i,j),'%.2f')];
%   end
% end
% frq1 = string(frq);
% dsp1 = string(dsp);

```

REFERENCES

- Jr Badia, R Farré, J Rigau, Me Uribe, D Navajas, & Jm Montserrat. (2001). Forced oscillation measurements do not affect upper airway muscle tone or sleep in clinical studies. *European Respiratory Journal*, 18(2), 335-339.
- E Fiona Bailey, & Ralph F Fregosi. (2004). Coordination of intrinsic and extrinsic tongue muscles during spontaneous breathing in the rat. *Journal of Applied Physiology*, 96(2), 440-449.
- Helen Bearpark, Lynne Elliott, Ron Grunstein, Stewart Cullen, Hartmut Schneider, Wilma Althaus, & Colin Sullivan. (1995). Snoring and sleep apnea. A population study in Australian men. *American Journal of Respiratory and Critical Care Medicine*, 151(5), 1459-1465.
- Sigfrid Blom. (1960). Afferent influences on tongue muscle activity. A morphological and physiological study in the cat. *Acta Physiologica Scandinavica. Supplementum*, 49(170), 1-97.
- David Burke, Karl-Erik Hagbarth, L Löfstedt, & B Gunnar Wallin. (1976a). The responses of human muscle spindle endings to vibration during isometric contraction. *The Journal of Physiology*, 261(3), 695-711.
- David Burke, Karl-Erik Hagbarth, L Löfstedt, & B Gunnar Wallin. (1976b). The responses of human muscle spindle endings to vibration of non-contracting muscles. *The Journal of Physiology*, 261(3), 673.
- Jean Edouard Desmedt, & Emile Godaux. (1975). Vibration-induced discharge patterns of single motor units in the masseter muscle in man. *The Journal of Physiology*, 253(2), 429-442.
- Elizabeth A Doble, James C Leiter, Susan L Knuth, Ja Daubenspeck, & D Bartlett Jr. (1985). A noninvasive intraoral electromyographic electrode for genioglossus muscle. *Journal of Applied Physiology*, 58(4), 1378-1382.
- Peter R Eastwood, Makoto Satoh, Aidan K Curran, Maria T Zayas, Curtis A Smith, & Jerome A Dempsey. (1999). Inhibition of inspiratory motor output by high-

frequency low-pressure oscillations in the upper airway of sleeping dogs. *The Journal of Physiology*, 517(1), 259-271.

Francis Echlin, & Alfred Fessard. (1938). Synchronized impulse discharges from receptors in the deep tissues in response to a vibrating stimulus. *The Journal of Physiology*, 93(4), 312.

David W Eisele, Philip L Smith, Daniel S Alam, & Alan R Schwartz. (1997). Direct hypoglossal nerve stimulation in obstructive sleep apnea. *Archives of Otolaryngology-Head & Neck Surgery*, 123(1), 57-61.

Göran Eklund, & K-E Hagbarth. (1966). Normal variability of tonic vibration reflexes in man. *Experimental Neurology*, 16(1), 80-92.

Ja Fiz, J Abad, R Jane, M Riera, Ma Mananas, P Caminal, . . . J Morera. (1996). Acoustic analysis of snoring sound in patients with simple snoring and obstructive sleep apnoea. *European Respiratory Journal*, 9(11), 2365-2370.

Robert B Fogel, Atul Malhotra, Giora Pillar, Jill K Edwards, José Beauregard, Steven A Shea, & David P White. (2001). Genioglossal activation in patients with obstructive sleep apnea versus control subjects: mechanisms of muscle control. *American Journal of Respiratory and Critical Care Medicine*, 164(11), 2025-2030.

Robert B Fogel, John Trinder, Atul Malhotra, Michael Stanchina, Jill K Edwards, Karen E Schory, & David P White. (2003). Within-breath control of genioglossal muscle activation in humans: effect of sleep-wake state. *The Journal of Physiology*, 550(3), 899-910.

Dd Fuller, Js Williams, Pl Janssen, & Rf Fregosi. (1999). Effect of co-activation of tongue protruder and retractor muscles on tongue movements and pharyngeal airflow mechanics in the rat. *The Journal of Physiology*, 519(2), 601-613.

C Gonzaga, A Bertolami, M Bertolami, C Amodeo, & D Calhoun. (2015). Obstructive sleep apnea, hypertension and cardiovascular diseases. *Journal of Human Hypertension*, 29(12), 705.

Karl Erik Hagbarth, Gustaf Hellsing, & L Löfstedt. (1976). TVR and vibration-induced timing of motor impulses in the human jaw elevator muscles. *Journal of Neurology, Neurosurgery & Psychiatry*, 39(8), 719-728.

- Kathe G Henke, & Colin E Sullivan. (1993). Effects of high-frequency oscillating pressures on upper airway muscles in humans. *Journal of Applied Physiology*, 75(2), 856-862.
- Keidai Hirayama, Saburo Homma, Muneaki Mizote, Yasuo Nakajima, & Shiro Watanabe. (1974). Separation of the contributions of voluntary and vibratory activation of motor units in man by cross-correlograms. *The Japanese Journal of Physiology*, 24(3), 293-304.
- Rl Horner, Ja Innes, Mj Morrell, Sa Shea, & A Guz. (1994). The effect of sleep on reflex genioglossus muscle activation by stimuli of negative airway pressure in humans. *The Journal of Physiology*, 476(1), 141.
- Jingtao Huang, Mesut Sahin, & Dominique M Durand. (2005). Dilation of the oropharynx via selective stimulation of the hypoglossal nerve. *Journal of Neural Engineering*, 2(4), 73.
- K Igarashi. (1996). Neurophysiological mechanism of jaw-tongue reflex in man. *Kokubyo Gakkai zasshi. The Journal of the Stomatological Society, Japan*, 63(1), 108-121.
- Y Ishiwata, S Hiyama, K Igarashi, T Ono, & T Kuroda. (1997). Human jaw-tongue reflex as revealed by intraoral surface recording. *Journal of Oral Rehabilitation*, 24(11), 857-862.
- Y Ishiwata, T Ono, T Kuroda, & Y Nakamura. (2000). Jaw-tongue reflex: afferents, central pathways, and synaptic potentials in hypoglossal motoneurons in the cat. *Journal of Dental Research*, 79(8), 1626-1634.
- Eric J Kezirian, George S Goding, Atul Malhotra, Fergal J O'donoghue, Gary Zammit, John R Wheatley, . . . Jennifer H Walsh. (2014). Hypoglossal nerve stimulation improves obstructive sleep apnea: 12-month outcomes. *Journal of Sleep Research*, 23(1), 77-83.
- Jason P Kirkness, Vidya Krishnan, Susheel P Patil, & Hartmut Schneider. (2006). Upper airway obstruction in snoring and upper airway resistance syndrome. In *Sleep Apnea* (Vol. 35, pp. 79-89): Karger Publishers.

- Dorit Koren, Magdalena Dumin, & David Gozal. (2016). Role of sleep quality in the metabolic syndrome. *Diabetes, Metabolic Syndrome and Obesity: Targets and Therapy*, 9, 281.
- Stephen W Kuffler, Carleton C Hunt, & Juan P Quilliam. (1951). Function of medullated small-nerve fibers in mammalian ventral roots: efferent muscle spindle innervation. *Journal of Neurophysiology*.
- Richard St Leung, & T Douglas Bradley. (2001). Sleep apnea and cardiovascular disease. *American Journal of Respiratory and Critical Care Medicine*, 164(12), 2147-2165.
- Aa Lowe. (1978). Mandibular joint control of genioglossus muscle activity in the cat (*Felis domesticus*) and monkey (*Macaca irus*). *Archives of Oral Biology*, 23(9), 787-793.
- Aa Lowe, Sc Gurza, & Bj Sessle. (1977). Regulation of genioglossus and masseter muscle activity in man. *Archives of Oral Biology*, 22(10-11), 579-584.
- Alan A Lowe, & Barry J Sessle. (1973). Tongue activity during respiration, jaw opening, and swallowing in cat. *Canadian Journal of Physiology and Pharmacology*, 51(12), 1009-1011.
- Micha T Maeder, Otto D Schoch, & Hans Rickli. (2016). A clinical approach to obstructive sleep apnea as a risk factor for cardiovascular disease. *Vascular Health and Risk Management*, 12, 85.
- Pb Matthews. (1984). Evidence from the use of vibration that the human long-latency stretch reflex depends upon spindle secondary afferents. *The Journal of Physiology*, 348(1), 383-415.
- Pbc Matthews. (1966). The reflex excitation of the soleus muscle of the decerebrate cat caused by vibration applied to its tendon. *The Journal of Physiology*, 184(2), 450-472.
- Mary K Milidonis, Charles G Widmer, Richard L Segal, & Steven L Kraus. (1988). Surface intraoral genioglossus EMG recording technique for kinesiologic studies. *American Journal of Orthodontics and Dentofacial Orthopedics*, 94(3), 240-244.

- Toshifumi Morimoto, Hiromitsu Takebe, Iwao Sakan, & Yojiro Kawamura. (1978). Reflex activation of extrinsic tongue muscles by jaw closing muscle proprioceptors. *The Japanese Journal of Physiology*, 28(4), 461-471.
- Peter D Neilson, Gavin Andrews, Barry E Guitar, & Peter T Quinn. (1979). Tonic stretch reflexes in lip, tongue and jaw muscles. *Brain Research*, 178(2-3), 311-327.
- Paul E Peppard, Terry Young, Jodi H Barnet, Mari Palta, Erika W Hagen, & Khin Mae Hla. (2013). Increased prevalence of sleep-disordered breathing in adults. *American Journal of Epidemiology*, 177(9), 1006-1014.
- Louise Plowman, Desmond C Lauff, Michael Berthon-Jones, & Colin E Sullivan. (1990). Waking and genioglossus muscle responses to upper airway pressure oscillation in sleeping dogs. *Journal of Applied Physiology*, 68(6), 2564-2573.
- Naresh M Punjabi. (2008). The epidemiology of adult obstructive sleep apnea. *Proceedings of the American Thoracic Society*, 5(2), 136-143.
- Jp Roll, Jp Vedel, & E Ribot. (1989). Alteration of proprioceptive messages induced by tendon vibration in man: a microneurographic study. *Experimental Brain Research*, 76(1), 213-222.
- Patricla Romaguere, Jean-Pierre Vedel, Jp Azulay, & S Pagni. (1991). Differential activation of motor units in the wrist extensor muscles during the tonic vibration reflex in man. *The Journal of Physiology*, 444(1), 645-667.
- Mesut Sahin, Dh Durand, & Musa A Haxhiu. (2000). Closed-loop stimulation of hypoglossal nerve in a dog model of upper airway obstruction. *IEEE Transactions on Biomedical Engineering*, 47(7), 919-925.
- R Schoen. (1931). Untersuchungen über Zungen-und Kieferreflexe: I. Mitteilung der Kieferzungen Reflex und andere proprioceptive Reflex der Zunge und der Kiefermuskulatur. *Arch Exp Pathol Pharmacoll*, 160, 29-48.
- Richard J. Schwab, Warren B. Geffer, Eric A. Hoffman, Krishanu B. Gupta, & Allan I. Pack. (1993). Dynamic upper airway imaging during awake respiration in normal subjects and patients with sleep disordered breathing. *American Review of Respiratory Disease*, 148, 1385-1400.

- Alan R Schwartz, David C Thut, Brad Russ, Marc Seelagy, Xiao Yuan, Roy G Brower, . . . Philip L Smith. (1993). Effect of electrical stimulation of the hypoglossal nerve on airflow mechanics in the isolated upper airway. *American Review of Respiratory Disease*, 147, 1144-1144.
- Eyal Shahar, Coralyn W Whitney, Susan Redline, Elisa T Lee, Anne B Newman, F Javier Nieto, . . . Jonathan M Samet. (2001). Sleep-disordered breathing and cardiovascular disease: cross-sectional results of the Sleep Heart Health Study. *American Journal of Respiratory and Critical Care Medicine*, 163(1), 19-25.
- Surendra K Sharma, Vishwa Mohan Katoch, Alladi Mohan, T Kadiravan, A Elavarasi, R Ragesh, . . . Manvir Bhatia. (2015). Consensus and evidence-based Indian initiative on obstructive sleep apnea guidelines 2014. *Lung India: Official Organ of Indian Chest Society*, 32(4), 422.
- J Sola-Soler, R Jane, Ja Fiz, & J Morera. (2002). *Pitch analysis in snoring signals from simple snorers and patients with obstructive sleep apnea*. Paper presented at the Engineering in Medicine and Biology, 2002. 24th Annual Conference and the Annual Fall Meeting of the Biomedical Engineering Society EMBS/BMES Conference, 2002. Proceedings of the Second Joint.
- Jordi Sola-Soler, Raimon Jane, Jose Antonio Fiz, & Jose Morera. (2000). *Towards automatic pitch detection in snoring signals*. Paper presented at the Engineering in Medicine and Biology Society, 2000. Proceedings of the 22nd Annual International Conference of the IEEE.
- Carl J Stepnowsky Jr, William C Orr, & Terence M Davidson. (2004). Nightly variability of sleep-disordered breathing measured over 3 nights. *Otolaryngology—Head and Neck Surgery*, 131(6), 837-843.
- Patrick J Strollo Jr, Ryan J Soose, Joachim T Maurer, Nico De Vries, Jason Cornelius, Oleg Froymovich, . . . M Boyd Gillespie. (2014). Upper-airway stimulation for obstructive sleep apnea. *New England Journal of Medicine*, 370(2), 139-149.
- Terri E Weaver, & Ronald R Grunstein. (2008). Adherence to continuous positive airway pressure therapy: the challenge to effective treatment. *Proceedings of the American Thoracic Society*, 5(2), 173-178.
- W Whitelaw. (1993). Characteristics of the snoring noise in patients with and without occlusive sleep apnea. *Am Rev Respir Dis*, 147, 635-644.

- Kent Wilson, Riccardo A Stoohs, Thomas F Mulrooney, Linda J Johnson, Christian Guilleminault, & Zhen Huang. (1999). The snoring spectrum: acoustic assessment of snoring sound intensity in 1,139 individuals undergoing polysomnography. *Chest*, 115(3), 762-770.
- B Tucker Woodson, M Boyd Gillespie, Ryan J Soose, Joachim T Maurer, Nico De Vries, David L Steward, . . . Sam Mickelson. (2014). Randomized controlled withdrawal study of upper airway stimulation on OSA: short-and long-term effect. *Otolaryngology--Head and Neck Surgery*, 151(5), 880-887.
- Paul B Yoo, Mesut Sahin, & Dominique M Durand. (2004). Selective stimulation of the canine hypoglossal nerve using a multi-contact cuff electrode. *Annals of Biomedical Engineering*, 32(4), 511-519.
- Shaoping Zhang, & Oommen P Mathew. (1992). Response of laryngeal mechanoreceptors to high-frequency pressure oscillation. *Journal of Applied Physiology*, 73(1), 219-223.